Turbulent Convection in Stars

by

Sashin Moonsamy

Thesis presented in fulfilment of the requirements for the degree of

Doctor of Philosophy
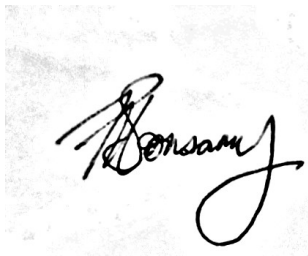
at the University of the Witwatersrand

Supervisor: F.A.M. Frescura

Co-supervisor: C.A. Engelbrecht

May 2017

Declaration

I declare that this thesis is my own unaided work. It is being submitted for the Degree of Doctor of Philosophy to the University of the Witwatersrand, Johannesburg. It has not been submitted previously for any degree or examination to any other university.

Sashin Lusane Moonsamy,

31 May 2017.

Acknowledgements

I would like to express my deepest gratitude to my principal supervisor, Fabio Frescura. Working alongside him has been one of the greatest experiences of my life. I am grateful for his unwavering guidance and support over the years. He has been and continues to be an inspiration and a role model to me.

I would also like to thank my co-supervisor Chris Engelbrecht for introducing me to the field of stellar astrophysics and for sparking my interest in the convection problem. I have benefited greatly from many useful discussions with him on several aspects of this work and look forward to working with him on future projects.

Finally, I would like to thank my family for all the laughter and joy they bring to my life and for always believing in me.

For my parents.

Abstract

Turbulent Convection in Stars

S.L. Moonsamy

School of Physics,
University of the Witwatersrand,
PO Box Wits, Johannesburg, 2050, South Africa

Thesis: PhD (Physics)

May 2017

This thesis investigates in detail the structure of models of turbulent convection with phenomenological closures for the eddy-viscosity. It explores the merits of replacing the canonical Mixing Length Theory of stellar convection with more realistic models of fluid turbulence that take into account the full spectrum of eddy sizes. The author provides a detailed exposition of the fundamental assumptions and the *modus operandi* of various approaches to the treatment of convective energy-transfer in stars. He focuses in particular on spectral descriptions of the convective process. The structure of several closure models developed by various authors are investigated, and he identifies and elucidates those aspects of these closures that lead to an improved description of convective turbulence in the stellar interior. The author also develops an implementation within the public-domain code, called Modules for Experiments in Stellar Astrophysics, of two of these models and reports and discusses the results of his numerical experiments.

Contents

List of Figures

Chapter 1

Introduction

"It remains to call attention to the chief outstanding difficulty of
our subject."
- H. Lamb [76]

Convection in stars is intrinsically a turbulent process. It is characterized by a wide spectrum of eddies whose interactions redistribute energy across the stellar interior in a highly non-linear way. Description of this phenomenon is complex both physically and mathematically. A theory of convection that can completely account for the turbulent dynamics of the stellar fluid, does not yet exist [131]. Lack of progress in this field is attributable to a lack of empirical data and to our inability to solve analytically the equations that describe turbulent flow.

The most commonly used model of convection in stars is Mixing Length Theory (MLT) [8; 47; 132]. The origins of the MLT can be traced back to the work of Prandtl [109] who, in the early 1900's, developed MLT to describe convection in incompressible terrestrial fluids. Prandtl's work was motivated by challenges in engineering at that time. The problem of channel flow was of considerable technological importance and the original form of the MLT was designed to model engineering problems of this type [10; 11; 109].

MLT was later adapted to the description of stellar convection first in the 1940's by Biermann [7], and later by Böhm-Vitense [8] in the mid to late 1950's. It has since undergone numerous modifications in an attempt to rectify its failures when applied to stellar interiors [49].

MLT is a primitive semi-empirical theory. It is based on a number of severe approximations which, depending on the efficiency of the convective process, can result in gross misrepresentations of the rate of energy transport through the stellar fluid [22; 23]. The inability of MLT to predict accurately the energetics of the convection zone may have severe consequences for our understanding of the structure and evolution of stars, and hence also of the evolution of galaxies and of the cosmos.

A major obstacle in developing more realistic models of stellar convection has been the lack of the computing power needed to perform realistic simulations of the stellar fluid. For example, there are two types of detailed three dimensional simulations that might be used. They are Direct Numerical Simulations (DNS) [46; 97; 110; 134] and Large Eddy Simulations (LES) [43; 51; 93]. These have the potential to provide significant inroads into our understanding of convective turbulence and its coupling to other physical phenomena in stars. While recent advances in technology have resulted in remarkable progress of computational speed and data storage capacity, simulations of the above types are still incapable of the resolution of scales needed for complete DNS and LES of turbulent convection, and are largely limited to the treatment of surface convection zones and stellar atmospheres [104]. Complete three-dimensional simulations of the stellar interior appear to be unattainable in the foreseeable future [73]. To avoid these difficulties, simulations of stellar structure and evolution are typically forced to rely on one-dimensional stellar evolution codes which use parametric representations of the stellar interior to bypass the

computational complexities associated with a full numerical treatment. The current generation of 1-D stellar evolution codes still rely in large part on the MLT for the calculation of the convective heat flux in the stellar interior [99].

The longevity of the MLT is especially surprising considering that, in fields other than stellar astrophysics, MLT has been replaced by more predictive models of turbulent convection which, unlike the MLT, are derived directly from the turbulence equations that govern the fluid [92; 127]. My purpose in this thesis is to investigate the structure of some of these models, to evaluate their merits, and to comment on their potential usefulness to models of stellar structure and evolution.

1.1 The origins of MLT

The pervasiveness of turbulence in astrophysical systems is a key obstacle to accurate description and prediction of the behaviour of systems such as stars. This is due the non-linear nature of the Navier-Stokes Equations (NSE) which present a major obstruction to the development of a complete, analytical model of fluid turbulence. A Reynolds averaging the NSE leads to an infinite sequence of equations for the velocity correlation terms. The equations that determine the n-th order correlation terms require knowledge of the corresponding terms of order $n + 1$. This leads to an infinite hierarchy of coupled equations. This is known as the closure problem. The closure problem appears, in principle, to be insoluble. Our only option, if we are to make progress requires us to cut the "Gordian knot" by appeal to semi-empirical models that develop a closure for the moment equations at a given order.

The first such models date back to the work of Boussinesq [10; 115]. In 1877, he introduced the concept of an eddy viscosity, ν_T, as a means of determining

the form of the Reynolds stress tensor in shear flows. According to Boussinesq's hypothesis, turbulence has the effect of renormalizing or "enhancing" the molecular viscosity by an amount that corresponds to ν_T. However, apart from stating that ν_T is an intrinsic property of the turbulence itself, Boussinesq's model did not provide any meaningful insight into the physical nature of the eddy viscosity which it proposed.

It was not until the development of Prandtl's mixing length model [109] that an explicit expression for ν_T was suggested. The theory was developed in analogy with similar processes in the kinetic theory of gases and was the first to relate the eddy viscosity to the turbulent kinetic energy of the fluid. The relation obtained came at the cost of a free parameter, the mixing length, l, which is a measure of the average distance travelled by a turbulent eddy before it dissipates its energy into the surrounding fluid. In the absence of a method for determining the mixing length, Prandtl's model effectively changed the problem from one of determining ν_T, to one of determining l. Prandtl himself appears to have had severe doubts concerning the validity of the model, describing it as "*only a rough approximation*" [11].

Despite its shortcomings, the mixing length model proved to be a useful "engineering" approach to problems in terrestrial fluid turbulence. For these, there is a wealth of experimental data on the time evolution of the turbulent velocity field, from which the form of ν_T can be inferred.

This type of data for astrophysical turbulence is currently unobtainable. In astrophysical systems, therefore, *prediction* rather than *description* of turbulent flow properties is of interest. The turbulent velocity and temperature fields, and the bulk quantities associated with them, should ideally be calculable from an astrophysical model of fluid turbulence, rather than being determined from data and supplied as inputs.

In the absence of a better alternative, Biermann and Böhm-Vitense adapted Prandtl's mixing length concept to the process of convective energy transport in stellar interiors. Their work laid the foundation for what later came to be known in stellar astrophysics as, the Mixing Length Theory (MLT).

As was the case with Prandtl's original model, the MLT suffers from a lack of predictive power with regard to the turbulence which it claims to describe. This lack of predictive power is "plastered over" in the model by the mixing-length parameter, α which needs to be fitted to the astrophysical data in order to be determined. No detailed model has yet been able to predict the value of α. Furthermore, fitted values of α have no universality even for restricted classes of stars. MLT is also devoid of any details regarding the structure and distribution of turbulent energy across the spectrum of eddies which carry the heat flux through the stellar convection zone. This is due to the fact that the original iteration of the model was not derived from the NSE, but rather from a purely phenomenological consideration of the kinematics of a putative fluid element subjected to a perturbation of its thermodynamic state [132].

Moreover, MLT is ignorant of the fundamental fluid equations. This makes the inclusion of new physical effects difficult and speculative. It was not until the work of Canuto and Goldman (CG) [17], nearly thirty years after Böhm-Vitense's original publication of the MLT's adaptation to stars, that a derivation of its flux formula from the general equations of turbulent flow was provided.

1.2 Eddy-viscosity models

Interestingly, at the same time that MLT was beginning to take shape, there was a renewed interest in turbulence modelling from a fundamental perspective. This renaissance was sparked by the work of G.I Taylor [125] who, in the late 1930's, began to develop the foundations of the spectral theory of homogeneous, isotropic turbulence. This introduced a new level of mathematical rigour into the description of turbulent flows which culminated a decade later in the work of Kolmogorov and Heisenberg, who produced an analytical theory of the inertial subrange [41; 55; 66].

The Kolmogorov-Heisenberg (KH) model was the first to provide a universal closure for the turbulent energy spectrum. The KH model has received extensive experimental verification [3; 63; 50; 98; 137] and is now widely regarded as one of the great milestones in the history of turbulence modelling. However, due the assumptions inherent in its construction, the KH model is necessarily valid only in a limited range of the energy spectrum of the flow known as the inertial subrange. This region is characterized by eddies that evolve freely and are thus insensitive to the detailed physical mechanisms that generate the turbulence and also to the processes that ultimately dissipate the energy of the eddies. It also does not take into account the backscattering of energy from smaller to larger scales. Its inability to describe the generation of the large eddies renders the KH model incapable of capturing fully the dynamics of the bulk flow which determines large-scale properties such as the convective heat flux.

To describe accurately the behaviour of astrophysical fluids, in which the effects of *large-scale turbulence* (LST) are most important, one needs a model of turbulence that incorporates a more complete description of the large eddy spectrum than is given by the KH model.

There are several ways in which one can attempt to construct LST models. For example, there is the formal, first principles approach, which attempts to treat analytically the non-linear nature of the NSE. Perhaps the most significant example of such a model is, the Direct Interaction Approximation (DIA) [67; 68; 69; 72], introduced by Kraichnan in the early 1960's. The DIA is arguably the most sophisticated model of fluid turbulence to have been developed using the eddy viscosity concept. It was formulated using the language of quantum field theory, and provides an advanced theoretical framework, free of ad hoc parameters, within which the properties of inhomogeneous anisotropic turbulence can be studied. This model is directly applicable to LST and also provides a method for treating the effects of non-local interactions in the fluid [71].

The DIA has given rise to a host of related models which are similar to it in structure. The most well known examples of such models are the Eddy Damped Quasi-Normal Markovian (EDQNM) model [81; 102] and the Test Field Model (TFM) [70], both of which simplify the full DIA theory with a view to obtaining a more tractable treatment of the turbulence problem.

The above models are categorized in the field of turbulence modelling as, *two-point closure* models. The term *two-point closure* refers to the fact that they deal with the correlation of fluid elements at two points in space (or two wavenumbers in Fourier-space). Due to the strong theoretical framework on which these models are based, they are capable of providing significant insights into the nature of turbulence and its interaction with the surrounding medium. However, these theories are often difficult to implement numerically. They are also computationally intensive. Depending on the strength of the turbulence of a given flow, the time required to generate a numerical solution of the model equations may be impractical. In fact, it was not until the work of Canuto and Mazzitelli [22] that the DIA/EDQNM model, was applied to the computation

of convective turbulence in stars.

To find middle ground between the theoretical sophistication of two-point closure models and the numerical limitations of one-dimensional stellar evolution codes, there is a second approach that can be taken. This approach involves providing a closure to the fluid equations by using *phenomenological* arguments that relate the eddy viscosity to other known or calculable quantities of the fluid. Models of this type typically rely on spectral descriptions of the turbulent flow field, and thus provide a natural framework for extracting information about the energetics of the flow. Furthermore, these models are significantly simpler to use and to implement numerically than are the DIA and its derivatives. This makes them ideal candidates for the description of stellar convection.

Analysis and evaluation of these types of models are the principal concern of this thesis, and I will discuss the benefits of using them in studies of stellar structure and evolution. It will be shown that, when applied to the description of convective turbulence, this class of models represents a significant improvement over the MLT, which fails to capture in a realistic way the dynamics of the eddy interactions that are known to occur in a turbulent fluid.

1.3 Outline of thesis

In addition to MLT, I will discuss in detail the following models of convection:

1. The Canuto and Goldman (CG) model [17].

2. The Canuto, Goldman and Chasnov (CGC) model [21].

3. The Canuto, Goldman and Mazzitelli (CGM) model [23].

I will present a thorough theoretical analysis of each of the above models, deriving and interpreting all of the major results and identifying the key elements required for an understanding of their predictions. I will then compare these models to one another, and to the MLT, in the context of convective turbulence in stars. This comparison will show that the predictions of the MLT are in severe disagreement with those made by more advanced models of convective turbulence. I will then report on my implementation of these models in the MESA code [106; 107; 108], and on the results of the numerical experiments that I have run. These results confirm quantitatively the disagreements inferred from the theoretical comparison.

The material in this thesis is structured as follows. In Chapter 2, I develop the theoretical framework required for a complete understanding of the models listed above. The fundamental aspects of spectral closure modelling for turbulent flows will be developed and discussed in detail in this chapter.

In Chapter 3, I provide a comprehensive discussion of the CG model of large-scale turbulence and show how this model improves in several ways on the shortcomings of the KH model. It will also be shown in this chapter that the MLT can be derived from the general equations of the CG model, when certain assumptions about the nature of the fluid are made.

Chapter 4 consists of a detailed theoretical analysis of the CGC model, which is in many ways an advanced extension of the CG model. I discuss the form of the CGC closure and show how this closure enables the model to naturally treat the physics of the *entire* eddy spectrum, including the region characterized by small-scale turbulence (SST). The CGC model also provides a unique method for determining the growth rates of the turbulence generating insta-

bilities from within the model itself. This remarkable aspect of the model is discussed in significant detail.

In Chapter 5, I consider the shortcomings of the MLT when applied to the description of stellar convection. I compare and contrast the flux predictions of the MLT with those of the models previously discussed, and show that the MLT makes an unphysical assumption about the nature of the turbulent energy spectrum. It will be shown in this chapter that, depending on the efficiency of the convective process, the MLT provides an extremely poor estimate of the convective heat flux.

Chapter 6 considers the CGM model of stellar convection. It will be shown that this model utilizes the framework of the CGC model to produce a flux equation that accounts for the full spectrum of fluid turbulence. This chapter also considers briefly the Canuto and Mazzitelli (CM) [22] model of stellar convection which, unlike the CG, CGC and CGM models, is based on the DIA/EDQNM treatment of the turbulence problem. The flux predictions of the CGM and CM models are also compared against those of the MLT.

In Chapter 7, I discuss the application of the CM and CGM models to simulations of stellar structure and evolution. As part of this work, numerical implementations of the above models were developed within the context of the Modules for Experiments in Stellar Astrophysics (MESA) code [106; 107; 108]. The results of a set of numerical experiments performed using this implementation are reported. It will be shown in this chapter that the previously discussed shortcomings of the MLT have important consequences on the predictions made by numerical simulations of stars. Several differences between the MLT, CM and CGM models are illustrated in this chapter via a set of evolutionary diagrams that were produced using the MESA code.

Finally, in Chapter 8 I conclude with a discussion of the implications of the analyses presented in this thesis, and discuss how the work detailed in it can be developed in future work.

Chapter 2

Theoretical Framework

"The smallest eddies are almost numberless, and large things are rotated only by large eddies and not by small ones, and small things are turned by small eddies and large."

- Leonardo Da Vinci [91]

2.1 Introduction

In this chapter I consider the theoretical framework within which phenomenological closures of the turbulent energy spectrum are developed.

I begin with a discussion of the factors which determine the dynamics of the eddies in key sectors of the turbulent energy cascade, and focus in particular on the differences between the large-scale and dissipation regions of the flow.

In sections 2.2.1 and 2.2.2, I relate the non-linear transfer of energy in the cascade to the action of the eddy viscosity, and define the closure problem as being equivalent to one of determining the form of the eddy correlation rate, $n_c(k)$.

In section 2.3, I discuss the physics underlying the KH model of the inertial subrange, and consider the limitations of this model in the context of large-scale turbulence.

A discussion of the generalized form of the energy equation is provided in section 2.4, where it is noted that its formulation in terms of the source growth rate allows for the incorporation of different physical processes in models of turbulence which aim to treat the LST sector of the spectrum.

I then derive, in section 2.5, the general expression for $\nu_t(k)$ in terms of $n_c(k)$, and then use this expression to comment on the balance of rates in a turbulent fluid.

Finally, section 2.6 contains a summary of the general procedure for determining the form of the turbulent energy spectrum. This procedure will be used in subsequent chapters within the context of several models of turbulence that provide better descriptions of convection than the MLT.

2.2   The turbulent energy spectrum

The largest eddies in a turbulent fluid are in general created as a result of an instability in the system which generates and maintains the turbulent state. The dynamics of these eddies is sensitive to the details of the physical process that causes the instability. Since there are an infinite number of ways in which a fluid instability can be created, spectral descriptions of these kinds of eddies do not in general exhibit any significant degree of universality.

The energy fed into the large eddies by the instability that generates them, (hereafter referred to as the *source instability*), is "cascaded" across a distri-

bution of eddy sizes until the Kolmogorov scale is reached. Eddies evolving at this length scale are the smallest ones present in the system. The dynamics of this region of the flow is almost entirely determined by the action of the molecular viscosity in the fluid, which causes the turbulent energy that was once fed into the system at the largest scales to be dissipated.

In order to study how the input energy is distributed across the various eddies in the cascade, one defines a spectral function for the turbulent energy, $F(k)$, by the equation,

$$\langle u^2 \rangle = \int_{k_0}^{\infty} F(k) dk \qquad (2.2.1)$$

where u is the turbulent velocity, k is the wavenumber, and the angular brackets, $\langle \cdot \rangle$, denote an ensemble average. The eddy size, l_k, is related to k via the formula $l_k = \pi/k$. The wavenumber, k_0, is therefore defined as the minimum value of k (and hence the maximum value of l_k) permitted by the system geometry.

The calculation of $F(k)$ is one of the primary objectives of any model of fluid turbulence. Its determination enables the calculation of several important properties of the flow which are of interest in stellar modelling. In this thesis, we will focus on the use of $F(k)$ to determine the convective heat flux in the stellar interior.

2.2.1   The energy equation

For the second order moment of the fluctuating velocity field, it has been shown that[1] [3],

---

[1] By an abuse of notation we have not distinguished the variable of integration from its value in the upper limit, this appears to be standard in the literature on the subject and is a convention which I have adopted in the rest of this thesis.
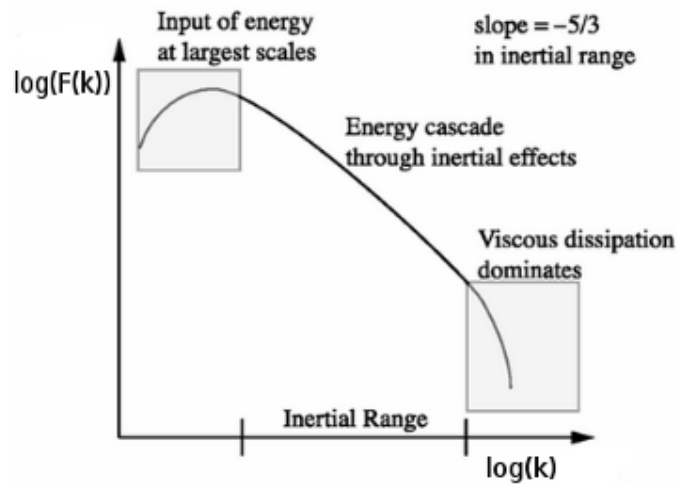
Figure 2.1: Plot of $\log F(k)$ vs $\log k$. [77]

$$\epsilon(k) = \left[\nu + \nu_t(k)\right] \int_{k_0}^{k} k^2 F(k) dk \qquad (2.2.2)$$

where $\epsilon(k)$ is the energy (per unit time, per unit mass) delivered to the fluid at wavenumber k, ν is the molecular viscosity, and $\nu_t(k)$ is the turbulent viscosity.

According to this equation, part of the turbulent kinetic energy fed into the system at wavenumber k, is converted into heat energy by the molecular viscosity, ν, and the remaining part is redistributed to eddies at wavenumbers larger than k, via non-linear interactions in the fluid.

In his seminal work on turbulent flows, Heisenberg proposed that the non-linear transfer be considered as a process consisting of two parts [55]: (1) the extraction of energy from the interval (k_0, k), and (2) the redistribution of this extracted energy into the interval (k, ∞). Heisenberg viewed process (2) as being the result of a turbulent viscosity, $\nu_t(k)$, exerted by the (k, ∞) eddies on the (k_0, k) eddies.

The non-linear transfer of energy inherent in equation (2.2.2) is thus described by the product of two terms which correspond to processes (1) and (2) respectively, ie.

$$\left(\int_{k_0}^{k} k^2 F(k) dk \right) \nu_t(k) \qquad (2.2.3)$$

where $\nu_t(k)$ must be of the form

$$\nu_t(k) = \int_{k}^{\infty} \Psi(k) dk \qquad (2.2.4)$$

This suggests that the turbulent viscosity exerted on eddies in the interval (k_0, k) must be built up from contributions made by all eddies with wavenumbers larger than k.

It is important to note that the turbulent viscosity transfers energy from low to high wave numbers in a non-dissipative manner. Unlike the molecular viscosity, it does not convert any of the turbulent kinetic energy present in the system into heat energy. This can be seen by integrating equation (2.2.2) from k_0 to ∞ to get,

$$\epsilon = \nu \int_{k_0}^{\infty} k^2 F(k) dk \qquad (2.2.5)$$

Note that the turbulent viscosity is no longer present in this equation. This is consistent with the notion that the non-linear interactions describe a non-dissipative process.

Equation (2.2.5) states that, *globally*, energy in the fluid is conserved, ie. the energy fed into the fluctuating velocity field by the source instability is completely dissipated by the action of viscous forces at a molecular level.

2.2.2   The closure problem

To solve for $F(k)$ in equation (2.2.1), one needs first to specify the function $\Psi(k)$. Therefore, the closure problem described in section 1.1 is, in k-space, equivalent to providing an analytic expression for $\Psi(k)$. Accordingly, this is known as a "closure" relation.

It will be shown in section 2.5, that in general,

$$\Psi = \Psi(k, F(k), n_c(k)) \qquad (2.2.6)$$

where $n_c(k)$ (which has the dimensions of inverse time) is the eddy correlation rate. The determination of $n_c(k)$ is the chief difficulty in the development of a closure model for the turbulent energy spectrum. The reason for this lies in the fact that the non-linear transfer, which is characterized by $n_c(k)$, does not appear to arise from a universal law which is valid throughout the entire k-space.

2.3   The Kolmogorov-Heisenberg (KH) model

2.3.1   The KH closure

Early attempts at providing a closure relation for $\Psi(k)$ were restricted to a specific region in k-space known as the *inertial subrange*. Eddies propogating in this wavenumber region have been formed as a result of several cascades of energy, and are sufficiently detached from the k_0 part of the spectrum that their evolution is independent of the precise details of the source instability. The only remnant of the stirring mechanism still felt by these eddies is the *total* input energy, ϵ. They are also sufficiently distant from the Kolmogorov microscale that the molecular viscosity does not affect their dynamics. Eddies in the inertial subrange are therefore freely evolving due to their distance (in

k-space) from both the input and dissipation length scales.

The only dimensionally correct expression for $n_c(k)$ that conforms to the above restrictions on the eddy type is,

$$n_c(k) \approx k^{3/2} F^{1/2}. \tag{2.3.1}$$

This is sufficient to fix the form of $\Psi(k)$ in the inertial region as,

$$\Psi(k) = \gamma F^{1/2}(k) k^{-3/2} \tag{2.3.2}$$

where γ is a coupling constant which can either be determined experimentally, or theoretically via the normalization of the mean-square vorticity (as discussed in section 4.2.1).

Under these assumptions, equation (2.2.1) can be solved for $F(k)$ to get [3],

$$
\begin{aligned}
F(k) &= \left(\frac{8\epsilon}{9\gamma} \right)^{2/3} k^{-5/3} \\
\\
&= (\mathrm{Ko})\, \epsilon^{2/3} k^{-5/3}
\end{aligned}
\tag{2.3.3}
$$

and

$$\nu_t(k) = \xi \nu_l l_l \tag{2.3.4}$$

where $\xi = \gamma \sqrt{3}/4\pi$, and Ko in equation (2.3.3) is the Kolmogorov number.

An important feature of the above expression for the energy spectrum is that its slope is independent of details of the turbulence generating mechanism. This lack of dependence on $n_s(k)$ gives the closure a universal characteristic. It is important to note, however, that this universality is a direct consequence of the assumptions inherent in its construction.

This *phenomenological* model of fluid turbulence is due to the work of both Kolmogorov [66] and Heisenberg [55] (KH), who developed the theory independently of each other in the mid to late 1940's. It is considered to be one of the great milestones in the history of turbulence modelling due to its experimental verification in laboratory studies of high wavenumber turbulence [3; 63; 137].

2.3.2 Limitations of the KH model

For several decades since its inception, the KH model was the only predictive theory of turbulence available to researchers. For lack of a better alternative, ad hoc adaptations of this model have often been used in the analysis of astrophysical systems [85; 135]. However, the assumptions used to construct the KH model limit its range of validity to a region of the k-space which is not populated by the large-scale eddies of interest in astrophysics. In particular, the absence of the source details from the KH closure make it unsuitable for studies of LST where source driven effects, such as buoyancy, are of key importance.

However, the experimental verification of the KH spectrum for the inertial subrange [50; 98] suggests that any proposed closure relation for $n_c(k)$ must be capable of reproducing the form of (2.3.1) in that region of the cascade.

2.4 Generalized form of the energy equation

In order to develop a turbulence model capable of treating the entire spectrum, one needs to establish an expression for $\epsilon(k)$ that incorporates the effects of different instabilities on the energetics of the flow. Such an expression has been derived by Ledoux, Schwarzschild and Spiegel [85], who have shown that,

$$\epsilon(k) = \int_{k_0}^{k} \left[n_s(k) + \nu k^2 \right] F(k) dk \qquad (2.4.1)$$

where $n_s(k)$ is the growth rate of the source instability. The dependence of

this equation on $n_s(k)$ allows it to encapsulate the net effect of buoyancy, viscosity, conduction, rotation, and magnetic fields on the energetics of the flow. Unlike the eddy correlation rate, $n_s(k)$ can be resolved using the linear theory [29][112], and is a direct measure of the energy per unit time which must be supplied to the system in order to sustain the turbulence.

Combining equations (2.2.2), (2.2.4) and (2.4.1) results in the following equation for $F(k)$,[2]

$$\int_{k_0}^{k} n_s(k)F(k)dk = \int_{k}^{\infty} \Psi(k)dk \int_{k_0}^{k} k^2 F(k)dk \qquad (2.4.2)$$

The left hand side of equation (2.4.2) represents the net energy delivered to the fluid, in the interval (k_0, k), by the instability described by $n_s(k)$.[3]

The right hand side of (2.4.2) represents the net loss of source energy from the interval (k_0, k) and its redeposition into the the interval (k, ∞) as a result of the non-linear interactions in the fluid.

2.5   The turbulent viscosity

The physical interpretion of the non-linear transfer as a two part process, implies that

$$\nu_t(k) = \int_{k}^{\infty} \Psi(k)dk = \int_{k}^{\infty} \frac{\nu_t^{(k)}}{k} \, dk \qquad (2.5.1)$$

where $\nu_t^{(k)}$ is the turbulent viscosity imposed on the unit interval $(k-dk, k+dk)$.

---

[2]A complete derivation of this equation starting from the NSE can be found in [85].
[3]Note that the molecular viscosity in equation (2.4.1) has been absorbed into $n_s(k)$ in equation (2.4.2).

Providing a closure relation for $\Psi(k)$ is therefore equivalent to determining the form of $\nu_t^{(k)}$, which is a priori unknown.

Studies of large scale turbulence in astrophysical systems require knowledge of $\nu_t^{(k)}$ in the interval (k_0, ∞) ie. throughout the entire k-space. This makes the determination of $\nu_t^{(k)}$ a formidable task compared to, say, studies of the inertial subrange, where one only needs knowledge of $\nu_t^{(k)}$ in a limited region of the spectrum. However, a guiding principle here lies in the fact that regardless of the exact form of $\nu_t(k)$, we must have from equation (2.4.2) that,

$$\nu_t(k_0) = \frac{n_s(k_0)}{k_0^2} \qquad (2.5.2)$$

Equation (2.5.1) may therefore be written as

$$\nu_t(k) = \nu_t(k_0) - \int_{k_0}^{k} \frac{\nu_t^{(k)}}{k} \, dk \qquad (2.5.3)$$

This simplifies matters considerably since we now only require the form of $\nu_t^{(k)}$ in the interval (k_0, k). Furthermore, equation (2.5.3) provides one with a unique means of checking the proposed form of $\nu_t^{(k)}$, since equation (2.5.2) must be satisfied by any expression for $\nu_t^{(k)}$ that is to be valid in the range (k, ∞).

Turning now to the issue of constructing an expression for $\nu_t^{(k)}$, we begin by noting that in general,

$$\nu_t^{(k)} = d_k u_k = \left[n_c^{-1}(k) \right] u_k^2 = \frac{kF(k)}{n_c(k)} \qquad (2.5.4)$$

where d_k is the mean free path of the eddy at k, and $n_c^{-1}(k)$ is the eddy correlation time.

Substituting equation (2.5.4) into equation (2.5.1) gives us the general expression for $\nu_t(k)$ in terms of $n_c(k)$,

$$\nu_t(k) = \int_k^\infty \frac{F(k)}{n_c(k)} dk \qquad (2.5.5)$$

Thus, as alluded to in section 2.2.2, in order to calculate ν_t and hence $F(k)$ via equation (2.4.2), we need to specify the rate $n_c(k)$, which governs the non-linear energy transfer in the cascade.

As an illustrative example, consider the inertial subrange. Since eddies in this region evolve freely, we have that $d_k = l_k \approx k^{-1}$. Equation (2.5.4) then gives $n_c(k) \approx (k^3 F)^{1/2}$. Solving for $F(k)$ with this choice of $n_c(k)$ results in the famous KH spectrum, $F_{KH} \approx k^{-5/3}$.

The form of $n_c(k)$ used to calculate the energy spectrum in the KH model, will of course need to be adjusted for studies of LST. In the $k \approx k_0$ region, where the nature of the source dominates the evolution of the large eddies, the eddy correlation rate must in some way depend on the growth rate of the source instability. It will be shown that closure relations which can account for this dependency, allow for the natural inclusion of compressiblity effects such as buoyancy within the model. The adaptation of these types of models to astrophysical systems is one of the primary concerns of this thesis, and will be elaborated in subsequent chapters.

2.5.1   The balance of rates

Differentiating equation (2.4.2) and substituting equation (2.5.5) into the result gives,

$$n_s(k) + y(k)n_c^{-1}(k) = k^2 \nu_t(k) \qquad (2.5.6)$$

where

$$y(k) \equiv \int_{k_0}^{k} F(k)k^2 dk \qquad (2.5.7)$$

is the mean-square vorticity.

Equation (2.5.6) has the following physical interpretation: *The rate at which energy is delivered to k (via the source and cascade) must be equal to the rate at which it is transferred out of k (via non-linear interactions in the fluid).*

This equation therefore describes the balance between the rates which govern the dynamics of the turbulent energy cascade. It is one of the basic equations of the closure models discussed in this thesis.

Taking the derivative of equation (2.5.6) and substituting the definitions of $\nu_t(k)$ and $y(k)$ given by equations (2.5.5) and (2.5.7) respectively, results in the following differential equation for the mean-square vorticity,

$$\left(\frac{2}{n_c(k)k^2} \right) \frac{d}{dk}\left[y(k) \right] + y(k)\frac{d}{dk}\left[\frac{1}{n_c(k)k^2} \right] + \frac{d}{dk}\left[\frac{n_s(k)}{k^2} \right] = 0 \qquad (2.5.8)$$

Since $y(k)$ and $F(k)$ are directly related to each other (via equation (2.5.7)), the above equation, in principle, provides one with a means of determining the structure of the turbulent energy spectrum *if* one has knowledge of both the eddy correlation and source growth rates. However, since $n_s(k)$ is assumed to be a known or calculable quantity, the only ingredient required for the solution of $F(k)$ from equation (2.5.8), is $n_c(k)$. This equation therefore serves to emphasise the fact that the calculation of the turbulent energy spectrum depends entirely on the determination of the eddy correlation rate, which defines the closure problem in k-space.

Assuming that a satisfactory closure model for $n_c(k)$ has been developed, one of course still needs to specify boundary conditions for equation (2.5.8) in order to solve for $y(k)$, and hence $F(k)$. It will be shown in sections 4.3.1 and 4.4 that the specification of these boundary conditions requires knowledge of the structure of the eddy anisotropies expected to occur in the LST sector of the spectrum.

2.6   Calculating the turbulent energy spectrum

With the aid of equation (2.5.5), equation (2.4.2) can now be rewritten in terms of $n_c(k)$ as,

$$\int_{k_0}^{k} n_s(k)F(k)dk = \int_{k}^{\infty} \frac{F(k)}{n_c(k)}dk \int_{k_0}^{k} k^2 F(k)dk \qquad (2.6.1)$$

This is the general form of the non-linear energy equation from which the turbulence spectrum can be calculated. It is important to note that, as with equation (2.5.8), $F(k)$ is completely determined by the above equation once the rates $n_s(k)$ and $n_c(k)$ have been specified.

To summarize, the general procedure for calculating the turbulent energy spectrum, $F(k)$, is as follows:

1. **Construct a closure model for turbulent viscosity, $\nu_t(k)$.**

   This amounts to prescribing a method for relating the eddy correlation rate, $n_c(k)$, to other known or calculable quantities in the problem of interest. The phenomenology used to construct the closure model determines the regions of the energy spectrum which it is capable of treating,

and hence its applicability to different fluid systems.

For example, in the CG model turbulence [17], it is assumed that $n_c^{-1}(k) \propto n_s^{-1}(k)$. The form of this closure makes the CG model ideal for studies of large-scale turbulence but unsuitable for studies of the dissipation region where the eddy dynamics are insensitive to the precise details of the source instability.

2. **Determine the form of $n_s(k)$ relevant to the problem of interest.**

Different physical processes will in general give rise to different types of fluid instabilities. This makes the form of $n_s(k)$ problem dependent. Once these processes have been identified for a given problem, $n_s(k)$ can, for example, be approximated via a linear mode analysis of the fluid equations.

According to this analysis, the general form of the dispersion equation satisfied by $n_s(k)$ for a rotating fluid undergoing thermal convection in the presence of a magnetic field is [29],

$$\left[\left(n_s + \chi k^2\right)\left(n_s + \nu k^2\right)\left(n_s + \eta k^2\right) + \frac{\mu}{4\pi\rho}\left(n_s + \chi k^2\right)(\mathbf{k}\cdot\mathbf{B})^2 - \right.$$

$$\left. g\alpha\beta\left(\frac{k_x^2 + k_y^2}{k^2}\right)\left(n_s + \eta k^2\right)\right]\left[\left(n_s + \eta k^2\right)\left(n_s + \nu k^2\right) + \frac{\mu}{4\pi\rho}(\mathbf{k}\cdot\mathbf{B})^2\right]$$

$$+4\left(n_s + \chi k^2\right)\left(n_s + \eta k^2\right)\frac{(\mathbf{k}\cdot\Omega)^2}{k^2} = 0$$

$$(2.6.2)$$

where χ is the thermometric conductivity, η is the magnetic diffusivity, μ is the permeability, ρ is the average density of the fluid, $\mathbf{k} = (k_x, k_y, k_z)$ is the wavevector, $\mathbf{B}$ is the magnetic field, g is the acceleration due to gravity, α is the coefficient of thermal expansion, β is the superadiabatic temperature gradient, and Ω is the angular velocity. Note that the argument of $n_s(k)$ has been dropped in the above formula for the sake of readability.

For the specific case in which $\Omega = 0$ and $\mathbf{B} = 0$, equation (2.6.2) reduces to,

$$n_s(k) = -\frac{1}{2}\left(\nu + \chi\right)k^2 + \frac{1}{2}\left[\left(\nu - \chi\right)^2 k^4 + 4g\alpha\beta\frac{\left(k_x^2 + k_y^2\right)}{k^2}\right]^{1/2} \quad (2.6.3)$$

In this case, $n_s(k)$ corresponds entirely to the buoyancy forces present in the fluid. We will return to this equation when calculating the convective heat flux in section 3.5.

It is worth noting here that several closure dependent alternatives to the linear theory exist [18; 21]. For example, Canuto and Battaglia [18] have proposed an *inversion method*, for the CG model of turbulence [17], which allows one to extract information about the structure of $n_s(k)$ from observational data. Their method has been successfully applied to the description of source instabilities in molecular clouds [18], and can be generalized to any fluid system where one can obtain velocity data of a specific type. The details of this method are discussed in section 3.6.

Furthermore, CGC [21] have also developed a *self-consistent method* for determining the form of $n_s(k)$ from within the turbulence model itself.

This approach, which forms the basis of the CGM model of stellar tur-
bulence [23], will be discussed in detail in section 4.4.

3. **Substitute the chosen expression for $n_s(k)$ and the closure rela-
tion constructed for $n_c(k)$ into either equation** (2.6.1) **or equation**
(2.5.8)**, and solve for** $F(k)$**.**

This will result in an expression for $F(k)$ from which several quantities
of interest can be calculated. For example, assuming that one has been
able to construct a closure model capable of probing the LST region of
the spectrum, bulk properties of the flow can be directly calculated from
the model once the form of the spectrum has been obtained using the
above procedure.

An example of a bulk quantity that is important in stellar astrophysics,
and to which we will devote several chapters, is the convective heat flux,
H_c. The general expression for H_c is given by,

$$H_c = c_p \rho \beta \chi \Phi \tag{2.6.4}$$

where where c_p is the specific heat at constant pressure, and

$$\Phi = \frac{1}{g\alpha\beta\chi} \int_{k_0}^{\infty} \left[n_s(k) + \nu k^2 \right] F(k) dk \tag{2.6.5}$$

$$= \frac{\epsilon}{g\alpha\beta\chi} \tag{2.6.6}$$

Since the above expression for Φ depends only on $F(k)$ and $n_s(k)$ for its
determination (g, α, β, χ, and ν are assumed to be known), H_c can be

directly calculated via the aforementioned procedure. A detailed derivation of equations (2.6.5) and (2.6.6) is provided in Appendix A.

Prior to the publication of the CGM model of convective turbulence [23], calculations of Φ, and hence of H_c, in stellar interiors, relied almost exclusively on (i) the linear theory for the specification of $n_s(k)$, via equation (2.6.3), and implicitly on (ii) the MLT for the specification of $F(k)$. These two aspects of the canonical convective flux calculation in stellar astrophysics will be discussed in detail in this thesis. In particular, I will provide a thorough theoretical analysis of the shortcomings of the current treatment of convection in stellar interiors within the context of these two points. I will also discuss more advanced models of turbulence than the MLT which are capable of circumventing these shortcomings.

Chapter 3

The CG Model

3.1 Introduction

In studies of astrophysical turbulence, one is typically interested in the calcula-
tion of the bulk properties of the flow [37; 40]. Examples of such properties are:
the energy fluxes associated with different heat transfer mechanisms, velocity
and temperature fluctuations, and the turbulent transport coefficients. These
quantities are determined by the large-scale eddies which carry a significant
portion of the energy present in the system. Since these eddies depend on the
nature of the instability generating the turbulence, one can no longer use the
KH model to study their dynamics [16; 120]. This is due the fact that the KH
model is limited to the inertial region of the spectrum, and is insensitive to
the details of the stirring mechanism.

In order to develop a model of turbulence which is capable of describing the
LST region of the spectrum, one has to abandon the KH restrictions on the
eddy type and construct a new closure relation for the nonlinear interactions.
This closure must allow for the probing of the $k \approx k_0$ part of the k-space if it
is to be applicable to fluids where LST is important. Such a model has been
proposed by Canuto and Goldman (CG) [17].

The nature of the closure used in the CG model of turbulence allows for $F(k)$ to be calculated analytically in terms of $n_s(k)$. Since, in the CG model, $F = F(n_s(k), k)$ (as opposed to $F = F(k)$ in the KH model), all of the physical effects associated with the source instability are naturally incorporated, making it ideal for studies of the large-scale properties of astrophysical fluids.

The CG model is phenomenological in nature, however, it is important to note that Hartke et al. [53; 54] were also able to derive the CG closure from Kraichnan's DIA [67; 68; 69]. The fact that the CG closure can be recovered from a fully predictive, theoretical model such as the DIA, serves as a strong justification of the phenomenology used in its the construction.

The CG model compares well with data from both laboratory and astrophysical studies of turbulent convection [17; 87; 95; 100]. A brief summary of these tests and applications is contained in section 3.7. It will also be shown in section 3.5 that the model predicts the exact form of the MLT expression for the convective heat flux. This is remarkable in and of itself since, prior to the publication of the CG model, no record existed in the literature of a derivation of the MLT flux equation from a general model of fluid turbulence.

Lastly, Canuto and Battaglia [18] have also provided a "retrieval method" whereby the form of $n_s(k)$ can be recovered from within the CG model, if one has knowledge of the structure of $F(k)$ at the start of a given problem. This is of particular importance in several types of astrophysical problems, such as molecular clouds, where one is often uncertain of the precise nature of the instability responsible for the turbulence. An outline of the method is discussed in section 3.6.

3.2   The KH model and LST

We begin by motivating the need for a replacement of the KH model with an improved model of turbulence that is tailored to LST and hence by implication to astrophysical fluid turbulence. To illustrate the shortcomings of the KH model in studies of LST, we consider here two examples of astrophysical systems where large-scale turbulence is known to occur. These are, molecular clouds, and stellar interiors. It will be shown that, when applied to the description of molecular clouds, the KH model leads to unphysical results, and, when applied to stellar convection, the KH model produces results that are in severe disagreement with the canonical MLT.

3.2.1   Turbulence in molecular clouds

Molecular clouds (MCs) are known to be regions of pronounced star formation that exhibit a high degree of fluid turbulence during a significant portion of their evolution [75; 88]. The determination of the distribution of turbulent kinetic in these systems has been the principal concern of several research endeavours [35; 36; 56]. However, early studies of the turbulence in these systems depended primarily on SST models which were in some way based on the KH model. As a result, these early models failed to capture several important large-scale effects, such as the cloud core formation. In this section I show how the KH model, when applied to the description of MCs, fails to predict correctly the form of the source instabilities that dictate their evolution.

Studies of the velocity-size relationship of MCs [59; 86] have in the past predicted that,

$$u(l_c) = u_0 \sqrt{l_c/l_0} \tag{3.2.1}$$

where $u_0 \approx 1 \text{km.s}^{-1}$ and $l_0 \approx 1 \text{pc}$. The use of equation (3.2.1) in equation

(2.2.1) results in the following power law for the turbulent energy spectrum,

$$F(k) \approx k^{-2} \tag{3.2.2}$$

Substituting equations (3.2.2) and (2.3.4) into equation (2.4.2) results in the following prediction of the form of $n_s(k)$ for this type of system,

$$n_s(q) \approx q^{-1/2}(1 - q/3) \tag{3.2.3}$$

where $q = k/k_0$.

However, detailed studies of the instabilities believed to be present in molecular clouds have shown that the growth rate represented by equation (3.2.3) is inapplicable to MCs [34]. As an example of one such instability, consider the Rayleigh-Taylor (R-T) instability. A detailed calculation of the growth rate associated with this type of instability can be found in [29]. Figure (3.1) shows the behaviour of the growth rates associated with the R-T instability for two cases of interest in studies of molecular clouds ($\mathbf{B} \parallel \mathbf{g}$ and $\mathbf{B} = 0$), versus the behaviour of the instability predicted by the KH model. This figure illustrates the fact that the growth rate predicted by KH model is a crude and inaccurate representation of the actual turbulence generating mechanisms expected to be present in molecular clouds.

3.2.2 Turbulence in stellar interiors

In this section, we will consider the differences in the energy fluxes predicted by the MLT and KH models when applied to stellar convection.

Stellar interiors are known to be highly turbulent [128]. The Sun, for example, is predicted to have a Reynolds number (Re) of approximately 10^{13} at the base of the solar convection zone [103], which is several orders of magnitude higher
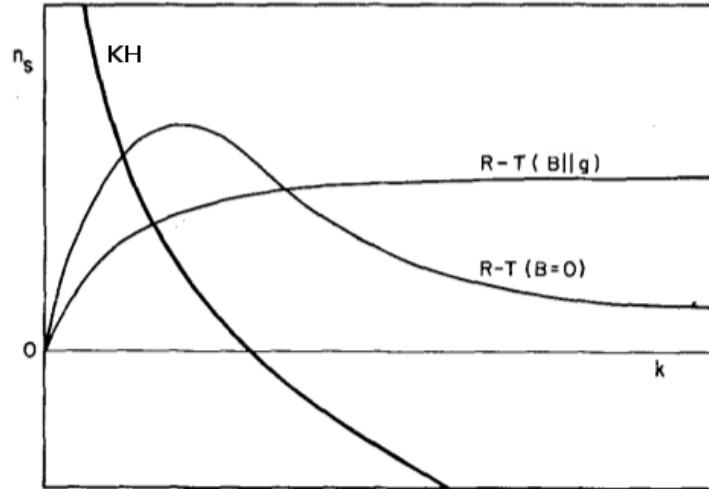
Figure 3.1: Plot of $n_s(k)$ vs k. The curve labelled KH corresponds to the growth rate predicted by the Kolmogorov-Heisenberg model. The curves labelled R-T ($\mathbf{B} = 0$) and R-T ($\mathbf{B} \parallel \mathbf{g}$) correspond to the growth rate of a Rayleigh-Taylor type instability in the absence of a magnetic field, and where the magnetic field is parallel to the direction of the gravitational acceleration, respectively. (Adapted from [16]).

than the most turbulent terrestrial fluids [136].

In the absence of a detailed model of stellar turbulence, studies of energy transport in the stellar interior have typically relied on the MLT for the calculation of the convective heat flux. According to this theory, the (dimensionless) convective heat flux, Φ, depends on the efficiency of convection, S, in the following way [132] ,

$$\Phi_{MLT} = AS^2, \qquad (S \ll 1) \qquad\qquad (3.2.4)$$

$$\Phi_{MLT} = B\sqrt{S}, \qquad (S \gg 1) \qquad\qquad (3.2.5)$$

where A and B are constants which can be determined via a calibration of the MLT in a stellar model. The efficiency parameter, S, is defined by,

$$S = g\alpha\beta l^4 \chi^{-2} = \sigma R \qquad\qquad (3.2.6)$$

where l is the mixing length, $\sigma = \nu/\chi$ is the Prandtl number, and $R = g\alpha\beta l^4 (\nu\chi)^{-1}$ is the Rayleigh number.

Using a solar model, Gough and Weiss [47] performed a calibration of the mixing length, and calculated that $A = 1.84 \times 10^{-4}$ and $B = 0.214$. (See Table I of [47])

Predictions of the convective flux using the KH model have also been performed by Ledoux, Schwarzschild and Spiegel [85] and Yamaguchi [135].

For $S \ll 1$, it was shown in [85] that,

$$\Phi_{LSS} = \left(\frac{\delta^8}{16\pi^{10}\gamma^2}\right) S^2, \qquad (S \ll 1) \qquad (3.2.7)$$

While for $S \gg 1$, it was shown in [135] that,

$$\Phi_Y = \left(\frac{3.2\delta^2}{4\gamma^2}\right) S^{1/2}, \qquad (S \gg 1) \qquad (3.2.8)$$

where $\delta = 8\pi^4/R$, and the coupling constant, γ, was determined from experimental data to be approximately equal to $\frac{1}{3}$.

If one now matches the KH results in equations (3.2.7) and (3.2.8) to the MLT in the *low efficiency regime* (ie. $S \ll 1$), it is found that $\delta = 1.53$. Equation (3.2.7) then implies that $A \approx 17$, which is an order of magnitude *higher* than the result in [47].

Similarly, if one matches the KH results to the MLT in the *high efficiency regime* (ie. $S \gg 1$), it is found that $\delta = 0.17$. Equation (3.2.8) then implies that $B \approx 4 \times 10^{-11}$, which is several orders of magnitude *lower* than the result

in [47].

A comparison of the aforementioned flux calculations is shown in figures 3.2
below, where it can be seen that the KH model is incapable of consistently
reproducing the form of the MLT flux throughout the entire efficiency space.
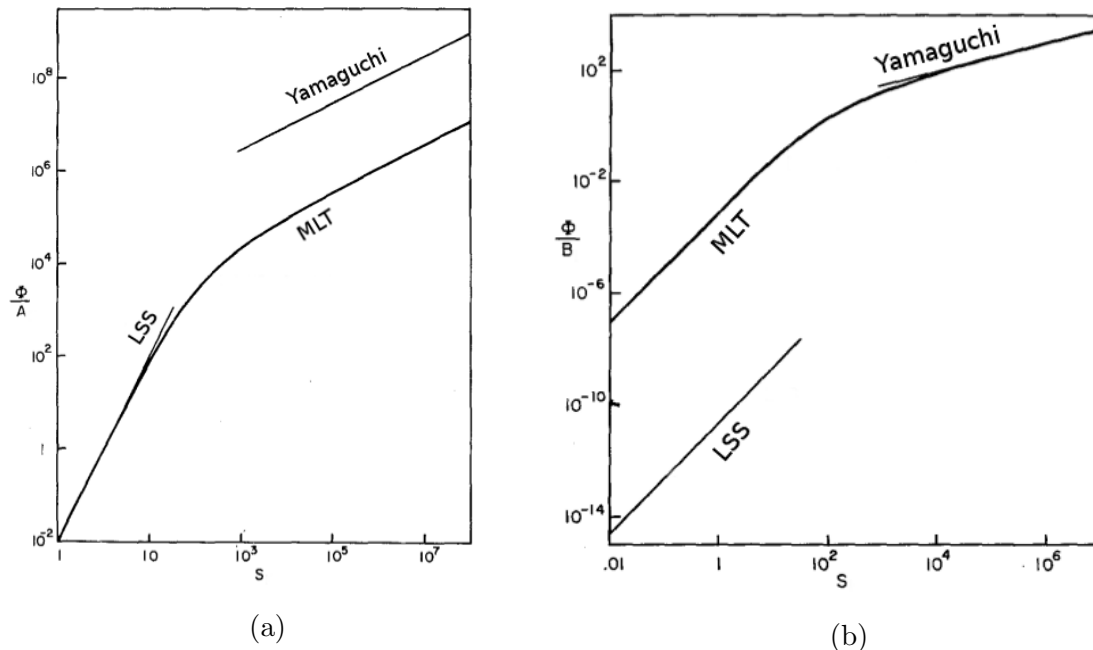
Figure 3.2: Plots of (Φ/A) vs S for (a) $S \ll 1$ and (b) $S \gg 1$. The curves la-
belled MLT correspond to the results of [47], while the curves labelled LSS and
Yamaguchi, correspond to the results of [85] and [135] respectively. (Adapted
from [16]).

One evidently has the option of either accepting the MLT results as being the
correct representation of convective flux and discarding the KH model as being
inapplicable to stellar interiors, or calling into question the MLT itself. This
is a difficult assessment to make since, owing to its purely phenomenological
derivation, the MLT does not provide any physical insight into the nature of
the turbulence spectrum which it implicitly assumes. Furthermore, since the
KH model is not directly reducible to the MLT, a comparison of the two con-

vection treatments is a non-trivial task. One would first need to deduce the form of $F(k)$ within the MLT treatment of convection and then compare the result against equation (2.3.3) for the KH spectrum, in the $\sigma \ll 1$ limit, in order to determine which of the two models provides a more accurate representation of the convective heat flux in the stellar interior. This analysis will be performed in section 5.2. For now, we will simply note that the fact that the canonical MLT flux equation cannot be directly recovered from the KH model is likely to be the reason why the KH model has been almost entirely ignored in studies of stellar structure and evolution.

In summary, the KH model has been shown to be unsuitable for description of large-scale turbulence in molecular clouds, and incapable of reproducing the predictions of MLT in stellar interiors. The inadequacy of the KH model when applied to astrophysical systems and LST in general, can be understood in terms of the fact that it was originally designed to treat only a limited region of the turbulence spectrum. In the absence of an extended inertial subrange, which is typical only of low viscosity systems, the KH model is bound to make predictions regarding the properties of the bulk flow which are in disagreement with observational data. One therefore needs a new model of turbulence which is capable of adequately describing the LST region of the spectrum. The CG model is one such example.

3.3   The CG closure

To provide a closure for $\nu_t(k)$, CG began by noting that the formation of eddies in the $k \approx k_0$ region of the spectrum is due almost entirely to the growth of the source instability. Once formed, nonlinear interactions in the fluid result in the fragmentation of these eddies into progressively smaller ones. Since these interactions are non-dissipative in nature, the generation of eddies in this region of the k-space should be at an optimum when the timescale

describing the input energy from the source matches the timescale describing their fragmentation ie. when $n_s(k_0) \propto n_c(k_0)$. CG applied this hypothesis to the entire LST region to derive the following expression for $n_c(k)$,

$$n_c(k) = \frac{n_s(k)}{n_s(k_0)} n_c(k_0) \equiv \gamma^{-1} n_s(k) \tag{3.3.1}$$

It is important to note that this expression is, by virtue of its construction, only valid in the LST portion of the energy spectrum where $n_s(k)$ is by definition positive. We therefore expect the form of $F(k)$ predicted by this model to also only be valid in the LST region. This will be shown in section 3.4.

With the aid of equations (2.5.4) and (3.3.1), equation (2.5.3) can now be rewritten as,

$$\nu_t(k) = \nu_t(k_0) - \gamma \int_{k_0}^{k} \frac{F(k)}{n_s(k)} dk \tag{3.3.2}$$

where $\nu_t(k_0) = n(k_0)/k_0^2$

In order to complete the expression for $\nu_t(k)$, one needs to specify the coupling constant γ. It can be seen from equations (2.5.4) and (3.3.1), that this is equivalent to providing an expression for $d(k_0)$. CG noted that, for LST, a natural first choice is to equate $d(k_0)$ to the longitudinal integral length scale, L_p, where [102]

$$L_p = \frac{3\pi}{4} \left(\int_{k_0}^{\infty} F(k) k^{-1} dk \right) \left(\int_{k_0}^{\infty} F(k) dk \right)^{-1} \tag{3.3.3}$$

This results in the following expression for γ,

$$-2n_s(k_0) = \frac{\gamma k_0}{L_p^2} \frac{d}{dk} \left(\frac{n_s(k)}{k^2} \right) \Bigg|_{k=k_0} \tag{3.3.4}$$

which is sufficient to complete the closure and allow us to rewrite (2.6.1) as

$$\int_{k_0}^{k} n_s(k)F(k)dk = \left(\nu_t(k_0) - \gamma \int_{k_0}^{k} \frac{F(k)}{n_s(k)}dk \right) \int_{k_0}^{k} k^2 F(k)dk \qquad (3.3.5)$$

Equation (3.3.5) is the closed form of equation (2.6.1) in the CG model of turbulence. It has the remarkable feature that it's solution depends only on the growth rate of the instability generating the turbulence. Since this growth rate is assumed to be a known quantity, one can use equation (3.3.5) to generate an analytic solution for the turbulent energy spectrum, $F(k)$.

3.4 Solving for F(k)

This section demonstrates the procedure for calculating the analytical solution of $F(k)$ using the above closure model for $n_c(k)$.

Start by differentiating equation (3.3.5) and dividing by $k^2 F(k)$ to get,

$$\frac{n_s(k)}{k^2} = \nu_t(k_0) - \gamma \int_{k_0}^{k} \left(\frac{d}{dk} y(k) \right) \left(\frac{1}{k^2 n_s(k)} \right) dk - \gamma \frac{y(k)}{k^2 n_s(k)} \qquad (3.4.1)$$

An integration of the above equation results in,

$$\frac{n_s(k)}{k^2} = \nu_t(k_0) - 2\gamma \frac{y(k)}{k^2 n_s(k)} + \gamma \int_{k_0}^{k} y(k) \frac{d}{dk} \left(\frac{1}{k^2 n_s(k)} \right) dk \qquad (3.4.2)$$

In order to simplify the ensuing algebra we define the following functions,

$$I(k) \equiv \gamma \int_{k_0}^{k} y(k) \frac{d}{dk} \left(\frac{1}{k^2 n_s(k)} \right) dk \qquad (3.4.3)$$

$$a(k) \equiv k^2 n_s(k) \tag{3.4.4}$$

$$b(k) \equiv \nu_t(k_0) - \frac{n_s(k)}{k^2} \tag{3.4.5}$$

Equation (3.4.2) can now be rewritten as,

$$\frac{d}{dk} I(k) + \frac{1}{2a(k)} \left[I(k) + b(k) \right] \frac{d}{dk} a(k) = 0 \tag{3.4.6}$$

Solving the above equation for $I(k)$ then gives,

$$I(k) = -\sqrt{\frac{1}{a(k)}} \int_{k_0}^{k} \left(\frac{d}{dk} \sqrt{a(k)} \right) b(k) \, dk \tag{3.4.7}$$

Taking the derivative of the above equation yields,

$$2\gamma y(k) = -\sqrt{n_s(k)k^2} \int_{k_0}^{k} \sqrt{n_s(k)k^2} \frac{d}{dk} \left(\frac{n_s(k)}{k^2} \right) dk \tag{3.4.8}$$

Finally, substituting the definition of $y(k)$ into equation (3.4.8) results in the following expression for $F(k)$ in terms of $n_s(k)$,

$$F(k) = -\frac{1}{2\gamma k^2} \frac{d}{dk} \left[k\sqrt{n_s(k)} \int_{k_0}^{k} k\sqrt{n_s(k)} \frac{d}{dk} \left(\frac{n_s(k)}{k^2} \right) dk \right] \tag{3.4.9}$$

Equation (3.4.9) is the CG expression for $F(k)$. It completely determines the energy spectrum in the LST region once the form of $n_s(k)$ has been specified. The dependence of this equation on the growth rate of the source instability ensures that the resulting expression for $F(k)$ embodies in a natural way the detailed nature of the turbulence generating mechanism. This makes the form

of $F(k)$ predicted by equation (3.4.9) well suited to the determination of bulk properties of the flow, such as the convective heat flux.

3.5 The convective heat flux

In this section, I apply the CG model to the calculation of the convective heat flux in a thermally driven fluid which exists in the absence of rotation and magnetic fields. It will be shown that the CG model predicts an expression for Φ which is identical in form to that of the MLT.

The linear growth rate relevant to this problem is given by equation (2.6.3). However, an equivalent form of this equation which simplifies considerably the algebra associated with the calculation of $F(k)$ via equation (3.4.9) is,

$$n_s(k) = n_0 \left[\left(1 + (1 - \mu) \Lambda^2 q^4 \right)^{1/2} - \Lambda q^2 \right] \tag{3.5.1}$$

where $n_0 = [g\alpha\beta\tau(k)]^{1/2}$, $\tau(k) = x(k)[1 + x(k)]^{-1}$, $\mu = 4\sigma(1 + \sigma)^{-2}$, $q = k/k_0$, and

$$\Lambda = \pi^2 \left(\frac{[1 + x(k)]^3}{x(k)\mu R} \right)^{1/2} \tag{3.5.2}$$

Note that, $x(k)$, is an eddy anisotropy factor which is defined such that, $x(k) = k_h/k_v$, where k_h and k_v are the horizontal and vertical wavenumbers, respectively. Throughout this thesis we will follow the suggestion of Spiegel [120] and adopt the following expression for $x(k)$,

$$x(k) = \left(\frac{kD}{\pi} \right)^2 - 1 \tag{3.5.3}$$

where D is the depth of the convective layer. This equation fixes the value of

k_0 at,

$$k_0 = \frac{\pi}{D} \left[x(k_0) + 1 \right]^{1/2} \tag{3.5.4}$$

Note that for $\mu \ll 1$ (ie. $\sigma \ll 1$ or $\sigma \gg 1$) equation (3.5.1) implies that $n_s(k) > 0, \forall k$. This choice of μ allows equation (3.4.9) to be solved analytically for $F(k)$. It is also physically consistent with the notion that the closure model inherent in equation (3.4.9) is only applicable to the LST region of the k-space, where $n_s(k)$ is by definition positive. With these considerations in mind, one can now solve equation (3.4.9) for $F(k)$ to get,

$$F(k) = F_0 \left[\frac{h^{3/2}}{q^2(1 + \Lambda^2 q^4)^{1/2}} \right] \tag{3.5.5}$$

where $F_0 = C_\Lambda n_0^2(k_0^3 \gamma)^{-1}$, $C_\Lambda = \left[(1 + \Lambda^2)^{1/2} + \Lambda \right]^{1/2}$ and $h = n_s(k)/n_0$.

Equation (2.6.5) can in turn be solved for the dimensionless convective flux, Φ, using the above determination of $F(k)$. The result is,

$$\Phi = \frac{\tau(k)}{2\gamma\Lambda} \left[C_\Lambda - \sqrt{2\Lambda} \right]^2 \tag{3.5.6}$$

To determine the coupling constant, γ, in the above equation we substitute equations (3.5.1) and (3.5.5) into equation (3.3.4) to get,

$$\gamma = \left(\frac{3\pi l}{4} \right)^2 \left(1 - \frac{\Lambda}{C_\Lambda^2} \right) \tag{3.5.7}$$

where

$$l = \frac{1 - 3\Lambda C_\Lambda \left(\tanh^{-1} C_\Lambda^{-1} - \tan^{-1} C_\Lambda^{-1} \right)}{2 \left(1 - p \tan^{-1} p^{-1} \right)} \tag{3.5.8}$$

and $p = C_\Lambda \sqrt{2\Lambda}$.

Finally, equation (3.5.6) can be rewritten in notation which is common in the field of stellar astrophysics as,

$$\Phi = aS^{-1} \left[(1 + bS)^{1/2} - 1 \right]^3 \tag{3.5.9}$$

where $a = \pi^4 [8\gamma]^{-1} [1 + x(k)]^2 A^2(\Lambda)$, $\quad A(\Lambda) = \left[1 + (2\Lambda)^{1/2} C_\Lambda^{-1} \right]^{-1}$, and $b = 4\pi^{-4} [1 + x(k)]^{-3} x(k)$.

The above equation is identical in structure to the expression for Φ predicted by the MLT model of stellar convection [132]. The associated expressions for the convective velocity are also identical. However in the case of the MLT, equation (3.5.9) was not explicitly derived from a model of fluid turbulence, but rather from a purely phenomenological consideration of the motion of a fluid element subjected to a perturbation of its initial state. It is also important to note that while the CG model recovers the MLT result for the convective heat flux in the LST region, it is certainly a much richer model than the MLT due to its direct dependence on $n_s(k)$, and its ability to determine the distribution of turbulent kinetic energy across the eddy spectrum. The CG model therefore represents a significant improvement over the MLT which neither provides information regarding the structure of the spectral function $F(k)$, nor allows for the direct inclusion of new physics via the presence of a turbulent growth rate.

3.5.1 Other important bulk quantities

In an analogy with the calculation of the convective heat flux, several other important bulk quantities can also be determined once the form of $F(k)$ is

known. For example, the equations for the mean-square temperature and velocity fluctuations ($\langle \theta^2 \rangle$ and $\langle u^2 \rangle$, respectively) can also be solved analytically for $\mu \ll 1$ to get,

$$\frac{\langle u^2 \rangle}{(g\alpha\beta\chi^2)^{1/2}} = \frac{\sqrt{S}}{\pi^2\gamma \left[1 + x(k)\right]^2} \left[1 - p\tan^{-1}\frac{1}{p}\right] \qquad (3.5.10)$$

and

$$\frac{\langle \theta^2 \rangle}{\beta^2 d^2} = \frac{p\,\tau(k)}{2\pi^2\gamma} \left[\frac{2}{p} - \frac{3 + 4\sigma}{(1+\sigma)^2}\tan^{-1}\frac{1}{p} + \frac{p}{(\sigma + 1)^2 (1+p)^2}\right] \qquad (3.5.11)$$

The ability to calculate these quantities for a given system provides one with deep insight into the physical effects of the turbulence on the structure and evolution of the bulk flow. They enable the probing of the phenomenology used to construct the closure model itself, and the validity of the use of the linear approximation to $n_s(k)$ for the flow in question. Furthermore, knowledge of $\langle u^2 \rangle$ and $\langle \theta^2 \rangle$ also allow for the determination of the coupling between the turbulent temperature and velocity fields. These considerations will be discussed in detail in section 4.4.

3.6   The retrieval method

In many types of astrophysical systems the precise nature of the source instability described by $n_s(k)$ is either unknown or difficult to predict. One often has data about the *effects* of the instability but not of the instability itself. For example, in studies of molecular clouds, one typically has data about the velocity-size relationship of the cloud, but not of the instability responsible for the relationship.

Since knowledge of $n_s(k)$ is vital to any theoretical study of fluid turbulence, one needs a method of inferring its form from the data at hand. Such a method

was provided, in the context of the CG model, by Canuto and Battaglia (CB) [18].

The method depends on one being able to extract information about $F(k)$ from the observed data. If this is possible, a simple inversion of the energy equation can be used to determine the structure of $n_s(k)$.

3.6.1   An illustrative example:

I illustrate here the general procedure for determining $n_s(k)$ from molecular cloud data. It is however important to note that this method can also be applied to other fluid systems where one has knowledge of the form of $F(k)$.

In the case of molecular clouds, knowing the velocity-size relation is equivalent to knowing $F(k)$, due to equation (2.2.1). Suppose that a $u(l)$ vs l relationship has been derived from the data. One can then determine an equation for $n_s(k)$ via the elimination of $F(k)$ from equations (3.4.9) and (2.2.1). The equation obtained for $n_s(k)$ will have the following structure

$$n_s(k) \quad = \quad n_0 f(q) \tag{3.6.1}$$

where, $n_0 = \gamma^{1/2} k_0 u_0$, $u(k) = u_0 U(q)$. Note that the form of $U(q)$ is assumed to be known from the data. In this notation the expression for $f(q)$ is,

$$\left[g(q) f^2(q) - q^2 g^2(q) \right] \left[\frac{d}{dq} f(q) \right] - A(q) f^3(q) + B(q) f(q) = 0 \tag{3.6.2}$$

where

$$g(q) = -\frac{2}{q^2} \int_1^q q^2 U(q) \left[\frac{d}{dq} U(q) \right] dq \tag{3.6.3}$$

$$A(q) = \frac{2g(q)}{q} \tag{3.6.4}$$
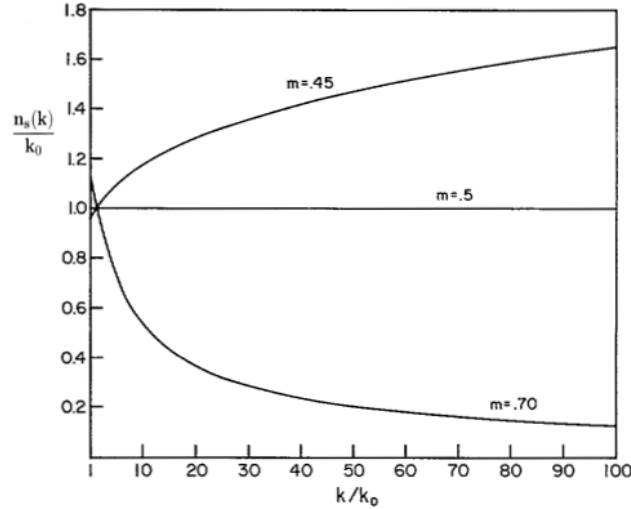
Figure 3.1: Plot of $n_s(k)/k_0$ vs k/k_0. The growth rate in this figure was determined via the retrieval method discussed in [18]. The $u(l)$ vs l relationship used to determine $n_s(k)$ was inferred from molecular cloud data. The three curves correspond to the three choices of m, as denoted in the graph. (Adapted from [18]).

and

$$B(q) = 2q\,g(q)\left[\frac{d}{dq}\Big(q\,g(q)\Big)\right] \tag{3.6.5}$$

The above procedure was applied by CB [18] to MCs where $U(q)$ is expected to be of the form,

$$U(q) = q^{-m}, \qquad 0.45 \le m \le 0.70 \tag{3.6.6}$$

Equation (3.6.2) was solved numerically using the above expression for $U(q)$, and the behaviour of $n_s(k)$ was subsequently determined via equation (3.6.1). The growth rate obtained via this method is shown in figure (3.1) for three values of m corresponding to $m = 0.45$, $m = 0.5$ and $m = 0.70$ respectively.

Since this method determines $n_s(k)$ directly from the data, one may consider the above procedure as a diagnostic tool for determining the nature of the turbulence generating mechanism in a fluid.

It is also worth noting here that CGC [21] have developed a self-consistent method for determining the growth rate in situations where one does *not* have the type of data from which the general form of $F(k)$ can be deduced. This method is the basis of the CGM model of convective turbulence and will be explained in detail in section 4.4.

3.7   Tests and applications of the CG Model

The CG model has been successfully applied to several problems in both astrophysical and terrestrial fluid turbulence (which differ by more than 12 orders of magnitude in σ). Some of the key studies that have been performed using the model are listed below:

Laboratory turbulence

The CG model was shown to predict the general form of the Nusselt vs Rayleigh number relationship [61], which is of significant importance in both theoretical and experimental studies of turbulent heat transfer. The experimentally deduced form of this relationship for water [45], has been the subject of much debate in the literature, and was explained for the first time from a model of turbulence by CG [17].

Rotation and magnetic fields

The CG model can also be extended to include the effects of both rotation and magnetic fields via equation (2.6.2) [19]. Such an extension has been used to study the propogation of electromagnetic signals through a turbulent fluid, with the theoretical predictions of the model in good agreement with experimental data [20].

Fluid instabilities

The model has also been tested extensively in studies of Richtmyer-Meshkov and Rayleigh-Taylor type instabilities [44; 95], where it was was shown to correctly predict the velocity-size relations of eddies associated with these types of flows [95].

The early solar nebula

The CG model has been utilized in studies of accretion disks and the early solar nebula [14; 15]. Studies of this type have in the past relied on a free parameter, known as the Shakura-Sunyaev parameter, for the calculation of $\nu_t(k)$ [111][118]. The CG model was used to develop a parameter free expression for the turbulent viscosity in these systems, resulting in temperature predictions of the early solar nebula that compared favourably with geophysical data [14].

3.8 Concluding Remarks

Despite its direct applicability to the type of large-scale turbulence encountered in stars, and its ability to predict the MLT expression for the convective heat flux, the original iteration of the CG model received little attention in the stellar astrophysics community. Shortly after its publication, Canuto, Goldman and Chasnov [21] began working on an extension of the model that was capable of treating the *entire* energy spectrum. It was not until this next iteration of the model was adapted by Canuto and Mazzitelli [22] and later Canuto, Goldman and Mazzitelli [23] for use in stellar evolution simulations, that the model appears to be recognized in the stellar modelling community as being a viable alternative to the MLT. In the next chapter I will discuss this extension of the CG model and develop the theory required for its application to calculations of stellar structure and evolution.

Chapter 4

The CGC Model

4.1 Introduction

The form of the closure relation used in the CG model of turbulence restricts its applicability to the extreme LST portion of the spectrum only. While this closure has been shown to be successful in studies of large-scale turbulence, its physical justification is not self evident.

Furthermore, in the absence of observational data from which the form of $n_s(k)$ can be extracted (via the retrieval method), the CG model depends entirely on the linear mode analysis for the determination of $n_s(k)$. This limits the predictive power of the model since the linear theory provides only an *approximation* to the actual form of $n_s(k)$.

Shortly after the development of the CG model, Canuto, Goldman and Chasnov (CGC) [21] constructed a new model of turbulence which addressed the above flaws in the CG model. The closure for $n_c(k)$ that was used to achieve this was inferred directly from the turbulence equations themselves, and therefore has a stronger phenomenological justification than that of the CG model.

Unlike the CG closure, this new expression for $n_c(k)$ is valid across the *entire*

spectrum making it applicable to studies of both large-scale and small-scale turbulence. Furthermore it will be shown in section (4.2) that the CGC closure reduces that of the CG model in the LST sector of the spectrum, ensuring that the deductions regarding the bulk properties of the flow presented in Chapter 3, are still valid here. The model also compares well with the DIA and has been shown to be in better agreement with laboratory studies of high Rayleigh number convection than the CG model [21].

Perhaps the most interesting feature of the CGC model is its ability to determine *self-consistently* the form of $n_s(k)$ when the coupling of the turbulent velocity and temperature fields are taken into account in a given problem. This allows one to abandon the use of the linear theory in favour of a more accurate representation of the physical mechanism which drives the turbulence. This approach is discussed in detail in section (4.4).

We will focus in this chapter only on the components of the CGC model that are relevant to the description of stellar turbulence.[1]

4.2   The CGC closure

The closure relation used in the CGC model of turbulence differs from that of the CG model in that it attempts to treat the *entire* energy spectrum. Unlike the CG model, which is limited to the LST region, the CGC model is also capable of describing the high wavenumber part of the spectrum where the effects of dissipation due to molecular viscosity are important.

The deduction of the CGC closure is based on the following physical argument: since non-linear interactions are described in terms of an eddy viscosity $\nu_t(k)$, and since the rate which governs the transfer of energy associated with these

---

[1] A discussion of the model's application to laboratory turbulence can be found in [21].

interactions is $n_c(k)$, these quantities should in some way be proportional to each other. This is evident from the definition of $n_c(k)$ in equations (2.5.4) and (2.5.5). The CGC model therefore assumes that,

$$\gamma n_c(k) = k^2 \nu_t(k) \tag{4.2.1}$$

where, as in sections (2.3) and (3.3), γ is a coupling constant which can either be fitted using experiment data, or determined via the normalization of $y(k)$ in the inertial subrange to ensure that the model reproduces the form of the KH spectrum in that region. The normalization of $y(k)$ in the inertial region will be discussed in section (4.2.1).

Substituting equation (4.2.1) into equation (2.5.6) results in the following closed equation for the rates,

$$n_s(k) + y(k)n_c^{-1}(k) = \gamma n_c(k) \tag{4.2.2}$$

from which it can be shown that,

$$2\gamma n_c(k) = n_s(k) + \sqrt{n_s^2(k) + 4\gamma y(k)} \tag{4.2.3}$$

The above equation defines the eddy correlation rate in terms of both the source instability *and* the mean-square vorticity. Unlike its counterpart, equation (3.3.1), in the CG model, this equation is positive-definite in $n_s(k)$ throughout the *entire* k-space. This allows one to calculate the form of the energy spectrum even in the $k \gg k_0$ region where $n_s(k)$ eventually becomes negative.

In the inertial subrange, where $n_s(k) \ll y(k)$, equation (4.2.3) predicts that

$$n_c(k) \approx \sqrt{y(k)} \tag{4.2.4}$$

Substituting the above result into equation (2.4.1), with $\epsilon(k) = \epsilon$, shows that the CGC model predicts a spectrum with the following shape,

$$F(k) \approx k^{-5/3} \tag{4.2.5}$$

This result, which will be derived in detail in section (4.2.1), is identical in structure to that of the KH spectrum in equation (2.3.3), implying that the CGC model exhibits the correct behaviour in the inertial subrange.

Furthermore, in the $k \approx k_0$ part of the spectrum (where $y(k)$ tends to to zero), the CGC closure reduces to

$$n_c(k) = \gamma^{-1} n_s(k) \tag{4.2.6}$$

This implies that the CG model can be recovered from within the CGC model in the LST sector, ensuring that the results and discussions presented in Chapter 3 regarding CG model's application to large-scale turbulence are still relevant here.

4.2.1 The normalization of $y(k)$

Any model of fluid turbulence which claims to treat the entire k-space must be able to reproduce the experimentally verified shape of the turbulent energy spectrum in the inertial subrange. In the CGC model, this achieved via the normalization of $y(k)$.

In order to perform this normalization, one needs to first determine the structure of the CGC spectrum in the region of the cascade where $\epsilon(k)$ saturates to ϵ (i.e., in the inertial subrange where $\epsilon(k)$ approaches its asymptotic value). Once this has been achieved, a comparison of the predicted spectrum with the observed spectrum can be used to fix the value of γ. This procedure is outlined below:

We begin by noting that, in the inertial subrange, equation (2.5.6) implies that,

$$|n_s(k)|n_c(k) \ll y(k) \tag{4.2.7}$$

Using this relation equation (4.2.3) becomes,

$$n_c(k) = \left(\frac{y(k)}{\gamma}\right)^{1/2} \tag{4.2.8}$$

We also have from equations (2.4.1) and (2.4.2) that,

$$\epsilon = \nu_t(k)y(k) \tag{4.2.9}$$

This shows that the eddy dynamics are unaffected by molecular viscosity in the KH region.

Substituting equations (4.2.1) and (4.2.8) into equation (4.2.9) gives the form of $y(k)$ and $n_c(k)$ in the inertial region of the spectrum as,

$$y(k) = \left(\frac{\epsilon^2 k^4}{\gamma}\right)^{1/3} \tag{4.2.10}$$

and

$$n_c(k) = \left(\frac{\epsilon k^2}{\gamma^2}\right)^{1/3} \tag{4.2.11}$$

Finally, the substitution of equation (2.5.7) into equation (4.2.10) gives the following expression for the energy spectral function,

$$F(k) = \frac{4}{3}\gamma^{-1/3}\epsilon^{2/3}k^{-5/3} \tag{4.2.12}$$

Comparing equation (4.2.12) with the expression for the KH spectrum given in section (2.3), shows that the CGC model indeed exhibits the correct behaviour in the inertial subrange.

Equations (4.2.12) and (2.3.3) then together determine the value of γ,

$$\gamma = \left(\frac{2}{3K_o}\right)^3 \qquad (4.2.13)$$

4.3   Solving for F(k)

Since the CGC closure specifies $n_c(k)$ in terms of both $n_s(k)$ *and* $y(k)$, the turbulent energy spectrum can be calculated directly from equation (2.5.8), which is stated here again for the sake of completeness,

$$\left(\frac{2}{n_c(k)k^2}\right)\frac{d}{dk}\left[y(k)\right] + y(k)\frac{d}{dk}\left[\frac{1}{n_c(k)k^2}\right] + \frac{d}{dk}\left[\frac{n_s(k)}{k^2}\right] = 0 \qquad (4.3.1)$$

However, due to the form of the CGC closure, the above equation does not allow solutions for $y(k)$, and hence also $F(k)$ (via equation (2.5.7)), to be obtained analytically for a given $n_s(k)$. Therefore, unlike its analogue in the CG model (equation (3.3.5)), this equation must in general be solved numerically for $F(k)$ once the closure for $n_c(k)$ has been substituted. Fortunately, given appropriate boundary conditions, the structure of the above equation permits a simple numerical treatment of its solution space.

4.3.1   Boundary conditions

The boundary conditions for equation (2.5.8) are determined by first fixing the value of k_0 via equation (3.5.4), and then using the fact that by definition $F(k_0) = 0$ and $y(k_0) = 0$ in the LST region. Equations (4.2.1) and (4.2.2) then

imply that,

$$n_s(k_0) = \gamma n_c(k_0) = k_0^2 \nu_t(k_0) \tag{4.3.2}$$

and

$$\frac{d}{dk}\left(\frac{n_s(k)}{k^2}\right)\bigg|_{k=k_0} = \frac{d}{dk}\left(\frac{\gamma n_c(k)}{k^2}\right)\bigg|_{k=k_0} = 0 \tag{4.3.3}$$

since from equations (2.5.7) and (2.5.8) we have that,

$$F(k_0) = \frac{1}{k_0^2}\left[\frac{d}{dk} y(k_0)\right] \tag{4.3.4}$$

$$= -\frac{n_s(k_0)}{2\gamma} \frac{d}{dk}\left(\frac{n_s(k)}{k^2}\right)\bigg|_{k=k_0} \tag{4.3.5}$$

It should be noted that in order to complete the specification of the above boundary conditions, one needs to determine the *exact* value of k_0. This amounts to prescribing the form the eddy anisotropies, represented by $\tau(k)$, since equation (3.5.4) fixes k_0 in terms of $x(k_0)$. However, since the anisotropic nature of the flow is governed by the physical mechanisms which generate the turbulent state, one expects $\tau(k)$ (and hence $x(k)$) to be directly determined by the structure of $n_s(k)$. Thus, in order to specify the value of k_0, an equation for $n_s(k)$ must first be provided. This can evidently be achieved using the linear analysis, as was done in Chapter 3 in the context of the CG model. However, since we plan to forgo the use of the linear theory in favour of a more accurate representation of the source instability, we will leave the treatment of the flow anisotropies to section (4.4) where it will be shown that a *self-consistent* determination of $n_s(k)$ leads to $k_0 = \sqrt{3/2}\ \pi D^{-1}$.

4.3.2 The procedure for determining $F(k)$

To summarize, the general procedure for calculating the turbulent energy spectrum within the CGC model is as follows:

(i) Decide on a method for determining the form of $n_s(k)$ and substitute the resulting expression into equation (4.2.3). This will generate an equation for the eddy correlation rate, $n_c(k)$.

(ii) Next, use the expression for $n_c(k)$ in equation (2.5.8) to determine the mean-square vorticity, $y(k)$.

(iii) Finally, using the above expression for $y(k)$, calculate the turbulent energy spectrum, $F(k)$, via equation (2.5.7) with boundary conditions specified by equations (4.3.2) and (4.3.3).

4.4 Self consistent treatment of $F(k)$ and $G(k)$

We have thus far limited our discussion of fluid turbulence to methods for determining the distribution of turbulent kinetic energy across the cascade. We have shown how the analysis of the spectral function, $F(k)$, can be used to extract information about the bulk properties of the flow and, via equation (2.2.1), related this function to the turbulent velocity field described by u. However, in several problems of interest in both astrophysical and laboratory turbulence, one needs a method of extending the analysis presented thus far to a description of the fluctuating *temperature* field. Such a method has been developed by CGC within the context of their turbulence model.

This aspect of the CGC model hinges on a simultaneous, self-consistent treatment of the spectral equations for the turbulent velocity and temperature fields. This self-consistent approach to the turbulence spectra, allows one to forgo the use of the linear analysis in favour of a more robust description of the

instability growth rates. For example, this method for determining $n_s(k)$ overcomes one of the major shortcomings of the linear analysis when applied to the case of turbulent convection, that is, the inability of the linear theory to predict correctly the behaviour of $n_s(k)$ in the dissipation region of a viscous fluid.

More precisely, the form of $n_s(k)$ predicted by the linear theory for a fluid undergoing turbulent thermal convection, has the following behaviour in the dissipation region [85],

$$n_s(k) \rightarrow -\nu k^2, \qquad \sigma < 1 \qquad\qquad (4.4.1)$$

$$n_s(k) \rightarrow -\chi k^2, \qquad \sigma > 1 \qquad\qquad (4.4.2)$$

Equation (4.4.1) is physically consistent with the fact that the molecular viscosity extracts energy from the eddy interactions at large wavenumbers. Thus, for an inviscid system, the linear theory predicts a source function which exhibits the correct behaviour in the dissipation region. However, in the $\sigma > 1$ regime, the behaviour predicted by equation (4.4.2) is clearly unphysical since it suggests that the damping of the velocity fluctuations is as a result of the thermometric conductivity. In models of turbulence designed for LST (such as the CGC model), this physical inconsistency is mitigated by the fact that, in the dissipation region, the overall contribution of $F(k)$ to the bulk properties of the flow is negligible. However for a theory of turbulence which aims to treat the entire k-space, this flaw in the description of $n_s(k)$ cannot be overlooked.

The spectral equations

Let $G(k)$ and $H(k)$ be the spectra of the mean-square temperature fluctuations ($\langle \theta^2 \rangle$) and mean convective heat flux ($\langle u_z \theta \rangle$) respectively. For steady state turbulence in a thermally driven system, the equations satisfied by these spectra are [135],

$$\nu k^2 F(k) - g\alpha H(k) \;=\; \frac{1}{2}\int_{k_0}^{\infty} Q(k,k')dk' \qquad (4.4.3)$$

$$\chi k^2 G(k) - \beta H(k) \;=\; \frac{1}{2}\int_{k_0}^{\infty} U(k,k')dk' \qquad (4.4.4)$$

In analogy with equation (2.5.6), the above equations describe the balance of rates in turbulent fluid undergoing thermal convection. For example, in equation (4.4.3), $g\alpha H(k)$ may be identified as the source instability responsible for the generation and maintenance of the convective turbulence. The energy fed into the fluid by this source is transferred to higher wavenumbers via the nonlinear interactions represented by $Q(k,k')$, and dissipated by the action of molecular viscosity described by $\nu k^2 F(k)$. Equation (4.4.4) for the temperature field can be interpreted in a similar way.

We also note here that in order to perform a complete theoretical analysis of the convective turbulence in the above system, a third equation describing the coupling between the turbulent velocity and temperature fields is needed, namely [135],

$$-\beta \tau(k)F(k) - g\alpha\tau(k)G(k) + (\nu + \chi)k^2 H(k) = \int_{k_0}^{\infty} Y(k,k')dk' \qquad (4.4.5)$$

As has been previously discussed, the nonlinear terms on the right hand side of the above equations represent the *rates* of transfer of some quantity per unit interval in k-space. In equation (4.4.3) this quantity corresponds to u^2, while in equation (4.4.4), the quantity is θ^2. In the case of equation (4.4.5), the quantity associated with the nonlinear transfer does not have a trivial physical interpretation. However, since the transfer term in this equation corresponds to the coupled fields, it must in some way be related to the *sum* of the transfers

associated with equations (4.4.3) and (4.4.4), which implies that its associated quantity is comprised of a combination of u and θ.

In order to simplify the algebra associated with the discussion of these nonlinear terms, we define two rates $N_s(k)$ and $N_s^*(k)$ such that,

$$N_s(k) = -\frac{1}{2F(k)} \int_{k_0}^{\infty} Q(k, k')dk' \qquad (4.4.6)$$

and

$$N_s^*(k) = -\frac{1}{2G(k)} \int_{k_0}^{\infty} U(k, k')dk' \qquad (4.4.7)$$

We then assume, based on the previous discussion, that the nonlinear term in equation (4.4.5) can be approximated as,

$$\int_{k_0}^{\infty} Y(k, k')dk' = -\Big[N_s(k) + N_s^*(k)\Big]H(k) \qquad (4.4.8)$$

which is equivalent to assuming that u and θ are in phase, i.e., that

$$H(k) \propto \Big[F(k)G(k)\Big]^{1/2} \qquad (4.4.9)$$

This assumption is physically consistent with the notion that in a system undergoing turbulent convection, $G(k)$ behaves as an active scalar which drives u.

The equivalence of equations (4.4.8) and (4.4.9) can easily be shown by substituting equation (4.4.8) into equation (4.4.5) and eliminating the rates using equations (4.4.6) and (4.4.7) to get,

$$-\beta\tau(k)F(k) - g\alpha\tau(k)G(k) + \Big[\nu + \chi\Big]k^2 H(k) =$$

$$\left[\nu k^2 F(k) - g\alpha H(k)\right]\frac{H(k)}{F(k)} + \left[\chi k^2 G(k) - \beta H(k)\right]\frac{H(k)}{G(k)} \qquad (4.4.10)$$

From which it follows that,

$$H(k) = \left[\tau(k)F(k)G(k)\right]^{1/2} \qquad (4.4.11)$$

Expressing F(k) in terms of G(k):

Substituting equations (4.4.6) and (4.4.7) into equations (4.4.3) and (4.4.4) and simplifying allows us to express $F(k)$ in terms of $G(k)$ as follows,

$$\left[N_s(k) + \nu k^2\right]F(k) = \frac{g\alpha}{\beta}\left[N_s^*(k) + \chi k^2\right]G(k) \qquad (4.4.12)$$

Expressing $N_s(k)$ in terms of $N_s^*(k)$:

Substituting equations (4.4.6) - (4.4.8) into equations (4.4.3) - (4.4.5) allows us to express $N_s(k)$ in terms of $N_s^*(k)$ as follows,

$$\left[N_s(k) + \nu k^2\right]\left[N_s^*(k) + \chi k^2\right] = g\alpha\beta\tau(k) \qquad (4.4.13)$$

The energy and temperature equations:

Integrating equations (4.4.6) and (4.4.7) from $k_0 - k$ and using analogues of the closure in equation (4.2.1) i.e.,

$$\int_{k_0}^{k} Q(k,k')dk' = -\nu_t(k)y(k) \tag{4.4.14}$$

and

$$\int_{k_0}^{k} U(k,k')dk' = -\chi_t(k)w(k) \tag{4.4.15}$$

results in the following equations for $F(k)$ and $G(k)$,

$$\int_{k_0}^{k} \left[N_s(k) + \nu k^2\right] F(k)dk = \left[\nu + \nu_t(k)\right]y(k) \tag{4.4.16}$$

$$\int_{k_0}^{k} \left[N_s^*(k) + \chi k^2\right] G(k)dk = \left[\chi + \chi_t(k)\right]w(k) \tag{4.4.17}$$

where

$$w(k) \equiv \int_{k_0}^{k} k^2 G(k)dk \tag{4.4.18}$$

is the analogue of $y(k)$ for the turbulent temperature field, and

$$\chi_t(k) \equiv \int_{k}^{\infty} \frac{F(k)}{N_c^*(k)}dk \tag{4.4.19}$$

is the *turbulent conductivity*.

Note that, as previously discussed, equation (4.4.16) can be solved for $F(k)$ via equation (2.5.8) once the form of $N_s(k)$ has been specified. Alternatively, if one wishes to solve for $G(k)$ directly from equation (4.4.17), then the form of $N_s^*(k)$ needs instead to be specified.

Determining $N_s(k)$ and $N_s^*(k)$:

The growth rates can be easily determined if one restricts equations (4.4.16) and (4.4.17) to *self-consistent solutions* only, i.e., solving either of them produces the same functions $F(k)$ and $G(k)$. Since $N_s(k)$ and $N_s^*(k)$ are related via equation (4.4.13), only one of them needs to be established in order for *both* of $F(k)$ and $G(k)$ to be determined via equations (4.4.16) and (4.4.17).

Integrating equation (4.4.12) and substituting equations (4.4.16) and (4.4.17) into the result gives,

$$\left[\chi + \chi_t(k)\right]w(k) = \left(\frac{\beta}{g\alpha}\right)\left[\nu + \nu_t(k)\right]y(k) \qquad (4.4.20)$$

The above equation can be rewritten in terms of a *generalized Prandtl number*, $\Sigma_t(k)$, which differs from σ in that takes into account the renormalization of ν and χ in flows which exhibit turbulent behaviour. This can be seen from the definition of $\Sigma_t(k)$, which is,

$$\Sigma_t(k) \equiv \frac{\nu + \nu_t(k)}{\chi + \chi_t(k)} \qquad (4.4.21)$$

Using equation (4.4.21) in equation (4.4.20) results in,

$$y(k)\Sigma_t(k) = \left(\frac{g\alpha}{\beta}\right)w(k) \qquad (4.4.22)$$

Now, solving for $w(k)$ from equations (4.4.12), (4.4.13) and (4.4.18) gives,

$$w(k) = \frac{1}{(g\alpha)^2}\int_{k_0}^{k}\tau^{-1}(k)\left[N_s(k) + \nu k^2\right]^2 k^2 F(k)dk \qquad (4.4.23)$$

Substituting the above expression for $w(k)$ into equation (4.4.20) and differentiating the result then yields the following expression for $N_s(k)$,

$$N_s(k) = -\nu k^2 + \left[g\alpha\beta\tau(k)\lambda(k) \right]^{1/2} \qquad (4.4.24)$$

where

$$\lambda(k) \equiv \left[\frac{d}{dk}\Big(y(k)\Sigma_t(k) \Big) \right] \left[\frac{d}{dk}\, y(k) \right]^{-1} \qquad (4.4.25)$$

Finally, from equation (4.4.13) the expression for $N_s^*(k)$ is determined to be,

$$N_s^*(k) = -\chi k^2 + \left[g\alpha\beta\tau(k)\lambda^{-1}(k) \right]^{1/2} \qquad (4.4.26)$$

Equations (4.4.24) and (4.4.26) are the self-consistently determined growth rates for the case of convective turbulence within the CGC model. Unlike the linear growth rate for this type turbulence (given by equation (2.6.3)), these growth rates exhibit the correct limiting behaviour in the dissipation region for *any* value of σ. In particular,

$$\lim_{k\to\infty} N_s(k) = -\nu k^2, \quad \forall \sigma \qquad (4.4.27)$$

This fact alone makes the CGC model a significant improvement over linear theory in studies of convective growth rates in the $\sigma > 1$ regime.

In order to complete the specification of these self-consistent growth rates, one needs only determine the function $\Sigma_t(k)$, which appears via $\lambda(k)$, in both of equations (4.4.24) and (4.4.26).

Calculating $\Sigma_t(k)$:

Determining $\Sigma_t(k)$ is equivalent to determining the form of $\nu_t(k)$ and $\chi_t(k)$. This can be achieved as follows:

Start by taking the derivative of equation (4.4.16) to get,

$$N_s(k) + \frac{y(k)}{N_c(k)} = k^2 \nu_t(k) \qquad (4.4.28)$$

which is equivalent to

$$N_s(k) + \frac{y(k)}{N_c(k)} = \gamma N_c(k) \qquad (4.4.29)$$

where the closure for $N_c(k)$ is given by,

$$k^2 \nu_t(k) = \gamma N_c(k) \qquad (4.4.30)$$

A similar approach can be taken for the temperature field to get, from equation (4.4.17),

$$N_s^*(k) + \chi k^2 + \left[\frac{w(k)}{N_c^*(k)}\right]\left[\frac{F(k)}{G(k)}\right] = \xi N_c^*(k) \qquad (4.4.31)$$

where the closure for $N_c^*(k)$ is written, in analogy with equation (4.4.30), as

$$k^2\left[\chi + \chi_t(k)\right] = \xi N_c^*(k) \qquad (4.4.32)$$

Note that ξ is the analogue of γ for the turbulent temperature field.

It also important to note that the expression for $\chi_t(k)$ derived from substituting equation (4.4.32) into equation (4.4.18), i.e.,

$$\chi_t(k) = \left(\chi^2 + 2\xi \int_k^\infty \frac{F(k)}{k^2} dk\right)^{1/2} - \chi \qquad (4.4.33)$$

is identical to the one derived by Howells [62], who used an independent method, based on the work of Batchelor et. al [4], to study the interaction between the turbulent velocity and temperature fields.

Finally, using the definition of $\nu_t(k)$ in equation (4.4.28) results in,

$$\nu_t(k) = \left(2\gamma \int_{k_0}^{\infty} \frac{F(k)}{k^2} dk \right)^{1/2} \tag{4.4.34}$$

A remarkable aspect of the above equation is that it determines $\nu_t(k)$ entirely in terms of $F(k)$. This result has been confirmed using other phenomenological models of turbulence [96], as well as fully predictive, theoretical models such as the DIA [72].

Equations (4.4.33) and (4.4.34) now complete the determination of $\Sigma_t(k)$, and hence $N_s(k)$ and $N_s^*(k)$, allowing one to calculate the energy and temperature spectral functions $F(k)$ and $G(k)$ via equations (4.4.16) and (4.4.17) respectively.

We also note here that the determination of $\chi_t(k)$ and $\sigma_t(k)$ allows one to study the behaviour of the *wavenumber-dependent* turbulent Prandtl number, $\sigma_t(k)$, where

$$\sigma_t(k) = \frac{\nu_t(k)}{\chi_t(k)} \tag{4.4.35}$$

According to equations (4.4.33) and (4.4.34), $\sigma_t(k)$ has the following asymptotic behaviour,

$$\text{Pe} \gg 1: \qquad \sigma_t(k) \;\; \rightarrow \;\; \sigma_t \equiv \sqrt{\gamma/\xi} \tag{4.4.36}$$

$$\text{Pe} \ll 1 : \qquad \sigma_t(k) \;\;\rightarrow\;\; 2\sigma_t^2 \chi \nu_t^{-1}(k) \qquad\qquad (4.4.37)$$

where $\text{Pe} = u_z l \chi^{-1}$, is the Péclet number. The limiting behaviour of $\sigma_t(k)$ with Pe is of particular importance in numerical treatments of stellar convection, with the current generation of hydrodynamical simulations unable to treat accurately the $\text{Pe} \gg 1$ regime [42].

For example, sub-photospheric convection in A-stars is associated with a significant amount of convective "overshooting" into the adjacent, stably-stratified region where decelerations due to the buoyancy force are unable to prevent the rapid exchanges of heat energy that occur between convective elements and the ambient fluid. Numerical simulations of the surface convection zone in these types of stars allow for a simple probing of this phenomenon due to it being characterized by small Péclet numbers [39; 42]. On the other hand, the $\text{Pe} \gg 1$ regime is typically associated with a "penetration" of convective elements into the adjacent radiative layer. This forces a near adiabatic temperature gradient to occur in the transition region between the two layers, with very little mixing beyond this transition region. This process is significantly more difficult to treat due to it being characterized by large Péclet numbers [80].

The above discussion suggests that the behaviour of $\sigma_t(k)$ should in some way be related to the efficiency of convection, which depends on the ratio of the radiative and buoyancy time-scales in the fluid. A discussion of these time-scales will be presented in section 5.3.

The determination of $\lambda(k)$

To simplify the calculation of the turbulence spectra, one can rewrite the expression for $\lambda(k)$, given in section 4.4, in a form which is easy to solve once

the basic properties of the flow have been determined for a given problem.

Substituting the definitions of $y(k)$ and $\nu_t(k)$ into the definition of $\lambda(k)$, equation (4.4.25), results in,

$$\lambda(k) = \Sigma_t(k) - \left(\frac{y(k)}{k^2 N_c(k)} \right) \left[\frac{d}{dk} \Sigma_t(k) \right] \left[\frac{d}{dk} \nu_t(k) \right]^{-1} \qquad (4.4.38)$$

Now from equation (4.4.28) we have that,

$$\frac{y(k)}{k^2 N_c(k)} = \left[\nu + \nu_t(k) \right] - \frac{1}{k^2} \left[N_s(k) + \nu k^2 \right] \qquad (4.4.39)$$

This equation can be rewritten in terms of $\lambda(k)$ using the expression for $N_s(k)$ given in equation (4.4.24). The result is,

$$\frac{y(k)}{k^2 N_c(k)} = \left[\nu + \nu_t(k) \right] - \frac{1}{k^2} \left[\lambda(k) g \alpha \beta \tau(k) \right]^{1/2} \qquad (4.4.40)$$

which when substituted into equation (4.4.38), gives the following general expression for $\lambda(k)$,

$$\lambda(k) = \left[\frac{d}{dk} \nu_t(k) \right]^{-1} \left(\Sigma_t^2(k) \left[\frac{d}{dk} \chi_t(k) \right] + \frac{1}{k^2} \left[\frac{d}{dk} \Sigma_t(k) \right] \left[\lambda(k) g \alpha \beta \tau(k) \right]^{1/2} \right)$$

$$(4.4.41)$$

The above equation is quadratic in $\lambda(k)$ and can be easily solved to get,

$$\lambda(k) = \frac{1}{2k^2} \left[\frac{d}{dk} \Sigma_t(k) \right] \left[\frac{d}{dk} \nu_t(k) \right]^{-1} \left[\lambda(k) g \alpha \beta \tau(k) \right]^{1/2} \times$$

$$\left[1 + \left(1 + \Sigma_t^2(k) \left[\frac{4k^4}{g\alpha\beta\tau(k)} \right] \left[\frac{d}{dk} \Sigma_t(k) \right]^{-2} \left[\frac{d}{dk} \chi_t(k) \right] \left[\frac{d}{dk} \nu_t(k) \right] \right)^{1/2} \right]$$

(4.4.42)

where equation (4.4.42) corresponds to the positive solution of equation (4.4.41). The other solution is unphysical. $\Sigma_t(k)$ and $\chi_t(k)$ can now be eliminated from the above equation via the use of equations (4.4.33) and (4.4.34) to get,

$$\lambda(k) = \frac{g\alpha\beta\tau(k)}{4\chi^2 k^4} \left[\frac{B(k)}{A(k)} \right]^2$$

(4.4.43)

where

$$A(k) = \left[1 + \frac{\nu_t^2(k)}{\sigma_t^2 \chi^2} \right]^{3/2}$$

(4.4.44)

and

$$B(k) = 1 - \frac{\nu\nu_t(k)}{\sigma_t^2 \chi^2} + \frac{1}{2} \left[1 - \frac{\nu\nu_t(k)}{\sigma_t^2 \chi^2} \right]^2 + A(k) \frac{4k^4 \nu_t(k) \left[\nu + \nu_t(k) \right]^2}{g\alpha\beta\chi\sigma_t^2 \tau(k)}$$

(4.4.45)

Finally, substituting equation (4.4.43) into equation (4.4.24) allows us to express $N_s(k)$ directly in terms of $\nu_t(k)$ as follows,

$$N_s(k) = -\nu k^2 + \frac{g\alpha\beta\tau(k)}{2k^2 \chi} \left[\frac{B(k)}{A(k)} \right]$$

(4.4.46)

The determination of $x(k_0)$

We return now to the determination of the flow anisotropies required for the complete specification of the boundary conditions for equation (2.5.8) within the CGC model. It should be noted that with the equations for the self consistent growth rates developed, the determination of $\tau(k_0)$ (and hence $x(k_0)$) is a trivial matter since this quantity features explicitly in the expression for

$N_s(k)$. The procedure is as follows:

First substitute equation (4.4.46) into equation (4.3.3) to get,

$$\frac{d}{dk}\left(\frac{\tau(k)}{k^4}\right)\bigg|_{k=k_0} = 0 \qquad (4.4.47)$$

Now, using equation (3.5.3), the exact value of k_0 can be calculated to be,

$$k_0 = \frac{\sqrt{3/2}\,\pi}{D} \qquad (4.4.48)$$

We therefore have that,

$$\tau(q) = 1 - \frac{2}{3q^2} \qquad (4.4.49)$$

from which it follows that,

$$x(k_0) = \frac{1}{2} \qquad (4.4.50)$$

With the values of the values of k_0 and $x(k_0)$ now fixed, the boundary conditions for equation (4.3.1) can be completely specified for a given problem. In particular, we note that in the $\sigma \to 0$ limit, which we will consider in this thesis as being applicable to the highly inviscid stellar interior (see section 5.3.2), equations (4.3.2), (4.3.3) and (4.4.46) fix the value of $n_c(k_0)$ at,

$$\gamma n_c(k_0) = \frac{\chi\sqrt{S}\,\psi_0(S)}{D^2} \qquad (4.4.51)$$

where the function $\psi_0(S)$ is given by,

$$\psi_0(S) = \sqrt{2S_*}\,\tau(k_0)\left[1 + \left[1 + 4S_*^2\sigma_t^{-2}\tau^2(k_0)\right]^{1/2}\right]^{-1/2} \qquad (4.4.52)$$

with,

$$S_* = \frac{S}{\pi^4\left[1 + x(k_0)\right]^2} \qquad (4.4.53)$$

As illustrated above, knowledge of k_0 and $x(k_0)$ has resulted in the determination $n_c(k_0)$ which, by way of equation (4.3.2), also completes the specification of $n_s(k_0)$ and $\nu_t(k_0)$. All of the ingredients required for the solution of $F(k)$ from equation (4.3.1) have therefore been obtained from within a self-consistent framework for the rates, thus freeing the calculated form of $F(k)$ from any physical inconsistencies associated with the linear approximation to $n_s(k)$.

4.5   Concluding Remarks

In summary, the CGC model of turbulence should be considered as being the natural successor to the CG model, which was originally designed to treat only a limited region of the k-space governed by the largest eddies present in the system. Since the CGC model is reducible to the CG model in the LST region of the spectrum, the predictions made by the CG model regarding the nature of the bulk flow are also true of the CGC model. However, unlike its predecessor, the CGC model is capable of determining the form of $F(k)$ throughout the entire k-space, including the inertial and dissipation regions. This remarkable aspect of the new model not only allows for deeper physical insight into the nature of the eddy dynamics in key regions of the flow, but also provides one with a means of estimating the *extent* of the LST, HK and SST sectors of the spectrum for a given problem.

The central difference between these two models of turbulence lies in their treatment of the eddy correlation rate, $n_c(k)$. In the CG model, this rate is assumed to depend entirely on the growth rate of the source instability, whereas in the CGC model $n_c(k)$ is assumed to be determined by the eddy viscosity itself. The form of the CGC closure is therefore obtained by setting $\gamma n_c(k) = k^2 \nu_t(k)$, an idea which is suggested by the turbulence equations themselves.

As a consequence of the structure of its closure, the CGC model allows for the possibility of self-consistently determining the growth rate of the source instability when both the turbulent temperature and velocity fields are accounted for in a given problem. This self-consistent treatment of the source ensures that the expression for its growth rate exhibits the correct limiting behaviour for any value of σ in the dissipation region. The model therefore represents a significant improvement over the linear approximation to $n_s(k)$ which predicts a behaviour for this rate which is unphysical in the $k \gg k_0$ portion of the spectrum. Therefore, in studies of SST in particular, the CGC model with the inclusion of its self-consistent determination of the rates, is likely to lead to a more accurate picture of the dissipation region, and the effects of molecular viscosity on the small scale eddies.

However, it must be noted that while the linear theory predicts an unphysical limit for $n_s(k)$ in the SST sector of the spectrum, this shortcoming is likely to be inconsequential in studies of bulk flow properties which are determined by eddies that reside in the extreme LST region of the k-space. The justification of this statement lies in the fact that the net contribution to $F(k)$ made by the SST eddies is negligible when compared to those belonging to LST sector. This makes the merits of using the self-consistent determination of $n_s(k)$ strongly dependent on the type of turbulence being considered in a given problem. For situations where details of the turbulent temperature field are required, the extra effort needed to determine growth rate via the self-consistent approach is certainly warranted, both due to the fact that the rates are predicted from *within* the model itself, and that the form of the spectral function for the temperature field can be easily deduced. That the latter is true can be seen by simply taking the derivative of equation (4.4.22) to get,

$$G(k) = \left(\frac{\beta}{g\alpha} \right) \lambda(k) F(k) \tag{4.5.1}$$

The self-consistent approach therefore provides one with a natural way of studying the dynamics of the turbulent temperature field from within the framework of the model.

Next, we note that an apparent shortcoming of both the CG and CGC models is that they inherently assume a unidirectional transfer of energy from high low to wavenumbers only. This neglects the effects of non-local interactions in the fluid which can result in a reverse transfer or "backscattering" of energy within the cascade, especially in regions of the k-space where $F(k)$ has not yet attained its maximum value [102]. This results in a smaller value of k_0 and a shallower gradient for $F(k)$ in the $k \approx k_0$ region of the spectrum, and is likely to be the reason for the mismatch between the CGC and DIA spectra [21], which are depicted in figure 4.1.
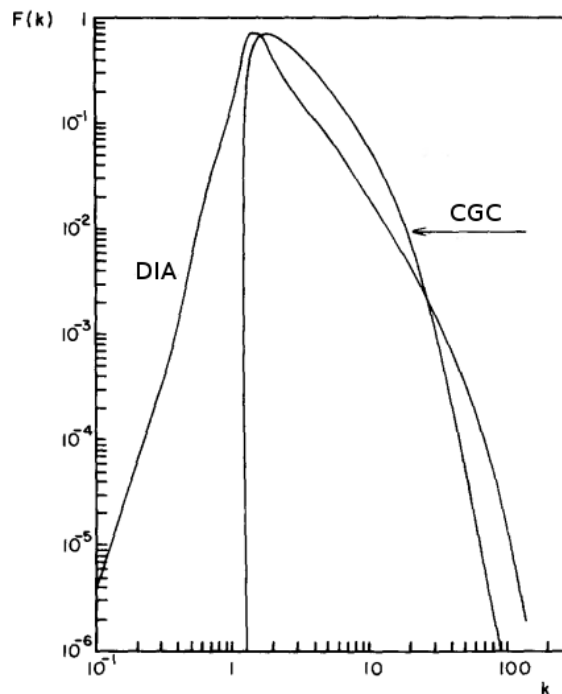
Figure 4.1: Plot of $F(k)$ vs k comparing the CGC and DIA models for the case of convective turbulence for $\sigma = 0.5$ and $S = 10^5$. (Adapted from [21])

The inclusion of this feedback mechanism is not however expected to be of great significance in studies of astrophysical turbulence which focus principally on the determination of bulk quantities, such as the convective heat flux [102]. Moreover, the effects of this process can to an extent be accounted for in a model of turbulent convection via a judicious choice of the eddy correlation rate. It is this extension of $n_c(k)$ that lies at the heart of the CGM model of stellar convection [23], which will be discussed in Chapter 6.

Furthermore, it should be noted that when directly compared with the MLT, the CGC model results in significantly different estimates of the heat flux magnitudes depending on the efficiency of the convective process. A discussion of this comparison is found in Chapter 5, where it is shown that this discrepancy is a direct consequence of the of the inadequacy of the MLT spectrum when applied to the description of high Reynolds number turbulence in inviscid systems.

Chapter 5

Mixing Length Theory

"Little attention is paid to assessing the accuracy of the models,
partly because there is a general feeling that mixing-length theory
is so uncertain that the task would be fruitless, and partly,
perhaps, because of an optimism that the theory will soon be
superseded by something better."
- D. Gough [48]

5.1   Introduction

For nearly sixty years, the treatment of convective heat transport in the stellar interior has relied almost exclusively on the MLT. The model was originally formulated by Prandtl [109], who developed it in the early 1900's in complete analogy with the theory of molecular heat transfer in terrestrial fluids. It was later adapted to the description of stellar convection by Biermann [?] and Bohm-Vitense [8] and has since been extended and modified in so many ways that there now exists several "versions" of the theory.

The theory is littered with seemingly arbitrary parameters which have been the source of some disagreement. A major source of uncertainty in the MLT is

the value to be used for the mixing length itself. Uncertainties like this have given rise to some of the variations of the theory.

In MLT, the convection zone is treated as if it effectively consists of one large, "average" eddy, which carries the entire heat flux across the convecting layer. This has the advantage of replacing the conceptually difficult treatment of a spectrum of eddies of different shapes, sizes, velocities and lifetimes, with one that is simpler to treat and easier to implement in stellar codes. But while this feature of the model simplifies the treatment of convection, it also makes the MLT wholly inadequate for the description of turbulence in stars.

MLT disregards the intrinsically turbulent nature of the convective process. This is due to the fact that the model was originally derived from a purely phenomenological consideration of a fluid element which, when subjected to an instability or perturbation of its initial state, rises under the action of buoyancy forces through a characteristic distance identified with the mixing length. The physics of the model is based entirely on the results of laboratory studies of convection centred around the Boussinesq approximation for buoyancy driven flows [119]. It will be shown in Chapter 7 that, when applied to the description of stellar convection, the MLT violates one of the basic assumptions of the Boussinesq approximation i.e., that the mixing-length should be less than the pressure scale height of the fluid.

While the MLT has served as a useful phenomenological tool for studies of convective heat transport, I will demonstrate in this chapter that the MLT is based on a crude model of turbulence which cannot be expected to generate results that are quantitatively either accurate or reliable. In particular, I will show that the form of the turbulent energy spectrum implicitly assumed by the MLT represents an extreme oversimplification of the true convective processes that occur in the stellar interior.

After deducing the form the MLT spectrum in section 5.2, I compare in section 5.3 its flux equation with other models of turbulence that incorporate more accurate representations of $F(k)$. A key result that emerges from this discussion is that the MLT either underestimates or overestimates the magnitude of the convective heat flux depending on the efficiency of convection in the fluid. This result, which was first suggested by the work of Ledoux, Schwarzschild and Spiegel [85] (and later Yamaguchi [135]), and which was also discussed in Chapter 3 of this thesis has far reaching consequences for our understanding of stars since miscalculation of the convective heat flux may have a significant impact on our ability to match the theoretical predictions of stellar codes with observational data. The discrepancy in the predictions of the MLT and those of more advanced models of convective turbulence, when applied to calculations of stellar structure and evolution, will be illustrated in Chapter 7.

5.2   The MLT energy spectrum

It will be shown in this section that *the MLT approximates the turbulent energy spectrum with a delta function* [22]. Physically, this implies that the flow consists of only a *single* large eddy that carries the entire convective heat flux. The stellar interior however, is characterized by a wide variety of eddy sizes due to its highly inviscid nature, making the single-eddy model a poor approximation. Errors associated with this approximation are typically masked by the uncertainty of the mixing-length itself, and manifest themselves in the lack of universality in its value for stars of a given class.

The basic equation for the heat flux Φ in MLT is,[1]

$$\Phi_{MLT} = \left(\frac{a_0}{2}\right) \Sigma^{-1} \left[\left(1 + \Sigma\right)^{1/2} - 1\right)\right]^3 \qquad (5.2.1)$$

where $a_0 = 9/4$, and Σ is defined to be,

$$\Sigma = \frac{2}{81} S$$

In what follows, I show that the MLT expression for Φ can be recovered by using first principles from the general expression for the convective heat flux (equation $(2.6.5)$) only if we assume that $F(k)$ is represented by a *delta function peaked about the largest eddy* in the fluid (ie. at wavenumber k_0) as follows,

$$F(k) = F_0 \, \delta\left(\frac{k}{k_0} - 1\right) \qquad (5.2.2)$$

We begin by substituting the expression for $\nu_t(k)$ in terms of $F(k)$ given by equation $(4.4.34)$ into the general non-linear equation for $F(k)$ given by $(2.6.1)$ to get,

$$\int_{k_0}^{k} n_s(k) F(k) dk = \left(2\gamma \int_{k_0}^{\infty} \frac{F(k)}{k^2} dk\right)^{1/2} \int_{k_0}^{k} k^2 F(k) dk \qquad (5.2.3)$$

Now, using the form of $F(k)$ given by equation $(5.2.2)$, and substituting equation $(2.6.3)$ for $n_s(k)$ into the above equation, results in the following expression for F_0,

$$F_0 = \frac{n_0^2}{\gamma k_0^3} \qquad (5.2.4)$$

With F_0 now determined, we can calculate the expression for the convective

---

[1]A detailed review of the basic equations of MLT can be found in [132].

heat flux corresponding to equation (5.2.2). This can be achieved by substituting equations (5.2.2), (5.2.4) and (2.6.3) into equation (2.6.5) to get,

$$\Phi = \left(\frac{\tau(k)}{\gamma} \right) \Sigma^{-1} \left[(1 + \Sigma)^{1/2} - 1 \right]^3 \qquad (5.2.5)$$

which is identical to equation (5.2.1) up to factors of order unity.

The above analysis allows us to conclude that, when considered in the context of the general turbulence equations, the MLT assumes a delta function for the turbulent energy spectrum. This result is not evident however from the standard formulation of the MLT, since the model was never derived by first principles from the NSE. This assumption is therefore hidden in the MLT expression for convective heat flux and is never made explicit in its equations.

5.3 The KH spectrum revisited

The delta function representation of the turbulent energy spectrum works well for highly viscous, low Reynolds number flows, where the separation of scales is small. However, in the highly inviscid stellar interior, where $Re \approx 10^{10}$, this turns out to be a poor approximation that fails to capture in a detailed way the energetics of the flow.

In this section, I discuss in detail the above statement and show that *the MLT provides an inaccurate estimate of the convective flux in both the high and low efficiency regimes.*

5.3.1 Turbulence in stellar interiors

In order to understand the physical origins of the MLT's inability to predict accurately the convective heat flux, we consider here the general variation in

the structure of the turbulent eddy spectrum across different viscosity and efficiency regimes.

Denote by l_{LST} the size of the largest eddy in the LST sector of the spectrum (defined by wavenumber k_0) and by l_{SST} the size of the smallest eddy in the SST sector of the spectrum (defined by k_d, where k_d is the wavenumber that corresponds to the dissipation length scale). Then the ratio of l_{LST} and l_{SST} can be used to define the width of the eddy spectrum (ie. the range of eddy sizes expected to occur in the cascade). In the case of the solar interior, this width can be calculated as follows [6; 84],

$$\frac{l_{LST}}{l_{SST}} \approx \text{Re}^{3/4} \tag{5.3.1}$$

$$\sim \left(10^{10}\right)^{3/4} \tag{5.3.2}$$

$$\sim 10^8 \tag{5.3.3}$$

The above spectrum, which is typical of stellar interiors, has a size ratio of roughly 10^8 between the largest and smallest eddies present in the flow. Such a spectrum cannot be accurately described in terms of a delta function. Doing so would effectively ignore the contributions to $F(k)$ made by all eddies smaller than the one described by k_0. In the case the case of stellar turbulence, this would result in a highly inaccurate description of the convective heat flux, since the width of the eddy spectrum in stars is correlated with a k-space of large extension. One would therefore expect a model of convection which assumes a spectrum of the form described by equation (5.2.2) to misrepresent severely the true nature of the energy transport in the stellar fluid.

We will consider this misrepresentation inherent in the MLT within the context of the two key limits of Σ, which correspond to highly efficient and highly inefficient convection, ie. $\Sigma \gg 1$ and $\Sigma \ll 1$ respectively. These limits are in accordance with the following physical scenarios:

The $\Sigma \gg 1$ regime:

Since, in general, we have that,

$$S = \sigma R = \frac{g\alpha\beta l^4}{\chi^2} = \left(\frac{t_\chi}{t_b}\right)^2 = \frac{81}{2}\Sigma \qquad (5.3.4)$$

where t_χ and t_b are the radiative and buoyancy time-scales respectively, the $\Sigma \gg 1$ regime may be interpreted as corresponding to a situation where convecting fluid elements transport their heat across the convective layer with little to no losses due radiation. Such a situation is therefore said to result in highly *efficient* convection. It is also interesting to note that in this case $n_s(k) \approx t_b^{-1}$.

The $\Sigma \ll 1$ regime:

When $\Sigma \ll 1$, fluid elements traverse the convective layer under the action of buoyancy forces while losing a significant portion of their heat energy via radiation into the surroundings. This situation therefore corresponds to a convective process which is said to be highly *inefficient*. The growth rate for such a situation corresponds to $n_s(k) \approx t_\chi t_b^{-2} \approx g\alpha\beta(\chi k^2)^{-1}$. Note that even though t_χ is the dominant time-scale in this scenario, $n_s(k)$ is still related to t_b here since it is the buoyancy which drives the turbulence and hence causes the convection to occur in the first instance.

With the above picture of the different convection regimes in mind, we now proceed calculate the expression for the convective heat flux predicted by KH model, and compare this expression with its counterpart in the MLT.

5.3.2 Derivation of the KH flux

Stellar interiors are known to be highly inviscid. For example, the Sun is esti-mated to have a Prandtl number of approximately 10^{-9} [6]. Inviscid systems with values of $\sigma \ll 1$ in general exhibit an extended inertial subrange which spans a large portion of the total k-space. This warrants the use of the KH spectrum as a first step in improving the delta function approximation to $F(k)$ used in the MLT.

In similar manner to the derivation of the MLT flux equation in section (5.2), we can calculate the expression for Φ predicted by the KH model by substi-tuting equations (2.3.3) and (3.5.1) into equation (2.6.5) to get,

$$\Phi_{KH} = \left(\frac{27}{16}\right) \tau(k) \, \text{Ko}^3 \, \Sigma^{-1} \left[(1+\Sigma)^{1/2} - 1\right]^3 \phi^3 \qquad (5.3.5)$$

The above equation is similar in structure to the MLT expression for Φ, how-ever, this expression contains an additional function, ϕ, given by,

$$\phi \equiv \frac{3}{2}\Sigma \left[(1+\Sigma)^{1/2} - 1\right]^{-1} \int_1^\infty \left(1 + \Sigma t^{-3}\right)^{-1/2} t^{-3} dt - 1 \qquad (5.3.6)$$

which causes an offset between the predicted KH and MLT fluxes. This can be seen by taking the ratio of equations (5.2.1) and (5.3.5) to get,

$$\frac{\Phi_{KH}}{\Phi_{MLT}} = \frac{8}{5}\left(\frac{3}{4}\,\text{Ko}\right)^3 \phi^3 \qquad (5.3.7)$$

In particular, since ϕ exhibits the following behaviour in the $\Sigma \gg 1$ and $\Sigma \ll 1$ limits,

$$\Sigma \gg 1: \qquad \phi^3 \;\rightarrow\; 8 \qquad (5.3.8)$$

$$\Sigma \gg 1: \qquad \phi^3 \;\rightarrow\; \frac{1}{8} \qquad (5.3.9)$$

we have from equation (5.3.7) that,

$$\Sigma \gg 1 : \qquad \frac{\Phi_{KH}}{\Phi_{MLT}} \;=\; 18 \left(\frac{\text{Ko}}{1.5} \right)^3 \qquad \qquad (5.3.10)$$

$$\Sigma \ll 1 : \qquad \frac{\Phi_{KH}}{\Phi_{MLT}} \;=\; 0.3 \left(\frac{\text{Ko}}{1.5} \right)^3 \qquad \qquad (5.3.11)$$

The results presented in equations (5.3.10) and (5.3.11) suggest that, due to its crude assumption about the form of $F(k)$, the MLT provides a severely inadequate measure of the actual convective fluxes propagating in the stellar interior. In particular, when a more accurate representation of the turbulence spectrum is taken into account, it is noticed that,

(i) *for $\Sigma \gg 1$: the MLT underestimates Φ*, and

(ii) *for $\Sigma \ll 1$: the MLT overestimates Φ*

This conclusion is verified by models of turbulence more complete that the KH model, whose description of the spectrum is of course limited to the inertial subrange only. For example, using the CGC model, a numerical calculation of the convective heat fluxes (via equations (4.3.1), (2.6.3) and (2.6.5)) for the above efficiency limits shows that [21],

$$\Sigma \gg 1 : \qquad \frac{\Phi_{CGC}}{\Phi_{MLT}} \;\approx\; 4, \qquad \qquad (5.3.12)$$

$$\Sigma \ll 1 : \qquad \frac{\Phi_{CGC}}{\Phi_{MLT}} \;\approx\; \frac{1}{12}, \qquad \qquad (5.3.13)$$

This situation is illustrated in figure 5.1, which shows plots of the Φ vs S relationship exhibited by the MLT and CGC models respectively.
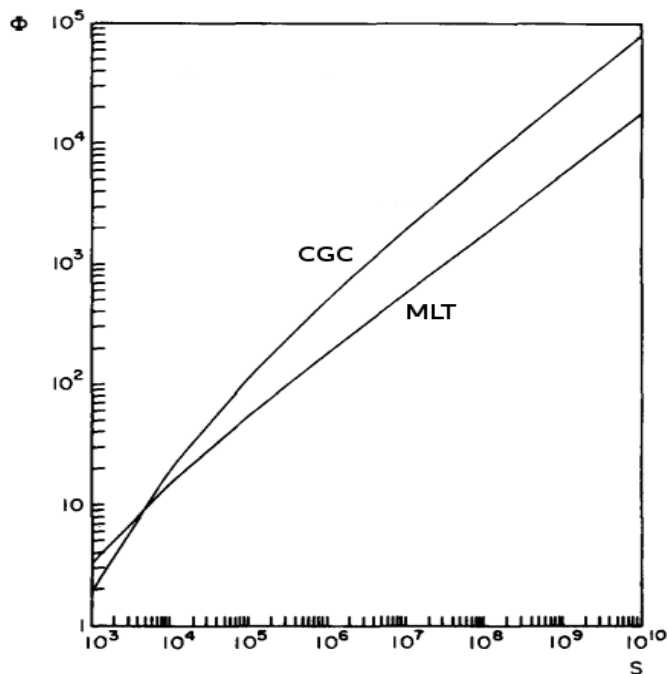
Figure 5.1: Plot of Φ vs S, comparing the CGC and MLT models for $\sigma = 0$ (adapted from [21])

The closeness of the curves in the above figure for small values of S is due to the fact that radiative losses in the low efficiency regime result in the bulk of the convective heat flux being carried by the large, energy containing eddies which reside in the $k \approx k_0$ region of the spectrum. Since the MLT approximation to $F(k)$ zones in on this region of the k-space through its preferential treatment of the dominant k_0 eddy, the difference between fluxes predicted by the models is relatively small. This is also evidenced by the low value of the offset coefficient in equation (5.3.13). Conversely, the strongly divergent behaviour of the fluxes in the $\Sigma \gg 1$ limit is a direct consequence of the fact that the one-eddy MLT model has its entire contribution to Φ given by $k = k_0$ only, whereas the CGC model accounts for contributions to made to Φ by eddies across the entire k-space. This "flux tilting in efficiency space" is a key feature of the CGC, CM and CGM models of convective turbulence, and is an effect which cannot be achieved through any adjustment of the α

parameter for the mixing-length (which is the typical approach taken within the MLT when attempting to circumvent any uncertainties in its treatment of the turbulence spectrum).

Furthermore, it must be noted that the general trend between the flux curves depicted in figure 5.1, and stated in points (i) and (ii) above, have also been confirmed by fully predictive, theoretical models of fluid turbulence such as the DIA/EDQNM [22]. An example of this type of comparison is shown in figure 5.2, which illustrates the change in the width of the spectrum predicted by the EDQNM model, for several values of σ and S, vs that of the MLT. The figure serves to emphasise the fact that fluids characterized by low values of σ exhibit extended spectra which encompass a broader k-space, and vice versa. This behaviour can be also be deduced on dimensional grounds from the standard relation between the dissipation length scale and the molecular viscosity given by, $l_{SST} \propto \nu^{3/4}$ [84].

Of particular importance here is the fact that as the value of ν is increased, the shape of the actual spectrum converges to that of a delta function peaked about k_0. This implies that the MLT becomes a progressively better approximation to $F(k)$ in the limit as ν tends to infinity, and conversely a progressively poorer approximation to $F(k)$ in the limit as ν tends to zero. Since stellar interiors are characterized by extremely low values of σ, the latter is true in stars, which calls into question the validity of the MLT in treatments of stellar turbulence.

Finally we note that the failure of the MLT to treat adequately the turbulence spectrum should be particularly exaggerated in regions of the star which exhibit a pronounced superadiabatic gradient due to the fact that [22],

$$\frac{l_{LST}}{l_{SST}} \;\; \propto \;\; (\nabla - \nabla_{ad})^{3/8} \qquad\qquad (5.3.14)$$

where ∇ and ∇_{ad} are the actual and adiabatic temperature gradients respectively. This is indeed suggested by the results of numerical simulations of stellar convection, which I will discuss further in Chapter 7.

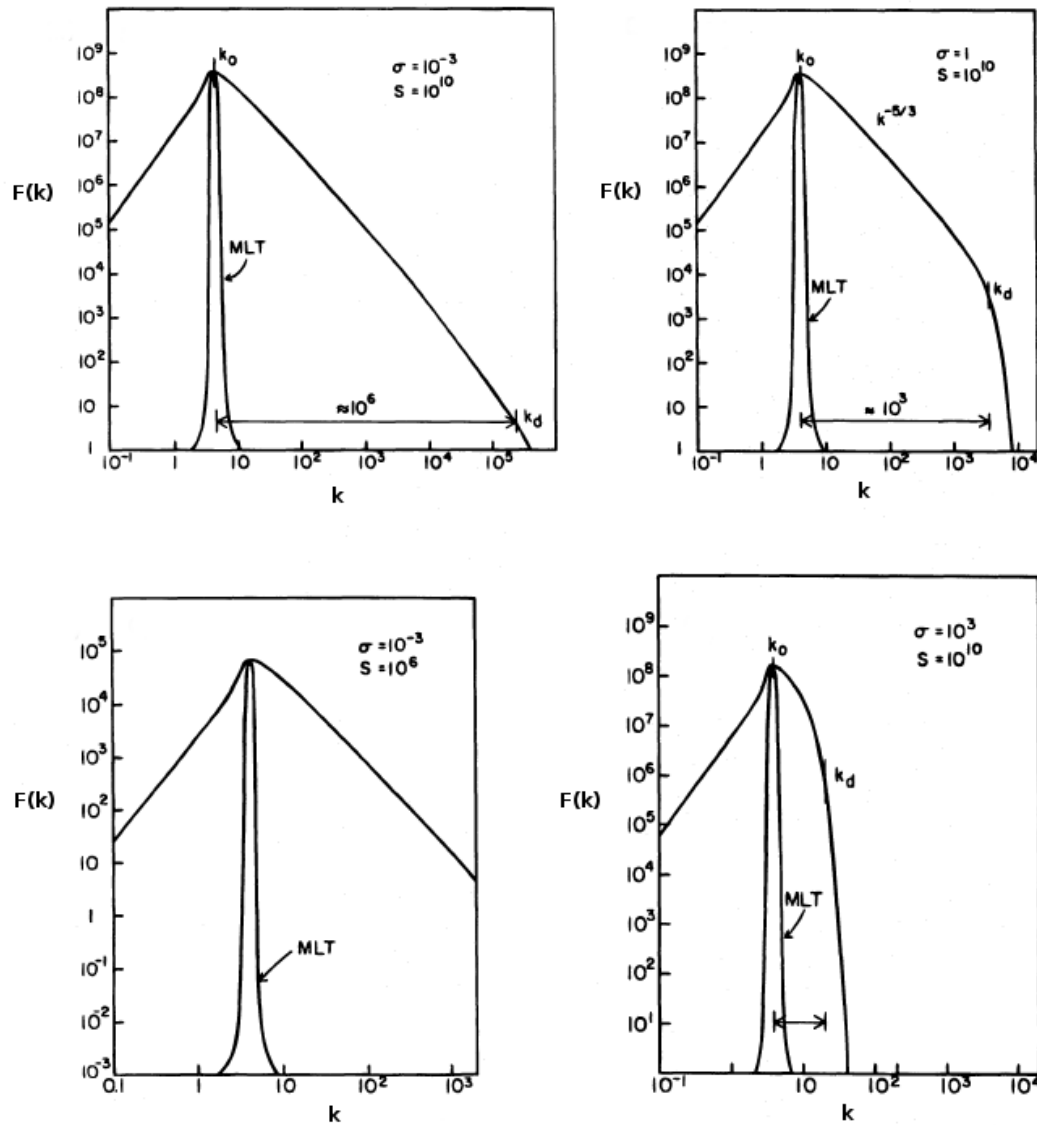Figure 5.2: Plots of $F(k)$ vs k, calculated numerically using the EDQNM model for several choices of σ and S. Superimposed on these graphs is the MLT spectrum, which is represented by a δ-function in each case. (adapted from [22])

5.4   Concluding Remarks

In this chapter, it has been shown that the MLT is inadequate for the treatment of convective turbulence in highly inviscid fluids. Since the stellar interior presents an example of such a fluid, the validity of the MLT in treatments of stellar convection is called into question. In particular, it has been shown that Φ_{MLT} can only be recovered from the general equations of turbulence if one assumes that the turbulent energy spectrum, $F(k)$, is represented by a delta function. It has also been shown that as a result of its implicit dependence on the above form of $F(k)$, the MLT is bound to misrepresent the magnitude of the convective heat flux in key regions of the efficiency space. To elucidate this fact we have compared the MLT with the KH, CGC and EDQNM models of turbulence. This comparison leads to the deduction that in the high efficiency regime the MLT underestimates the true magnitude of Φ, while the opposite is true in the low efficiency regime [22].

The inability of the MLT to match the predictions of more robust models of convective turbulence represents a major shortcoming of the theory. In light of this fact it is certainly remarkable that the vast majority of stellar evolution codes today still rely on the model for the calculation of the convective heat flux in the stellar interior, especially since the discrepancy between the flux predictions of the MLT and the KH model in particular have been known since the work of Ledoux, Schwarzschild and Spiegel [85] (see section 3.2.2).

In the next chapter I will show that a re-evaluation of the expression for $F(k)$ within models of convection that account for the *full spectrum of turbulence* leads to a new set of expressions for Φ which, due to their structure, are capable of being implemented in modern day stellar evolution codes. A key feature of such models is that they naturally exhibit the flux behaviour described in figure 5.1, and have turbulence spectra that are consistent with the results of figure 5.2.

Chapter 6

The FST Models of Stellar Convection

"Despite the great achievements of the stellar evolution theory, there are many points of disagreement between theory and observations which are ultimately related to our poor knowledge of the extension of convectively unstable regions and associated mixing processes."

- C. Chiosi [60]

6.1   Introduction

In this chapter, I discuss the application of models which account for the Full Spectrum of Turbulence (FST) to stellar interiors. The two models which will be discussed are, the Canuto, Goldman and Mazzitelli (CGM), and Canuto and Mazzitelli (CM) models of stellar convection. These models are based on significantly more complete descriptions of fluid turbulence than the MLT which, in Chapter 5, was shown to be inadequate for the treatment of convection in stars.

Section 6.2 considers the key ingredients of the CGM model required for the development of a new FST flux equation. I begin in section 6.2.1, with a discussion of the phenomenology used to construct the CGM closure. This closure is then compared to those of previous models discussed in this thesis. The fundamental equations of the CGM model are then derived in section (6.2.2), where it is noticed that the construction of this model is analogous to that of the CGC model, discussed in Chapter 4.

Section 6.3 considers the core aspects of the CM model which unlike the CGM model, is based directly on the more advanced Eddy Damped Quasi-Normal Markovian (EDQNM) model of turbulence. It is shown in section 6.3.2 that the framework of the EDQNM approach also allows for the development of a FST flux equation which is similar in structure to that of the CGM model.

In section 6.4, I compare the FST and MLT flux predictions across the different efficiency regimes. It is noticed that, depending on the efficiency of convection, the FST models predict fluxes that differ by up to an order of magnitude relative to the MLT.

Finally, in section 6.5, I end with a discussion of the astrophysical implications of the flux differences between the FST and MLT models of turbulent convection.

6.2 The CGM model

The Canuto, Goldman and Mazzitelli (CGM) model of stellar convection utilizes the CGC framework for the self-consistent determination of the turbulence rates, as discussed in Chapter 4. However, the principal difference between the CGM and CGC models lies in their interpretation of the eddy correlation time.

In the CGM model, this time-scale is viewed as depending on *both* the source and the turbulence itself, thus allowing for the natural inclusion of the feedback mechanism discussed in Section 4.5.

It will be shown that the inclusion of this mechanism leads to a new expression for the convective heat flux which takes into account the full spectrum of fluid turbulence. Furthermore, the parametrization of this expression in terms of the convective efficiency allows it to be naturally incorporated into present day 1-D stellar evolution codes, whose numerics typically require the flux model to be parametrized in this way.

6.2.1 The CGM closure

While the CGM model is based in large part on the CGC model, the key difference between the two lies in their treatment of the eddy correlation rate. CGM provided a reinterpretation of this rate that allows for the possibility of the eddies being "scattered" in the cascade. Doing so causes the effective energy input from the source to be regulated by the turbulence it creates, and incorporates into the model an aspect of the reverse feedback mechanism discussed in Section 4.5. A self consistent treatment of the rates is then used to develop a new expression for the convective heat flux which can be solved numerically for Φ.

In what follows, we will refer to CGM's reinterpretation of the correlation rate as $N_{cgm}(k)$. This rate is defined in terms of the eddy viscosity as follows,

$$\nu_t(k) = \int_{k_0}^{\infty} \frac{F(k)}{N_{cgm}(k)} \tag{6.2.1}$$

In the CGM model, the eddy lifetime, described by $N_{cgm}^{-1}(k)$, is viewed as depending on the following set of processes:

(i) the input of energy from the source, described by $N_s(k)$,

(ii) the removal of energy via the action of the eddy viscosity, described by $k^2\nu_t(k)$.

(iii) the random walks that occur as a result of the interaction between the above two processes, described by $2[k^2\nu_t(k)N_s(k)]^{1/2}$. For example during the time interval between successive scatterings as a result of process (i), the eddy is assumed to undergo a random walk as a result of process (ii), and vice-versa.

Taking the sum of the rates associated with the above three processes results in the CGM expression for the correlation rate, which is given by,

$$
\begin{aligned}
\gamma N_c^{CGM}(k) &= k^2\nu_t(k) + N_s(k) + 2\sqrt{k^2\nu_t(k)N_s(k)} \\
&= \left[\sqrt{k^2\nu_t(k)} + \sqrt{N_s(k)}\right]^2
\end{aligned}
\tag{6.2.2}
$$

As in the CGC model, the closure for $\nu_t(k)$ within the self-consistent treatment of rates is still given by equation (4.4.30) as,

$$
k^2\nu_t(k) = \gamma N_c(k)
\tag{6.2.3}
$$

However, $N_c(k)$ is to be interpreted here as applying *only* to process (ii). To draw a comparison between the models discussed thus far, note that in the CG model we had $N_{cgm}(k) = N_s(k)$, while in the CGC model we had $N_{cgm}(k) = N_c(k)$. The CG model therefore accounted only for process (i) and neglected process (ii) (and by implication process (iii)), while the CGC model accounted only for process (ii) while neglecting process (i) (and by implication process (iii)). In other words, the CG model treated the eddy correlation time

as depending only on the source instability and ignored the effects of the turbulence itself on the correlation time, while the CGC model did the opposite.

The CGM model may therefore be viewed as an attempt to overcome the shortcomings of the CG and CGC treatments of the correlation time by allowing it to depend on *both* the source and the turbulence which it generates.

6.2.2   The model equations

This section considers the ingredients of the CGM model required for the the determination of the convective heat flux. The method for constructing the governing equations in this model is analogous to that of the CGC model with the inclusion of the self-consistent approach to the rates. However, due to the differences in the description of the correlation time between these two models, the equations involving $N_c(k)$ in Section 4.4 have to be reinterpreted via equation (6.2.1) in order to ensure that $N_{cgm}(k)$ enters the formalism in a physically consistent manner.

6.2.2.1   The differential equation for $N_c(k)$

In the CGM model, the differential equation for $N_c(k)$ should be thought of as being the analogue of equation (4.3.1) which, in the CGC model, determined the structure of mean-square vorticity, and hence the turbulent energy spectrum. It will be shown that in addition to describing the interplay between the rates that govern the flow, the solution of the differential equation for $N_c(k)$ enables the calculation of several important quantities which characterize the turbulence described by the CGM model.

To derive this equation, begin by substituting equation (4.4.30) into equation (6.2.1) and taking the derivative of the result to get,

$$F(k) = -\gamma N_{cgm}(k) \left[\frac{d}{dk} \left(\frac{N_c(k)}{k^2} \right) \right] \tag{6.2.4}$$

Next, we note that by taking the derivative of equation (4.4.16) we have,

$$N_s(k) - \frac{y(k)}{F(k)} \left[\frac{d}{dk} \nu_t(k) \right] = k^2 \nu_t(k) \tag{6.2.5}$$

which, with the aid of equations (6.2.1) and (4.4.30), results in

$$y(k) = N_{cgm}(k) \left[\gamma N_c(k) - N_s(k) \right] \tag{6.2.6}$$

Finally, substituting the definition of the mean-square vorticity into the above equation and combining the result with equation (6.2.4) gives the differential equation obeyed by $N_c(k)$ as,

$$2 N_{cgm}(k) \left[\frac{d}{dk} N_c(k) \right] + \left[\frac{d}{dk} N_{cgm}(k) \right] \left[N_c(k) - \frac{1}{\gamma} N_s(k) \right]$$

$$-\frac{1}{\gamma} N_{cgm}(k) \left[\frac{d}{dk} N_s(k) \right] - \left(\frac{2}{k} \right) \left[N_c(k) N_{cgm}(k) \right] = 0$$

$$\tag{6.2.7}$$

Since $N_s(k)$ and $N_{cgm}(k)$ are also expressed in terms of $N_c(k)$ via equations (4.4.46) and (6.2.2) respectively, the solution of equation (6.2.7) completely determines the rates, and hence the turbulent energy spectrum (via equation (6.2.4)). Equation (6.2.7) may therefore be viewed as being the fundamental equation of the CGM model.

6.2.2.2 The energy equation

In order to determine the form of the energy equation obeyed by $\epsilon(k)$ we simply combine equations (4.4.16), (4.4.30) and (6.2.4) to get,

$$\epsilon(k) = N_{cgm}(k) \left[\nu + \frac{\gamma N_c(k)}{k^2} \right] \left[\gamma N_c(k) - N_s(k) \right] \qquad (6.2.8)$$

Again, since the three rates $N_s(k)$, $N_c(k)$ and $N_{cgm}(k)$ are related to each other via equations (4.4.46), (6.2.2) and (6.2.7), a solution of equation (6.2.7) for $N_c(k)$ completely detemines $\epsilon(k)$ via equation (6.2.8) above.

6.2.2.3 The convective heat flux

The convective heat flux is calculated, as usual, from equation (2.6.5) or equivalently from equation (2.6.6),

$$\Phi = \frac{\epsilon}{g\alpha\beta\chi} \qquad (6.2.9)$$

In order to determine the asymptotic value of $\epsilon(k)$ required to generate a numerical solution for Φ via the above equation, CGM have taken the usual approach of following the solution of $N_c(k)$ from k_0 into the inertial subrange where $\epsilon(k)$ saturates to ϵ.

6.2.2.4 Boundary conditions

In order to solve equation (6.2.7) for $N_c(k)$ one to needs to specify a set of appropriate boundary conditions. Due to the analogous nature of equations (6.2.7) and (4.3.1), the procedure for determining these boundary conditions is identical to the one discussed in sections (4.3.1) and (4.4) within the context

of the self-consistent framework of CGC model.

For the sake of completeness, we list these conditions again below:

$$N_s(k_0) = \gamma N_c(k_0) = k_0^2 \nu_t(k_0)$$ (6.2.10)

$$\frac{d}{dk}\left(\frac{N_s(k)}{k^2}\right)\bigg|_{k=k_0} = \frac{d}{dk}\left(\frac{\gamma N_c(k)}{k^2}\right)\bigg|_{k=k_0} = 0$$ (6.2.11)

with the form of the eddy anisotropies given, as in the CGC model, by equations (4.4.47) - (4.4.50).

6.2.3   Numerical solution of the model equations

Due to its non-linear structure, equation (6.2.7) must in general be solved numerically for $N_c(k)$. As is common practice in numerical treatments of the turbulence equations, CGM chose to normalize the rates in their model in order ensure a sufficient degree of numerical accuracy in the solutions of $N_{cgm}(k)$ at both high, and low values of S (or equivalently Σ). The normalizations were all taken relative to $N_s(k_0)$ as follows:

$$\eta_s(k) = \frac{N_s(k)}{N_s(k_0)}$$ (6.2.12)

$$\eta_c(k) = \frac{\gamma N_c(k)}{N_s(k_0)}$$ (6.2.13)

$$\eta_{cgm}(k) = \frac{\gamma N_{cgm}(k)}{N_s(k_0)}$$ (6.2.14)

Notice that for $q = k/k_0 = 1$, equations (6.2.12) - (6.2.14) imply that,

$$\eta_c(q) = \eta_s(q) = 1 \quad \text{and} \quad \eta_{cgm}(q) = 1 \tag{6.2.15}$$

Using equations (6.2.12) - (6.2.14), equations (6.2.7) and (6.2.8) for $n_{cgm}(k)$ and $\epsilon(k)$ can be rewritten in terms of the normalized rates as,

$$2\eta_{cgm}(q)\left[\frac{d}{dq}\,\eta_c(q)\right] \;+\; \left[\frac{d}{dq}\,\eta_{cgm}(q)\right]\left[\eta_c(q) - \eta_s(q)\right]$$

$$-\; \eta_{cgm}(q)\left[\frac{d}{dq}\,\eta_s(q)\right] \;-\; \frac{2\eta_c(q)\eta_{cgm}(q)}{q} = 0$$

$$\tag{6.2.16}$$

and,

$$\epsilon(q) = \gamma^{-1} S_*^{1/2} q^{-2} g\alpha\beta\chi\,\psi_0^3(S)\,\eta_c(q)\eta_{cgm}(q)\left[\eta_c(q) - \eta_s(q)\right] \tag{6.2.17}$$

respectively. Furthermore, since equation (2.6.6) relates ϵ directly to Φ, the expression for the dimensionless convective heat flux can also easily be written in terms of the normalized rates as,

$$\Phi(S) = \gamma^{-1} S_*^{1/2} q_f^{-2}\,\psi_0^3(S)\,\eta_c(q_f)\eta_{cgm}(q_f)\left[\eta_c(q_f) - \eta_s(q_f)\right] \tag{6.2.18}$$

where q_f is defined such that $\epsilon(q_f) = \epsilon$ (i.e., q_f is the normalized wavenumber at which $\epsilon(k)$ saturates in the inertial subrange).

6.2.3.1   The CGM flux

To determine the behaviour of Φ in the different efficiency regimes, CGM employed an iterative procedure which consisted of the computation of $\eta_c(q)$

from equation (6.2.16) for values of S in the interval $[10^{-4}, 10^{20}]$, with the initial conditions being specified by equation (6.2.15). For each solution of $\eta_c(q)$, $\epsilon(q)$ was determined via equation (6.2.17). The saturation point, q_f, and the associated value of $\epsilon(q_f) = \epsilon$ were noted for each iteration. This procedure then allowed for the determination of $\Phi(S)$ via equation (6.2.18). Using the data generated from the above procedure CGM produced an analytically fit formula for $\Phi(S)$ which has the following structure,

$$\Phi_{CGM} = \left(\frac{\text{Ko}}{1.5}\right)^3 aS^m \left[(1 + bS)^n - 1\right]^p \left[1 + \frac{cS^q}{1 + dS^r} + \frac{eS^s}{1 + fS^t}\right] \quad (6.2.19)$$

and a, b, c, d, e, f, k, m, n p, q, r, s and t are constants determined by the fitting procedure[1].

The above expression for the convective heat flux is extremely similar to that of the MLT (equation (5.2.1)). However unlike Φ_{MLT}, this expression for Φ takes into account the full spectrum of turbulence associated with the convective process. In section 6.4, I will compare Φ_{CGM} against Φ_{MLT} across both efficiency regimes in order to determine the relative improvement in the estimation of the convective flux provided by the CGM model.

6.3   The CM model

It must be noted that prior to the development of the CGM model, Canuto and Mazzitelli (CM) [22] had already attempted to derive a full spectrum of turbulence equation for Φ within the framework of the EDQNM model [114], which may be viewed as a simplification of the full DIA formalism. Unlike the phenomenological closures discussed in this thesis, the DIA is a fully predictive, theoretical model of fluid turbulence which is derived directly from the

---

[1]A list of the numerical values associated with these constants can be found in [23].

NSE using ideas from quantum field theory [67; 71]. Since a comprehensive discussion of this class of two-point closure models is beyond the scope of this thesis, we simply state in this section the model equations used by CM, and refer the reader to the excellent review of the DIA and its derivatives given by Leslie [82].

6.3.1   The model equations

Due to the highly complex nature of the DIA equations and the fact that they must in general be solved using advanced numerical procedures, little progress has been made in the application of the DIA formalism to problems in the field of stellar astrophysics. In fact, the CM model appears to be one of the first attempts at applying a version of the DIA (EDQNM) to the description of turbulent convection in stars.

The basic equations of the CM model are [22],

$$\left[\frac{\partial}{\partial t} - 2n_s(k) \right] F(k,t) = T(k,t) \tag{6.3.1}$$

where $T(k,t)$, which describes the transfer of energy due to the non-linear interactions, is given by

$$T(k,t) = \int \int_{\Delta} [k^2 F(p,t) - p^2 F(k,t)] k(pq)^{-1} b_{kpq} \theta_{kpq}(t) F(q,t) dp \, dq \tag{6.3.2}$$

where Δ denotes the fact that the domain of integration is restricted to wave vectors $\mathbf{p}$ and $\mathbf{q}$ such that $|\mathbf{p} - \mathbf{q}| \le k \le |\mathbf{p} + \mathbf{q}|$ and b_{kpq} is a geometrical factor for the eddy anisotropies. Note that $\theta_{kpq}(t)$ in this notation corresponds to the eddy correlation time which as usual must be specified in order to complete the model equations. According to the DIA, the equations obeyed by θ are

[72],

$$\frac{\partial \theta\,(k,t)}{\partial t} = 1 - 2n_c(k,t)\theta(k,t) \tag{6.3.3}$$

$$n_c(k,t) = k^2\left[\nu + \nu_t(k,t)\right] \tag{6.3.4}$$

$$\nu_t(k,t) = \frac{1}{15}\int_k^\infty \left(5E(p,t) + p\left[\frac{d}{dp}\,E(p,t)\right]\right)\theta(p,t)dp \tag{6.3.5}$$

Once $n_s(k)$ has been specified, equations (6.3.1) - (6.3.5) can then be used to determine the form of the turbulent energy spectrum relevant to the problem being considered.

6.3.2   The CM flux

Using equation (2.6.3) for growth rate of a convective instability, CM solved the model equations numerically and used the resulting $F(k)$ to generate a new expression for Φ via equation (2.6.5). The result obtained was,

$$\Phi_{CM} = a_1\Sigma^m\left[(1 + a_2\Sigma)^n - 1\right]^p \tag{6.3.6}$$

where as in the CGM model, the constants a_1, a_2, m, n and p are determined from the fitting procedure [2].

As with equation (6.2.19), equation (6.3.6) provides an expression for the convective heat flux which now incorporates the full spectrum of turbulence. However, the difference between the two is that due to its derivation from within the EDQNM framework, equation (6.3.6) is based an inherently more robust

---

[2]The values of these constants as well as a discussion of the numerical procedure can be found in [22].

description of the non-linear interactions than equation (6.2.19) which assumes a phenomenology for these interactions.

6.4 Comparison of the CGM and CM fluxes with MLT

With the form of the Φ_{CGM} and Φ_{CM} now determined via equations (6.2.19) and (6.3.6) respectively, we can now compare the CGM and CM flux treatments to that of the MLT across both efficiency regimes. As with the analogue of this comparison in section (5.3.2) for the KH model, we expect the convective fluxes in the FST models to be higher in the high S regime and lower in the low S regime when compared to the MLT. Taking the ratios of the respective flux equations confirms that this is indeed the case:

$$S \gg 1: \qquad \frac{\Phi_{CM}}{\Phi_{MLT}} \approx 9.8 \qquad ; \qquad \frac{\Phi_{CGM}}{\Phi_{MLT}} \approx 9.5 \left(\frac{\mathrm{Ko}}{1.5}\right)^3 \left(\frac{\sigma_t}{0.72}\right)^{3/2}$$

$$(6.4.1)$$

$$S \ll 1: \qquad \frac{\Phi_{CM}}{\Phi_{MLT}} \approx 0.11 \qquad ; \qquad \frac{\Phi_{CGM}}{\Phi_{MLT}} \approx 0.31 \left(\frac{\mathrm{Ko}}{1.5}\right)^3 \qquad (6.4.2)$$

Therefore, the FST models predict fluxes that can differ by up to an *order of magnitude* relative to the MLT. Furthermore, the inability of the MLT to correctly predict the true magnitude of the convective flux in highly inviscid fluids has also been confirmed by DNS simulations of turbulent convection [13; 30]. This suggests that the FST models do indeed provide a better description of convection in stars than the MLT.

6.5   Discussion

The inclusion of the "feedback/backscattering mechanism" in the CGM expression for the eddy correlation rate results in a closure for the turbulent energy spectrum which overcomes the deficiencies of its predecessor, the CGC model. As stated in section 4.5, the inability of the CGC model to match the DIA spectrum in the LST region is due in large part to the omission of this mechanism from its closure (which was based on a simple proportionality relation between $\nu_t(k)$ and $n_c(k)$). One would therefore expect the CGM model to be in good agreement with the form of the energy spectrum predicted by a model of turbulent convection based on the DIA or one of its derivatives. This indeed appears to be the case, with both the CGM model, and the EDQNM based CM model, making very similar flux predictions in both the high and low efficiency regimes. While a direct comparison between the CGM and CM spectra is not trivial, the differences in the absolute magnitude of their fluxes can certainly be attributed to the following facts,

1. The CGM model utilizes a self-consistent framework for the determination of the source growth rate (which in the case of turbulent convection corresponds to the buoyancy force), whereas the CM model relies exclusively on the linear approximation to $n_s(k)$.

2. The CGM model uses a phenomenological closure for the energy spectrum, whereas the CM model is based directly on the EDQNM model, and hence incorporates a more complete description of the non-linear interactions associated with the eddy viscosity.

However, it should be noted that neither of these differences are likely to result in a *significant* discrepancy between the CM and CGM spectra. In particular the CM model's use of the linear approximation to $n_s(k)$ should be of lit-

tle consequence for the calculation of bulk quantities, such as the convective heat flux, which are determined principally by eddies in the LST region of the k-space. It is for these reasons that one would expect the application of these models to simulations of stellar structure and evolution to result in fairly similar predictions for stars across various regions of the Hertzsprung-Russell (HR) diagram. This is indeed a feature exhibited by the evolutionary tracks produced from our numerical implementation of the CM and CGM models, which is discussed in Chapter 7.

In summary, both of the CGM and CM models presented in this chapter are designed to treat the full spectrum of eddies that contribute to the convective heat flux in a turbulent fluid. When compared to the MLT, they confirm the general trend that, when a more complete description of the turbulence spectrum is accounted for, the flux magnitudes predicted by the MLT are lower than they should be in the high efficiency regime, and higher than they should be in the low efficiency regime.

Furthermore, the parametric nature of the flux equations in the CGM and CM models make them ideal for implementation in stellar evolution codes. However, despite the fact that from a theoretical point of view, these models provide an unquestionably better description of convection than the MLT, much of the research work currently being performed using 1-D stellar evolution codes still relies on the MLT for the treatment of convection in the stellar interior [139; 140].

In light of this, I have developed an implementation of the CGM and CM models (hereafter referred to collectively as the full spectrum of turbulence (FST) models) for one of the most widely used stellar evolution codes at present. The details of this implementation will be discussed in the next chapter.

Chapter 7

Numerical Simulations

7.1 Introduction

Numerical simulations are of vital importance in stellar astrophysics. They provide valuable insights into the complex nature of the stellar interior. The extreme conditions found in stars cannot be realised in laboratory based experiments. We therefore have no other means to investigate the processes that occur under these extremes.

Convection in stellar evolution codes have relied, and still largely rely, principally on MLT which was developed in the mid to late 1950's as a first order approximation to the convective process in stars. The mixing-length treatment has been found adequate for stellar models whose sole purpose is the description of the gross features of stellar evolution. But MLT has well known shortcomings in specific applications. Almost all versions of MLT approximate the equations of motion in the manner set out by Boussinesq. The Boussinesq approximation is known to be valid only when the mixing-length is less than the pressure and density scale heights, and assumes in particular that the convective motion is subsonic. However, stellar models based on the MLT disagree with observations when the mixing length is less than these scale heights. To force agreement, the mixing length must be assumed greater than the scale

heights. This makes the model internally inconsistent.

To assess the theoretical analysis presented in this thesis, I have devised a method for implementing the CM and CGM models in the MESA code library [106; 107; 108]. MESA is widely regarded as the premier open-source numerical tool for research in stellar astrophysics at present.

In this chapter I will show that, when implemented in a modern state-of-the-art stellar evolution code, the FST models produce results which differ significantly from those of the MLT.

7.2 MESA

MESA is a highly modularized, open-source code library for stellar astrophysics that began as an effort to improve the now defunct EZ stellar evolution code [99; 106]. The MESA modules are thread safe. This means that more than one process can execute the module routines at the same time, and allows for the utilization of multicore processors. This type parallelizability is particularly useful in simulations of stellar evolution.

The MESA library includes a one-dimensional feature-rich code called MESA `star`. The numerical and computational methods used in MESA `star`, which include adaptive mesh refinement and sophisticated time-step adjustment, allow it to evolve stellar models consistently through phases of stellar evolution that have posed substantial challenges for evolutionary codes in the past. These include the helium core flash in low mass stars and the advanced nuclear burning phases in massive stars. A detailed review of MESA's extensive feature set can be found in the MESA instrument papers [106; 107; 108].

As of September 2016, the MESA user base consists of approximately 915 registered users across six continents. The code serves as the basis of a vast array of research currently being pursued in the field. This is evidenced by the fact that the MESA instrument papers have at present been cited collectively more than 1500 times in academic articles, with the number of citations continuing to grow.
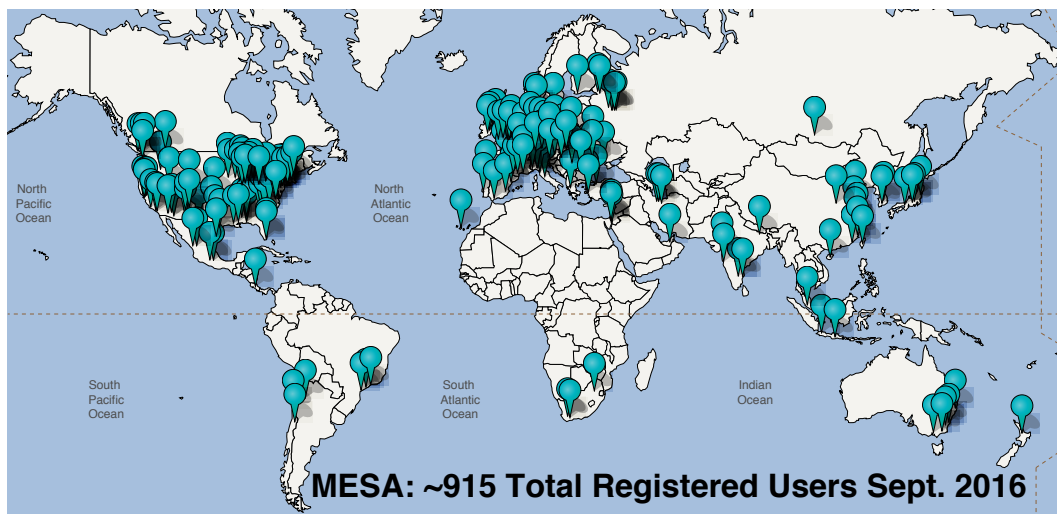

MESA: ~915 Total Registered Users Sept. 2016

Figure 7.1: The MESA user map as of September 2016. [138]

7.2.1 Treatment of convection in MESA

The default treatment of convection in MESA is based on the standard version of the MLT [132], with the core flux calculation in the code being described by equation (5.2.1). Several variations of the MLT are also included to allow a wider range of physical scenarios to be studied. The full list of convection options currently present in MESA are listed below:

(i) `Cox:` based on Cox and Giuli (1968) [132]

(ii) `Henyey:` based on Henyey, Vardya, and Bodenheimer (1965) [58]

(iii) `Mihalas:` based on Mihalas (1978) [94] and Kurucz (1979) [74]

(iv) `ML1:` based on Böhm-Vitense (1958) [8]

(v) `ML2:` based on Bohm and Casinelli (1971) [9]

As shown by the above list, the current version of MESA does not include any official support for either the CM or CGM treatments of turbulent convection. In light of this, I have developed numerical implementations of both of these FST models in such a way that they can be naturally incorporated within the framework of the code. The key motivation for developing this implementation is based on the analysis in the previous chapters of the severe theoretical shortcoming of the MLT as a model of fluid turbulence. I will show in this chapter that these shortcoming have observable consequences on numerical studies of stellar structure and evolution.

7.3 Implementation of the FST models in MESA

My implementation of the FST models allows replacement of the standard MLT calculation of the convective heat flux with that of either the CM or CGM models (described in sections 6.2.3 and 6.3.2). To achieve this, I used MESA's `run_star_extras` platform, which provides an interface to the core numerics contained in MESA `star`.

One of the key differences between the present implementation of the FST models in MESA and the one used by CM and CGM in their ATON code [130], is the treatment of the mixing-length parameter α. This will be discussed in detail below.

7.3.1   The mixing length

Implementation of a convection model within a stellar evolution code requires the specification of methods for determining two key quantities associated with the mixing process. These are, the convective heat flux, Φ, and the mixing-length, l.

The form of Φ is in general determined from a fluid model of the convective process, such as the MLT or CGM models. However, these models typically require a set of parameters to be specified before a numerical solution of the convective heat flux can be obtained. In models of astrophysical turbulence, the key parameter required for the calculation of Φ is the mixing length. However, the mixing-length is itself a-priori unknown, and in the absence of a complete analytical model of convective turbulence, one usually determines the form of l by some ad hoc prescription.

In stellar astrophysics, the standard method for determining l is by the following equation,

$$l = \alpha H_p \qquad\qquad (7.3.1)$$

where α is a free parameter (the mixing length parameter), and H_p is the pressure scale height. Since H_p is assumed to be a known or calculable quantity, equation (7.3.1) reduces the problem of determining l to one of specifying the value of α.

As part of their publication of the CM model, Canuto and Mazzitelli proposed a new method for determining the mixing-length [22]. Their method is based on the concept of "vertical stacking", which treats eddies at the top of the convection zone as having smaller sizes than those in the deep interior. The inclusion of this effect within the FST models is an attempt to account for

the effects of compressibility in turbulent flows, however, as will be discussed below, it is unclear whether this prescription for l is significantly better than that of equation (7.3.1) [83].

The CM expression for the mixing length is given by [22][83],

$$l = \alpha_{cm} z \qquad (7.3.2)$$

where α_{cm} is a variable coefficient of order unity, and z is the distance from the location of the eddy to the boundary of the convective layer. CM have recommended setting $\alpha_{cm} = 1$, which effectively results in a parameter free expression for l which, in principle, should be applicable to any star irrespective of its position on the HR diagram.

Simulations of stellar convection which are based on the CM/CGM treatments typically couple the FST flux routines in the code with equation (7.3.2) for the calculation of the mixing-length [99; 130]. However, calibrations of this equation, performed using two-dimensional hydrodynamical simulations, have shown that the variation in α_{cm} is comparable to that of α over extended regions of the HR diagram [83].

Therefore, even though the physical interpretation of α_{cm} is different to that of α, equation (7.3.2) is not truly parameter free since α_{cm} must also be fitted to astrophysical data in order for credible results to be obtained from a stellar model which used the CM prescription for l.

It is also worth noting that in addition to equations (7.3.1) and (7.3.2), several alternative forms of the mixing-length have also been proposed in the literature. Some examples of these additional prescriptions for the l include taking the mixing-length as being proportional to the density scale height [116], or

regarding it as equal to the width of the superadiabatic region [8].

Due to the uncertainty in the correct prescription for l, and since no major contradictions with the data have arisen in previous studies based on equation (7.3.1), I have chosen to set $l = \alpha H_p$ in the present simulations.

I have also adopted the standard practice of fixing the value of alpha via a solar calibration of the models. This is an acceptable approach since it allows direct comparison of the flux calculations across all three models, and removes the differences that arise from the various definition of l. However, future versions of this implementation will be extended to take into account the different prescriptions for the mixing length to allow for a wider range of studies to be performed.

7.3.2   Calibration of the Models

Based on the discussion above, I have calibrated the models presented to within 0.1% of the observed effective temperature of the Sun. To achieve this I constructed a set of $1 M_\odot$ pre-main sequence models, with $Z = 0.02$ and $Y = 0.28$, for each of the MLT, CM and CGM treatments of convection.[1] Each of these models were then evolved from the pre-main sequence phase onto the zero-age main sequence, and then from the zero-age main sequence to the present age of the Sun.

In each of the convection models, the mixing-length parameter was fixed by requiring that the model match the currently accepted effective temperature of the Sun, $T_{\text{eff}} = 5777K$, to within 0.1% accuracy at an age of 4.7×10^9yrs (where this age includes the pre-main sequence lifetime). In the case of the

---

[1]Note that throughout this chapter I follow the standard astrophysical convention of referring to Y and Z as the initial stellar helium and metal mass fractions, respectively. Note also, that quantities subscripted by $\odot$ refer to Solar values.

MLT treatment, this was achieved with $\alpha_{MLT} = 1.9$, while in the case of the CM and CGM treatments, the desired result was achieved with $\alpha_{CM} = 0.9$ and $\alpha_{CGM} = 0.6$ respectively. The complete set of evolutionary tracks corresponding to this calibration are shown in figure 7.1.
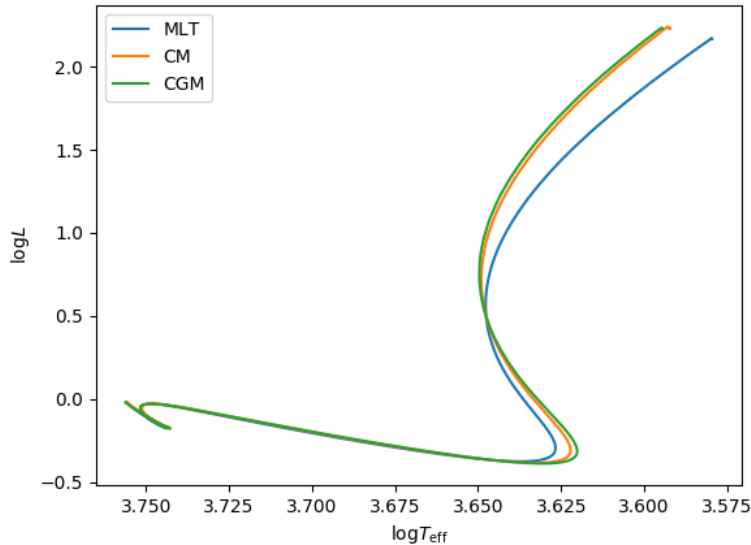

Figure 7.1: Evolutionary tracks for a $1M_\odot$ star with $Z = 0.02$ and $Y = 0.28$, from pre-main sequence to present solar age.

It is important to note that, in general, when this type of calibration is performed using the MLT model, it places a constraint on the allowed value of α_{MLT} such that $1.4 \leq \alpha_{MLT} \leq 2.0$, where the exact value of the parameter within this range depends on the specific details of the stellar code being used [89; 126]. As already noted, a solar calibration of the MLT in MESA results in a value of $\alpha = 1.9$. However, from a theoretical point of view, values of $\alpha > 1$ should be considered unphysical since in the vast majority of cases, the extent of the superadiabatic region is only a fraction of the total pressure scale height. Furthermore, the use of $\alpha > 1$ leads to a violation of the Boussinesq approximation,[2] on which all convection models considered in this

---

[2]See reference [119] and appendix (A)

thesis, including the MLT, are based. The Boussinesq approximation implicitly assumes that the mixing length is shorter than any scale length associated with the structure of the star. In order for progress to made, the unphysical values of alpha predicted by the MLT in stellar codes are typically overlooked, with the violation of the Boussinesq approximation usually being attributed to other uncertainties in the modelling of the fundamental input physics in the code.

It is remarkable, therefore, that when used in a stellar evolution code the CM and CGM models yield values of α that lie in a physically acceptable range of values (ie. $\alpha_{CGM} < \alpha_{CM} < 1$) and are hence fully consistent with the Boussinesq approximation on which they are based. This is an important and useful result since it implies that the model used for convective energy transport in the stellar interior is internally self-consistent and incorporates successfully a credible and physically realistic framework.

As a further check of the accuracy of the present numerical implementation of the FST treatments, I evolved the $1 M_\odot$ model up to a value of $\log L = 1.5 L_\odot$ on the red giant branch. This allows comparison of the results of the simulation against those originally published by CM. Figure 7.2 compares the evolutionary tracks that were produced using MESA, against figure 6 of Canuto and Mazzitelli (1991) [22], which they produced using the ATON code. As illustrated by these graphs, the evolutionary tracks are nearly identical. The slight differences in T_{eff} between the two graphs is due to the fact CM used an initial helium abundance of $Y = 0.27$ in their solar model, whereas I have updated the simulation to include the most recent estimate of $Y = 0.28$ [117].
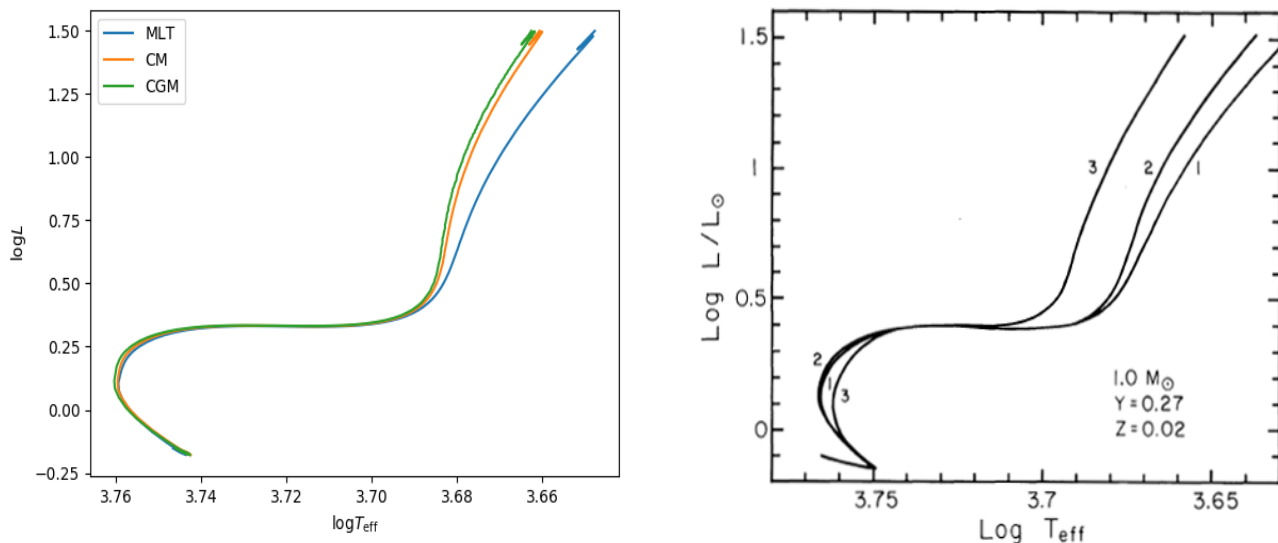
Figure 7.2: Comparison of the MESA implementation of the FST models for a $1M_\odot$ star with $Y = 0.28$ and $Z = 0.02$ (*left panel*), against figure 6 of Canuto and Mazzitelli (1991) [22] (*right panel*) which considers the same evolution, but with $Y = 0.27$, within the context of the ATON code . Note that the curves labelled '1' and '2' correspond to the solar calibrated MLT and CM models respectively, whereas the curve labelled '3' corresponds to the CM model with $l = z$ (which I have not implemented).

7.3.3 Numerical exploration of the FST models

This section provides several illustrations of the major differences in predictions made by the MLT and FST models when applied to calculations of stellar structure and evolution. The results of several simulations that were run using the FST and MLT treatments in MESA are shown in the figures below.

Note that all simulations used the following input physics:

- OPAL equation-of-state (EOS) tables [113].

- Ferguson et.al low temperature opacities [38].

- OPAL tables for high temperature opacities [64].

- Nuclear reaction networks according to the JINA REACLIB database [32].

- Mixing according to each of the MLT [132], CM [22] and CGM [23] models.

Note that I have not incorporated into the present simulations the effects of turbulent pressure, since they are not expected to lead to any significant differences in the locations of the evolutionary tracks on the HR diagram [22].

The quantitative differences between MLT and FST treatments of convection become most apparent in my calculations for stars with convective cores, and at the post main-sequence stages of evolution respectively (see for example, figures 7.2 and 7.4).

In figure 7.3, we notice that episodes of rapid extension of the convective core (the "spikes" in the plots) during main-sequence hydrogen-burning are seen to occur at substantially different ages in the CGM model compared with the MLT and CM treatments. The physical reason for this is not understood.

Figure 7.4 illustrates the substantial difference in the evolutionary tracks that occur when switching between the Schwarzschild and Ledoux criteria respectively. This figure emphasises the fact that, when computing stellar models, it is essential to use the Ledoux criterion which takes into account gradients in the chemical composition of the stellar fluid, rather than the simpler Schwarzschild criterion. However, we note that even across changes in the choice of stability criterion, the relative behaviour of the CM, CGM and MLT curves is still preserved.

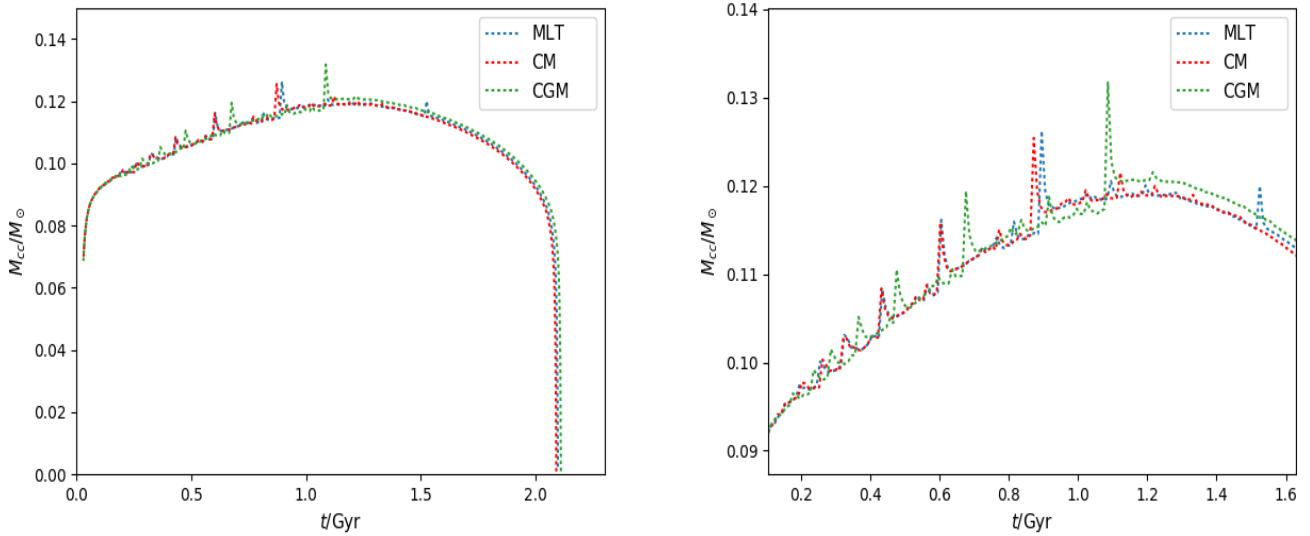Note also that the evolutionary tracks corresponding to the MLT, CM and

Figure 7.3: Plot of the mass fraction of the convective core of a $1.5M_\odot$ star as a function of its age in Gyr. The left panel plots the total evolution of the core from near the onset of hydrogen burning up until core hydrogen depletion. The right panel is a magnified version of the graph in the left panel.

CGM models exhibit a general trend. That is, they initially follow each other very closely while the star is on the main-sequence and undergoing core hydrogen burning. This feature extends onto the sub-giant branch (SGB) until the formation of an extended convective envelope (see for example, figures 7.2 and 7.4). Once the red-giant branch (RGB) is reached, the differences between the models start to become severely exaggerated, with the FST curves exhibiting larger effective temperatures at a given luminosity.

This can be understood in terms of the fact that in the surface regions of a star, where there is a large decrease in the density of the stellar fluid, ∇ begins to deviate from ∇_{ad} and the region becomes superadiabatic, resulting in a pronounced difference between the FST and MLT models. Figure 7.5 shows the profile of the superadiabatic gradient in the outer region of a $0.8M_\odot$ star with $Z = 0.0001$ and $Y = 0.25$ on the RGB. The peak of the superadiabatic gradient

is several times larger in FST model than it is in the standard MLT treatment.

Figure 7.6 shows a remarkable change in the extent of the horizontal branch for a $5M_\odot$ star. This finding could have important implications for the study of classical pulsators (specifically: Cepheids and RR Lyrae stars) as well as the study of subdwarf B (sdB) pulsators.

Finally, figures 7.7 and 7.8 show the differences in the predicted temperatures of the main-sequence turn-offs, and red giant branches for low-mass (convective envelope) stars. In figure 7.7 (*left panel*) and figure 7.8 (*left panel*), it can be seen that the MLT treatment delivers a hotter main-sequence turn-off and a significantly cooler RGB than FST models for a $0.8M_\odot$ globular cluster star with $Z = 0.0001$. However, for a $1.2M_\odot$ star with $Z = 0.02$, while the behaviour of the RGBs is preserved, the location of the turn-off points is reversed, with the MLT predicting a cooler main-sequence turn-off than the FST treatments.
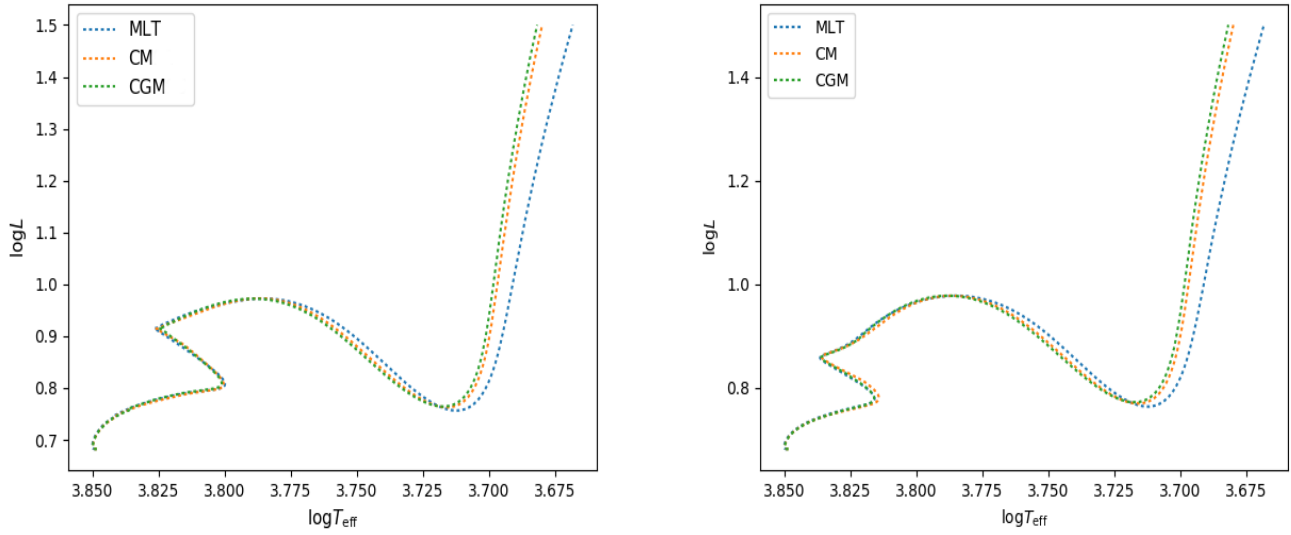
Figure 7.4: Evolutionary tracks for a $1.5M_\odot$ star with solar abundances. This figure illustrates the differences in the evolutionary tracks that result from the use of the Schwarzschild criterion (*left panel*) and the Ledoux criterion (*right panel*) respectively.
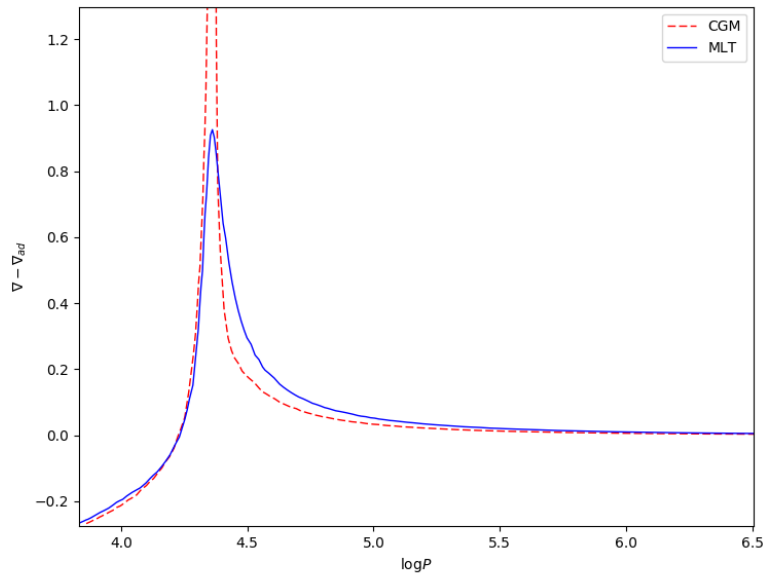

Figure 7.5: Plot of $(\nabla - \nabla_{ad})$ vs $\log P$, in the surface region of a $0.8M_\odot$ star with $Z = 0.0001$ and $Y = 0.25$.
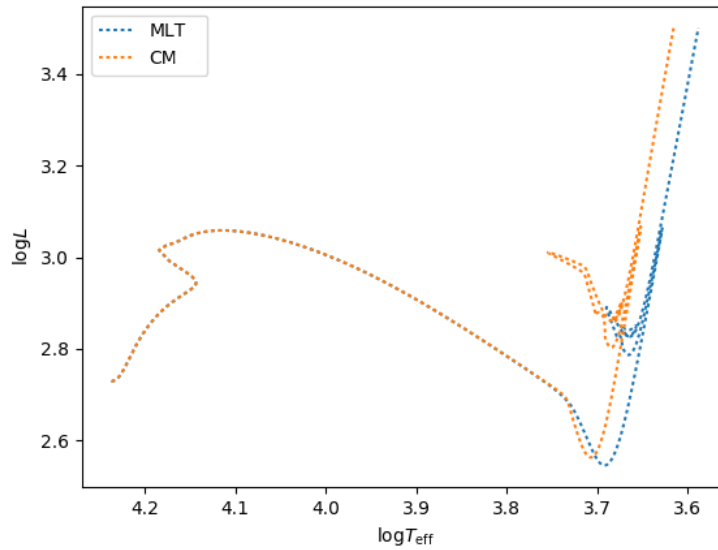
Figure 7.6: Evolutionary tracks comparing the CM and MLT models for a $5M_\odot$ star with solar abundances. The star has been evolved through core He burning. Note the significant difference in the Horizontal Branch (HB) location on this diagram.
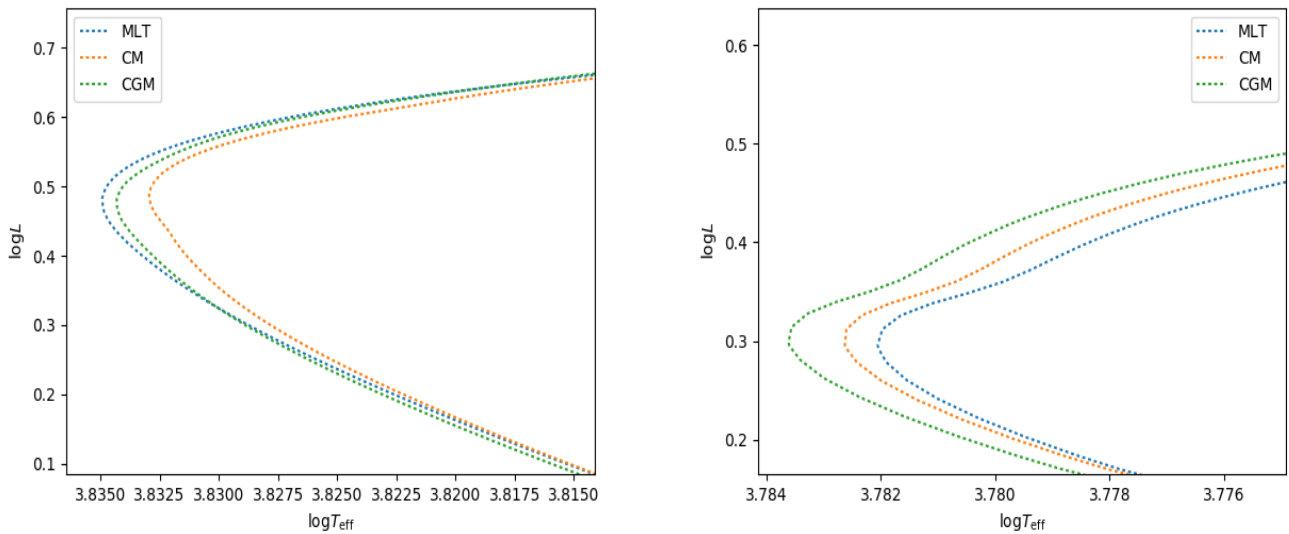

Figure 7.7: Evolutionary tracks centred and magnified at the main sequence turn-off for: (*left panel*) a $0.8M_\odot$ star with $Z = 0.0001$, $Y = 0.25$; and (*right panel*) a $1.2M_\odot$ star with $Z = 0.02$, $Y = 0.25$
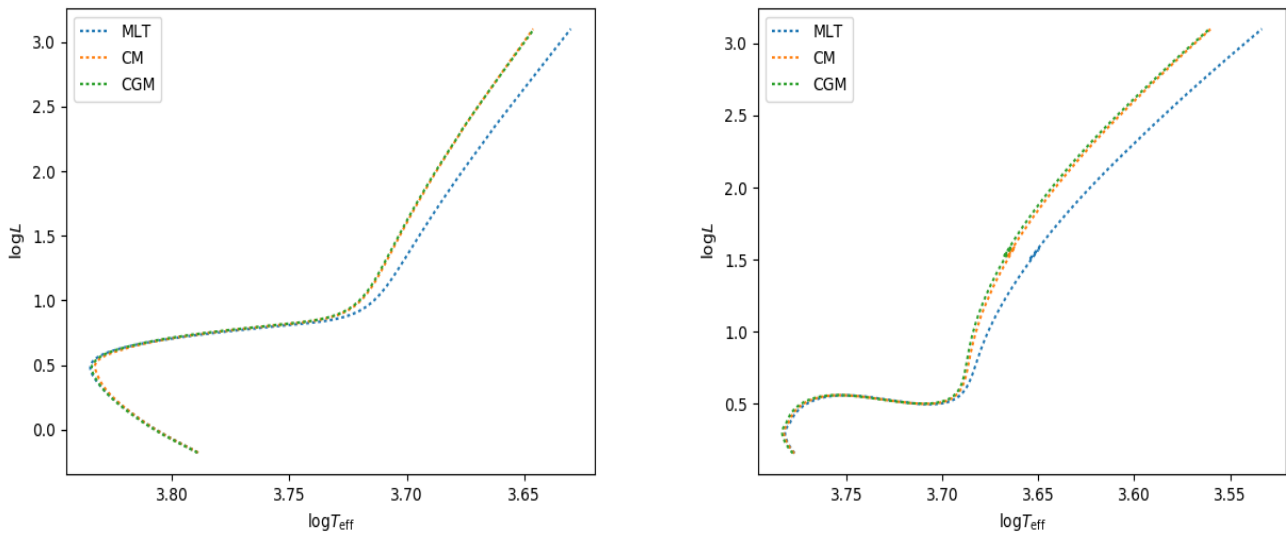
Figure 7.8: Evolutionary tracks for: (*left panel*) a $0.8M_\odot$ star with $Z = 0.0001$, $Y = 0.25$; and (*right panel*) a $1.2M_\odot$ star with $Z = 0.02$, $Y = 0.25$

7.4   Concluding Remarks

The above results serve to illustrate the significant differences between the FST and MLT treatments of convection when applied to calculations of stellar structure and evolution.

The figures demonstrate the fact that when applied to a modern, state-of-the-art stellar evolution code, the FST models make predictions that are in severe enough disagreement with those of the MLT, that they should not be ignored.

We also note that, through numerical simulations of their own, other groups have extensively tested the FST and MLT treatments, against observational data where possible, and shown that in each of the applications considered, the FST models perform at least as well as the MLT eg. [1; 2; 5; 31; 33; 90; 124].

In view of the theoretical arguments made elsewhere in this thesis for the significant problems associated with the use of the MLT in stellar models, the numerical results reported in this chapter suggest that the current, standard MLT evolutionary paths published in the literature (and used in a plethora of applications in stellar astrophysics) may be in need of substantial revision.

Future extensions of this work will include a further exploration of the differences between these models, as well as the inclusion of oscillation modelling into the FST-modified MESA models represented here. I also plan to implement several different prescriptions for the mixing length, as discussed in section 7.3.1.

Summary

The benefits of using the FST models in simulations of stellar structure and evolution can be summarized as follows:

- The flux expression obtained from the FST models include the full spectrum of eddy sizes. These are expected to provide a significantly more accurate representation of the convective energy transfer in stellar convection zones.

- Unlike the MLT, when implemented in a stellar evolution code, the CM and CGM models both predict values of $\alpha < 1$. This indicates that the treatment of convection in the stellar interior is consistent with the Boussinesq approximation and ensures that the convection model incorporates a credible and physically realistic framework.

- The FST models make several predictions regarding the structure and evolution of stars which are expected to be in better agreement with

astrophysical data than the MLT. This is consistent with the results of several authors eg. [1; 2; 5; 31; 33; 90; 124].

Chapter 8

Conclusion

"Although the turbulent motion has been extensively discussed in the literature from different points of view, the very essence of this phenomenon is still lacking sufficient clearness."

- L.D. Landau. [78]

Turbulence in fluids is a remarkably complex and fascinating phenomenon that manifests itself in a myriad of ways. Numerous difficulties are associated with its description. This has forced researchers to resort to a variety of models that approximate its effect on the evolution of the stellar interior. In the absence of a complete, analytical model of turbulence, this appears to be the only viable approach via which progress in our understanding of the behaviour of the stellar fluid can be made.

For several decades the MLT has been the default model for treating convective energy transfer in stars. While this model has played a useful role in providing a qualitative description of the stellar convection zone, it is not without flaw. In this this thesis I have discussed several alternative models which, from both a qualitative and quantitative point of view, provide a significantly better description of convection than does MLT. The purpose of this thesis has been to

motivate replacement of MLT in present day studies of stellar structure and evolution by alternative theories.

8.1   Review of the CG/CGC/CGM models

In this thesis I have presented a detailed theoretical analysis of several models of turbulent convection that have been developed by Canuto et. al. [17; 21; 23]. The fundamental assumptions, equations and predictions associated with each of these models have been derived and explained in significant detail. The CG, CGC and CGM models were shown to be parts of a chain of successive attempts aimed at improving our ability to describe accurately the phenomenon of convective turbulence.

8.1.1   The CG model

The CG model arose as an attempt to improve on the limitations of the KH model. Since the KH model is limited to only a small region of the k-space, which is in general far removed from the LST sector of the flow, it is not well suited to the description of astrophysical systems that fail to exhibit an extended inertial subrange. To address this shortcoming, CG proposed a closure relation which leads to an analytical expression for the energy spectrum in the LST region. The CG model has been shown to perform well in studies of LST, with the theoretical predictions of the model being in good agreement with experimental data in several different applications.

One of the great achievements of this model is that it is able to predict the MLT equation for the convective heat flux in the $k \approx k_0$ region of the spectrum. This appears to be the first derivation in the literature of the MLT from a model of turbulence [17]. The fact that the CG model reproduces the form

of the MLT flux when $k \approx k_0$, is completely consistent with the notion that the MLT is a *single-eddy* model of turbulence since, if one reduces the description of turbulent energy spectrum to the extreme LST sector only, then the bulk of the convective heat flux *is* indeed carried by the k_0 eddy. Unlike the the MLT however, the CG model is also capable of describing the distribution of turbulent kinetic energy across the entire region where $n_s(k_0) > 0$. This makes the CG model much richer than the MLT in both its theoretical foundations and in its predictive power.

8.1.2 The CGC model

The closure relation used to provide an analytic solution for the turbulent energy spectrum in the CG model limits the applicability of the model to the LST region of the flow. The CGC model therefore arose as an attempt to improve on the CG model by allowing for a treatment of the *entire k*-space. This was a achieved through an improved closure for the correlation rate which related it directly to the eddy viscosity. In addition to being able to treat the SST region of the spectrum, the CGC model also provides a method for *self-consistently* determining the turbulent growth rates from within the model itself. This approach to the determination of growth rates freed the model from any physical inconsistencies associated with the use of the linear approximation to $n_s(k)$. The shortcoming of the CGC model is its omission of the feedback mechanism expected to occur between the source instability and eddies in the cascade.

8.1.3 The CGM model

The CGM model is based directly on the self-consistent framework of the CGC model, however, the difference between the two lies in their interpretation of the eddy correlation time. The CGM model incorporates into the definition

of the correlation time the phenomenology associated with the scattering of eddies that generates the feedback mechanism discussed in section 4.5. The net effect of this mechanism is to regulate the source input energy by the turbulence itself. This allows for a significantly improved closure compared with that of the CGC model, and is the reason why the energy spectrum predicted by the CGM model is likely to be in better agreement with the DIA/EDQNM spectra than the CGC model.

Furthermore, the parametric nature of the CGM expression for the convective heat flux, allows it to be implemented numerically in 1-D stellar evolution codes, making it an ideal replacement to the MLT in studies of stellar structure and evolution.

8.1.4 The CM model

In this thesis, I also considered briefly the formulation of the CM model which, unlike the models discussed above, is based on the DIA/EDQNM approach to turbulence. The merit of using this approach is that it allows the CM model to incorporate a more complete description of the non-linear interactions than the CGM model. However, due to the difficulties associated with incorporating a self-consistent method for determining the rates within the DIA/EDQNM framework, the CM model is still limited to the use of the linear theory for its description of the turbulence generating instability.

The reason for including this model in this thesis was to illustrate the fact that even though the CGM model is based on a phenomenological closure for the eddy viscosity that is not derived directly from the NSE, the physical basis of this closure is robust enough that the model produces results which are comparable to those of the DIA/EDQNM approach, which incorporates a much more sophisticated treatment of the non-linear energy transfer in the fluid.

Furthermore, since the CM model also produces a parametric expression for the convective heat flux, it allows for a direct comparison with the results of the CGM model when applied to numerical simulations of stellar structure and evolution. The closeness between the evolutionary tracks predicted by the CGM and CM models in chapter 7 speak to the strength of the CGM closure and its inclusion of a method for determining the growth rates in a way that is independent of the linear mode analysis of the fluid equations.

8.2 The need for a replacement of the MLT

It has been shown in this thesis that several models exist which provide a better description of turbulent convection than the MLT. Each of the models discussed above form part of a hierarchy of improvements to the MLT. However, while these models have existed for some time, the MLT still remains the de facto standard model when it comes to the treatment of convection in stars. This is remarkable in light of the fact that all the models discussed use more complete representations of the turbulent energy spectrum than the MLT, which assumes a δ-function for $F(k)$.

The convective fluxes predicted by these models differ significantly from those predicted by the MLT, especially for the situation of highly efficient convection. These differences should not be ignored for they are bound to result in inaccurate descriptions of the structure and evolution of stars. This is reflected in the set of evolutionary diagrams displayed in Chapter 7. It was noted there that the differences between alternative treatments of convection become most apparent for stars with convective cores, and at the post main-sequence stages of evolution respectively. Most prominent among these results are the following:

1. A significantly hotter red giant branch.

2. Substantial changes in the position of the terminal age main-sequence.

3. A substantially extended horizontal branch (including a hotter blue edge).

In summary, the figures of Chapter 7 serve to justify the fact that the current, standard evolutionary paths published in the literature using the MLT, may be in need of substantial revision and that the use of more realistic models for convective energy transfer is imperative for future calculations of stellar structure and evolution.

8.2.1 Future work

The phenomenological closure models discussed in this thesis are designed to provide detailed information about the structure and distribution of energy in turbulent flows. They have also been shown to provide a significantly better description of the convective process than the canonical MLT. However, these models are not capable of treating accurately turbulence which is incompressible, inhomogeneous, or strongly anisotropic. They also lack the ability to describe the physics of non-local effects such convective overshooting. These deficiencies prevent the FST models from being able to probe in a direct way the coupling of convection to other key physical processes that occur in the stellar fluid, such as pulsation.

A model which is capable of circumventing these deficiencies, and which has recently been adapted by the principle author of the CG, CGC, CGM and CM models to the description of stellar turbulence, is the Reynolds Stress Model (RSM) [24; 25; 26; 27; 28]. The RSM belongs to a class of turbulence models which do not employ the concept of an eddy-viscosity. They deal rather with

the second-order moments of the NSE in real coordinate space, and incorporate in a natural way the dynamics of non-local fluid effects [79; 122].

When we investigated these models, we concluded that their implementation in current stellar codes was beyond the scope of this project. I have therefore not undertaken this task in the present thesis. In fact, there do not at present appear to be any 1-D stellar evolution codes that incorporate the full set of partial differential equations suggested by the RSM for the treatment of convective turbulence [99]. Investigation of how to implement these equations in current or new stellar codes thus provides a natural avenue for future work, in which I propose exploring the possibility of implementing this model within the MESA code library.

The CGM and CM models therefore represent the best currently available alternatives to the MLT that can be feasibly incorporated into present day, 1-D stellar evolution codes. While this thesis was being written, a new version of MESA (-r9575) was released which added several new features to the code library. These include significant updates and improvements to the opacity, pulsation and accretion modules. I therefore plan to update and extend the present FST implementation to ensure full compatibility with these recent changes (in particular the MESA-Gyre pulsation package) and, having done so, to make our FST convection module available to the MESA user base in the hope that it will reignite an interest in these models, and provide the large number of researchers who use the MESA code with an alternative method for calculating convective energy transfer in their models.

8.2.2   Final remarks

The convection problem has vexed stellar astrophysics for several decades. It is the prototype of many astrophysical problems in which the bottle-neck preventing significant progress is the difficulty involved in solving the Navier-

Stokes equations. With the current generation of hydrodynamical simulations unable to perform full evolutionary calculations, one has no choice but to resort to phenomenological models of convective turbulence that can be implemented in a tractable way in 1-D stellar evolution codes. In this thesis I have presented a detailed analysis of such models and, through this analysis, have suggested that the MLT is in need of replacement. In particular I have focused on the theoretical foundations of models of convective turbulence which improve on the MLT by incorporating the full spectrum of turbulent eddies in their predictions of the convective heat flux. I have argued in several ways that these FST type models represent a significantly more robust and improved description of convective turbulence than the MLT. It is hoped that the analysis presented in this thesis will shed light on the origins and theoretical foundations of the FST models, and stimulate interest in their use as a replacement for the MLT in studies of stellar structure and evolution.

Appendix A

The Convective Heat Flux

In this appendix I provide a first principles derivation of the formula for the convective heat flux stated in equation (2.6.4). This quantity is also related to, ϵ, the total input energy from the source.

Consider a fluid constrained between two boundaries of infinite horizontal extent. Let the vertical distance between these boundaries be denoted by D. Now suppose that the fluid is subjected to a heat flux from the lower boundary. Applying the Boussinesq approximation [119] to the above fluid results in the following equations for the fluctuating velocity and temperature fields, denoted by $\mathbf{u}$ and θ respectively,

$$\left(\frac{\partial}{\partial t} - \nu\nabla^2\right)\mathbf{u}(\mathbf{x},t) \;=\; (\mathbf{u}\cdot\nabla)\,\mathbf{u}\,(\mathbf{x},t) - \frac{1}{\rho}\nabla p + \mathbf{g}\alpha\theta(\mathbf{x},t) \quad \text{(A.0.1)}$$

$$\left(\frac{\partial}{\partial t} - \chi\nabla^2\right)\theta(\mathbf{x},t) \;=\; -(\mathbf{u}\cdot\nabla)\theta(\mathbf{x},t) + \beta(z)u_z(\mathbf{x},t) \qquad \text{(A.0.2)}$$

$$\nabla\cdot\mathbf{u} \;=\; 0 \qquad\qquad\qquad\qquad \text{(A.0.3)}$$

where $\mathbf{u} = (u_x, u_y, u_z)$.

The equation for the heat flux in the above system is given by,

$$-\chi\frac{d\overline{T}(z)}{dz} + \overline{u_z\theta}(z) = \chi N\beta_0 \tag{A.0.4}$$

where $\overline{T}(z)$ is the average temperature at z, N is the Nusselt number, and $\beta_0 = \Delta T/D$, where ΔT is the temperature difference between the upper and lower boundaries. Note that the bars in the above equation refer to horizontal averages, which will be assumed to be equal to ensemble averages.

The volume average of equation (A.0.4) is given by,

$$H_c = \left(\frac{\rho c_p}{V}\right)\int_V \overline{(w\theta)}\, dV = (N-1)\, c_p\rho\chi\beta_0 \tag{A.0.5}$$

In the above notation, the expression for the turbulent convective heat flux is given by,

$$H_c = c_p\rho\overline{u_z\theta} \tag{A.0.6}$$

where the angular brackets, $\langle\cdot\rangle$, denote an ensemble average. In order to develop a spectral representation of this equation, we begin by using Fourier expansions of $\mathbf{u}(\mathbf{x},t)$ and $\theta(\mathbf{x},t)$ to generate equations for the second order moments of these fields. The procedure is as follows:

Starting from,

$$\mathbf{u}(\mathbf{x},t) = V\sqrt[3]{2\pi}\int_V \mathbf{U}(\mathbf{k},t)e^{i\mathbf{k}\cdot\mathbf{x}}\, dV \tag{A.0.7}$$

$$\theta(\mathbf{x},t) = V\sqrt[3]{2\pi}\int_V \theta(\mathbf{k},t)e^{i\mathbf{k}\cdot\mathbf{x}}\, dV \tag{A.0.8}$$

we can write down volume averages of the fluctuating quantities as follows:

$$\overline{u^2} \equiv \frac{1}{V}\int_V \langle\mathbf{u}\mathbf{u}^*\rangle dV = \int_{k_0}^{\infty} F(k)dk \tag{A.0.9}$$

$$\overline{\theta^2} \equiv \frac{1}{V} \int_V \langle \theta\theta^* \rangle dV = \int_{k_0}^{\infty} G(k)dk \tag{A.0.10}$$

$$\overline{u_z\theta} \equiv \frac{1}{2V} \int_V \langle w\theta^* + w^*\theta \rangle dV = \int_{k_0}^{\infty} H(k)dk \tag{A.0.11}$$

$F(k)$, $G(k)$ and $H(k)$ may now be identified as spectral functions describing the turbulent velocity, temperature fluctuations and turbulent convective heat flux, respectively.

It has been shown [135] that, for the case of stationary turbulence, the spectral equations obeyed by these functions are,

$$g\alpha H(k) = \nu k^2 F(k) + T_F(k) \tag{A.0.12}$$

$$\beta H(k) = \chi k^2 G(k) + T_G(k) \tag{A.0.13}$$

Combining equations (A.0.12) and (2.4.2) results in,

$$H(k) = \frac{1}{g\alpha}\left[n_s(k) + \nu k^2\right]F(k) \tag{A.0.14}$$

The volume average of (A.0.4) is

$$F_c = c_p\left(\frac{\rho}{V}\right) \int (\overline{w\theta})dV = (N-1)\, c_p\rho\chi\beta_o \tag{A.0.15}$$

Using equations (A.0.6), (A.0.11), (A.0.12), this becomes

$$H_c = c_p\rho \int_{k_0}^{\infty} H(k)dk = c_p\rho\beta\chi\Phi \tag{A.0.16}$$

where the dimensionless convective flux, Φ, is given by

$$\Phi = \frac{1}{g\alpha\beta\chi} \int_{k_0}^{\infty} \left[n_s(k) + \nu k^2 \right] F(k) dk \qquad \text{(A.0.17)}$$

Finally, combining the above equation with equation (2.4.1), results in,

$$\Phi = \frac{\epsilon}{g\alpha\beta\chi} \qquad \text{(A.0.18)}$$

Bibliography

[1] Althaus, L.G. and Benvenuto, O.G., 1996. Evolution of DB white dwarfs in the Canuto and Mazzitelli theory of convection. Monthly Notices of the Royal Astronomical Society, 278(4), pp.981-984.

[2] Basu, S. and Antia, H.M., 1995. Helium abundance in the solar envelope. Monthly Notices of the Royal Astronomical Society, 276(4), pp.1402-1408.

[3] Batchelor, G.K., 1953. The theory of homogeneous turbulence. Cambridge university press.

[4] Batchelor, G.K., Howells, I.D. and Townsend, A.A., 1959. Small-scale variation of convected quantities like temperature in turbulent fluid Part 2. The case of large conductivity. Journal of Fluid Mechanics, 5(01), pp.134-139.

[5] Baturin, V.A. and Mironova, I.V., 1995. The method of acoustic potential for the analysis of oscillating solar models with revised convection theory. Astronomy Reports, 39(1), pp.105-114.

[6] Berthomieu, G. and Cribier, M. eds., 2012. Inside the Sun: Proceedings of the 121st Colloquium of the International Astronomical Union, Held at Versailles, France, May 22-26, 1989 (Vol. 159). Springer Science & Business Media.

[7] Biermann, L., 1945. Neuere Fortschritte der Theorie des inneren Aufbaues und der Entwicklung der Sterne. In Ergebnisse der exakten naturwissenschaften (pp. 1-49). Springer Berlin Heidelberg.

[8] Böhm-Vitense, E., 1958. Uber die Wasserstoffkonvektionszone in Sternen verschiedener Effektivtemperaturen und Leuchtkrafte. Mit 5 Textabbildungen. Zeitschrift fur Astrophysik, 46, p.108.

[9] Bohm, K.H. and Cassinelli, J., 1971. Convective envelopes and acoustic noise generation in white dwarfs. Astronomy and Astrophysics, 12, p.21.

[10] Boussinesq, J., 1877. Théorie de l'écoulement tourbillant. Mem. Présentés par Divers Savants Acad. Sci. Inst. Fr, 23(46-50), pp.6-5.

[11] Bradshaw, P., 1974. Possible origin of Prandtl's mixing-length theory. Nature, 249(5453), pp.135-136.

[12] Buzzoni, A., Pecci, F.F., Buonanno, R. and Corsi, C.E., 1983. Helium abundance in globular clusters-The R-method. Astronomy and Astrophysics, 128, pp.94-101.

[13] Cabot, W., Hubickyj, O., Pollack, J.B., Cassen, P. and Canuto, V.M., 1990. Direct numerical simulations of turbulent convection: I. Variable gravity and uniform rotation. Geophysical & Astrophysical Fluid Dynamics, 53(1-2), pp.1-42.

[14] Cabot, W., Canuto, V.M., Hubickyj, O. and Pollack, J.B., 1987. The role of turbulent convection in the primitive solar nebula: I. Theory. Icarus, 69(3), pp.387-422.

[15] Canuto, V.M., Goldman, I. and Hubickyj, O., 1984. A formula for the Shakura-Sunyaev turbulent viscosity parameter. The Astrophysical Journal, 280, pp.L55-L58.

[16] Canuto, V.M., Cabot, W., Hartke, G.J. and Battaglia, A., 1985. Is the Kolmogoroff model applicable to large-scale turbulence?. Astrophysics and space science, 116(2), pp.367-375.

[17] Canuto, V.M. and Goldman, I., 1985. Analytical model for large-scale turbulence. Physical review letters, 54(5), p.430.

[18] Canuto, V.M. and Battaglia, A., 1985. Turbulence in molecular clouds-A new diagnostic tool to probe their origin. The Astrophysical Journal, 294, pp.L125-L129.

[19] Canuto, V.M. and Hartke, G.J., 1986. Convective turbulence with rotation and magnetic fields. Astronomy and Astrophysics, 168, pp.89-104.

[20] Canuto, V.M. and Hartke, G.J., 1986. Propagation of electromagnetic waves in a turbulent medium. JOSA A, 3(6), pp.808-817.

[21] Canuto, V.M., Goldman, I. and Chasnov, J., 1987. A model for fully developed turbulence. The Physics of fluids, 30(11), pp.3391-3418.

[22] Canuto, V.M. and Mazzitelli, I., 1991. Stellar turbulent convection-A new model and applications. The Astrophysical Journal, 370, pp.295-311.

[23] Canuto, V.M., Goldman, I. and Mazzitelli, I., 1996. Stellar turbulent convection: a self-consistent model. The Astrophysical Journal, 473(1), p.550.

[24] Canuto, V.M., 2011. Stellar mixing-I. Formalism. Astronomy & Astrophysics, 528, p.A76.

[25] Canuto, V.M., 2011. Stellar mixing-II. Double diffusion processes. Astronomy & Astrophysics, 528, p.A77.

[26] Canuto, V.M., 2011. Stellar mixing-III. The case of a passive tracer. Astronomy & Astrophysics, 528, p.A78.

[27] Canuto, V.M., 2011. Stellar Mixing-IV. The angular momentum problem. Astronomy & Astrophysics, 528, p.A79.

[28] Canuto, V.M., 2011. Stellar mixing-V. Overshooting. Astronomy & Astrophysics, 528, p.A80.

[29] Chandrasekhar, S., 2013. Hydrodynamic and hydromagnetic stability. Courier Corporation.

[30] Chan, K.L. and Sofia, S., 1989. Turbulent compressible convection in a deep atmosphere. IV-Results of three-dimensional computations. The Astrophysical Journal, 336, pp.1022-1040.

[31] Christensen-Dalsgaard, J., Monteiro, M.J. and Thompson, M.J., 1995. Helioseismic estimation of convective overshoot in the Sun. Monthly Notices of the Royal Astronomical Society, 276(1), pp.283-292.

[32] Cyburt, R.H., Amthor, A.M., Ferguson, R., Meisel, Z., Smith, K., Warren, S., Heger, A., Hoffman, R.D., Rauscher, T., Sakharuk, A. and Schatz, H., 2010. The JINA REACLIB database: its recent updates and impact on type-I x-ray bursts. The Astrophysical Journal Supplement Series, 189(1), p.240.

[33] D'Antona, F. and Mazzitelli, I., 1994. New pre-main-sequence tracks for M less than or equal to 2.5 solar mass as tests of opacities and convection model. The Astrophysical Journal Supplement Series, 90, pp.467-500.

[34] Elmegreen, B.G., 1982. The Parker instability in a self-gravitating gas layer. The Astrophysical Journal, 253, pp.634-654.

[35] Elmegreen, B.G. and Scalo, J., 2004. Interstellar turbulence I: observations and processes. Annu. Rev. Astron. Astrophys., 42, pp.211-273.

[36] Scalo, J. and Elmegreen, B.G., 2004. Interstellar turbulence II: implications and effects. Annu. Rev. Astron. Astrophys., 42, pp.275-316.

[37] Featherstone, N.A. and Hindman, B.W., 2016. The spectral amplitude of stellar convection and its scaling in the high-Rayleigh-number regime. The Astrophysical Journal, 818(1), p.32.

[38] Ferguson, J.W., Alexander, D.R., Allard, F., Barman, T., Bodnarik, J.G., Hauschildt, P.H., Heffner-Wong, A. and Tamanai, A., 2005. Low-temperature opacities. The Astrophysical Journal, 623(1), p.585.

[39] Freytag, B., Ludwig, H.G. and Steffen, M., 1996. Hydrodynamical models of stellar convection. The role of overshoot in DA white dwarfs, A-type stars, and the Sun. Astronomy and Astrophysics, 313, pp.497-516.

[40] Freytag, B., Steffen, M., Ludwig, H.G., Wedemeyer-Bohm, S., Schaffenberger, W. and Steiner, O., 2012. Simulations of stellar convection with CO5BOLD. Journal of Computational Physics, 231(3), pp.919-959.

[41] Frisch, U. and Donnelly, R.J., 1996. Turbulence: the legacy of AN Kolmogorov.

[42] Fröhlich, C., Huber, M., Solanki, S.K. and von Steiger, R. eds., 2012. Solar Composition and Its Evolution-from Core to Corona: Proceedings of an ISSI Workshop 26-30 January 1998, Bern, Switzerland (Vol. 5). Springer Science & Business Media.

[43] Ghizaru, M., Charbonneau, P. and Smolarkiewicz, P.K., 2010. Magnetic cycles in global large-eddy simulations of solar convection. The Astrophysical Journal Letters, 715(2), p.L133.

[44] Goldstein, R.J., Chiang, H.D. and See, D.L., 1990. High-Rayleigh-number convection in a horizontal enclosure. Journal of Fluid Mechanics, 213, pp.111-126.

[45] Goldstkin, R.J. and Tokuda, S., 1980. Heat transfer by thermal convection at high Rayleigh numbers. International Journal of Heat and Mass Transfer, 23(5), pp.738-740.

[46] Goluskin, D. and van der Poel, E.P., 2016. Penetrative internally heated convection in two and three dimensions. Journal of fluid mechanics, 791, p.R6.

[47] Gough, D.O. and Weiss, N.O., 1976. The calibration of stellar convection theories. Monthly Notices of the Royal Astronomical Society, 176(3), pp.589-607.

[48] Gough, D.O., 1977. Mixing-length theory for pulsating stars. The Astrophysical Journal, 214, pp.196-213.

[49] Gough, D., 1977. The current state of stellar mixing-length theory. In Problems of Stellar Convection (pp. 15-56). Springer Berlin Heidelberg.

[50] Grant, H.L., Stewart, R.W. and Moilliet, A., 1962. Turbulence spectra from a tidal channel. Journal of Fluid Mechanics, 12(02), pp.241-268.

[51] Grinstein, F.F., Margolin, L.G. and Rider, W.J. eds., 2007. Implicit large eddy simulation: computing turbulent fluid dynamics. Cambridge university press.

[52] Haselgrove, C.B. and Hoyle, F., 1956. A mathematical discussion of the problem of stellar evolution, with reference to the use of an automatic digital computer. Monthly Notices of the Royal Astronomical Society, 116(5), pp.515-526.

[53] Hartke, G.J., Canuto, V.M. and Dannevik, W.P., 1988. A direct interaction approximation treatment of high Rayleigh number convective turbulence and comparison with experiment. The Physics of fluids, 31(2), pp.256-262.

[54] Hartke, G.J., Canuto, V.M. and Alonso, C.T., 1988. A direct interaction approximation treatment of turbulence in a compressible fluid. I. Formalism. The Physics of fluids, 31(5), pp.1034-1050.

[55] Heisenberg, W., 1948. On the Theory of Statistical and Isotropic Turbulence. Proceedings of the Royal Society of London Series A, 195, pp.402-406.

[56] Heitsch, F., 2006. The Formation of Turbulent Molecular Clouds: A Modeler's View. Reviews in Modern Astronomy, The Many Facets of the Universe: Revelations by New Instruments, 19, p.157.

[57] Henyey, L.G., Forbes, J.E. and Gould, N.L., 1964. A New Method of Automatic Computation of Stellar Evolution. The Astrophysical Journal, 139, p.306.

[58] Henyey, L., Vardya, M.S. and Bodenheimer, P., 1965. Studies in Stellar Evolution. III. The Calculation of Model Envelopes. The Astrophysical Journal, 142, p.841.

[59] Heyer, M. and Dame, T.M., 2015. Molecular clouds in the milky way. Annual Review of Astronomy and Astrophysics, 53, pp.583-629.

[60] Houdek, G., Balmforth, N.J., Christensen-Dalsgaard, J. and Gough, D.O., 1999. Stellar Structure: Theory and Test of Connective Energy Transport. In ASP Conf. Ser (Vol. 173).

[61] Howard, L.N., 1963. Heat transport by turbulent convection. Journal of Fluid Mechanics, 17(03), pp.405-432.

[62] Howells, I.D., 1960. An approximate equation for the spectrum of a conserved scalar quantity in a turbulent fluid. Journal of Fluid Mechanics, 9(01), pp.104-106.

[63] Hunt, J.C.R. and Vassilicos, J.C., 1991, July. Kolmogorov's contributions to the physical and geometrical understanding of small-scale turbulence and recent developments. In Proceedings of the Royal Society of London A: Mathematical, Physical and Engineering Sciences (Vol. 434, No. 1890, pp. 183-210). The Royal Society.

[64] Iglesias, C.A. and Rogers, F.J., 1996. Updated OPAL opacities. The Astrophysical Journal, 464, p.943.

[65] Izotov, Y.I., Stasinska, G. and Guseva, N.G., 2013. Primordial 4He abundance: a determination based on the largest sample of H II regions with a methodology tested on model H II regions. Astronomy and Astrophysics, 558, p.A57.

[66] Kolmogorov, A.N., 1991. The local structure of turbulence in incompressible viscous fluid for very large Reynolds numbers. Proceedings: Mathematical and Physical Sciences, 434(1890), pp.9-13.

[67] Kraichnan, R.H., 1958. Irreversible statistical mechanics of incompressible hydromagnetic turbulence. Physical Review, 109(5), p.1407.

[68] Kraichnan, R.H., 1965. Lagrangian-history closure approximation for turbulence. The Physics of Fluids, 8(4), pp.575-598.

[69] Kraichnan, R.H., 1966. Isotropic Turbulence and Inertial-Range Structure. The Physics of Fluids, 9(9), pp.1728-1752.

[70] Kraichnan, R.H., 1972. Test-field model for inhomogeneous turbulence. Journal of Fluid Mechanics, 56(02), pp.287-304.

[71] Kraichnan, R.H., 1976. Eddy viscosity in two and three dimensions. Journal of the Atmospheric Sciences, 33(8), pp.1521-1536.

[72] Kraichnan, R.H., 1987. An interpretation of the Yakhot-Orszag turbulence theory. The Physics of fluids, 30(8), pp.2400-2405.

[73] Kupka, F., Roxburgh, I. and Chan, K.L., 2007. Convection in Astrophysics (IAU S239) (Vol. 239). Cambridge University Press.

[74] Kurucz, R.L., 1979. Model atmospheres for g, f, a, b, and o stars. The Astrophysical Journal Supplement Series, 40, pp.1-340.

[75] Lada, C.J., Lombardi, M. and Alves, J.F., 2010. On the star formation rates in molecular clouds. The Astrophysical Journal, 724(1), p.687.

[76] Lamb, H., 1932. Hydrodynamics. Cambridge university press.

[77] Landahl, M.T. and Mollo-Christensen, E., 1992. Turbulence and random processes in fluid mechanics. Cambridge University Press.

[78] Landau, L.D., 1944. On the problem of turbulence. In Dokl. Akad. Nauk SSSR (Vol. 44, No. 8, pp. 339-349).

[79] Launder, B.E., Reece, G.J. and Rodi, W., 1975. Progress in the development of a Reynolds-stress turbulence closure. Journal of fluid mechanics, 68(03), pp.537-566.

[80] Latour, J., Toomre, J. and Zahn, J.P., 1981. Stellar convection theory. III-Dynamical coupling of the two convection zones in A-type stars by penetrative motions. The Astrophysical Journal, 248, pp.1081-1098.

[81] Lesieur, M., 2012. Turbulence in fluids (Vol. 40). Springer Science & Business Media.

[82] Leslie, D.C., 1973. Developments in the theory of turbulence. Oxford, Clarendon Press.

[83] Ludwig, H.G., Freytag, B. and Steffen, M., 1999. A calibration of the mixing-length for solar-type stars based on hydrodynamical simulations. I. Methodical aspects and results for solar metallicity. Astronomy and Astrophysics, 346, pp.111-124.

[84] Landau, L.D. and Lifshitz, E.M., 2013. Fluid mechanics: Landau and Lifshitz: course of theoretical physics (Vol. 6). Elsevier.

[85] Ledoux, P., Schwarzschild, M. and Spiegel, E.A., 1961. On the Spectrum of Turbulent Convection. The Astrophysical Journal, 133, p.184.

[86] Larson, R.B., 1981. Turbulence and star formation in molecular clouds. Monthly Notices of the Royal Astronomical Society, 194(4), pp.809-826.

[87] Lombardini, M., Hill, D.J., Pullin, D.I. and Meiron, D.I., 2011. Atwood ratio dependence of Richtmyer-Meshkov flows under reshock conditions using large-eddy simulations. Journal of fluid mechanics, 670, pp.439-480.

[88] Mac Low, M.M. and Klessen, R.S., 2004. Control of star formation by supersonic turbulence. Reviews of modern physics, 76(1), p.125.

[89] Maeder, A. and Meynet, G., 1989. Grids of evolutionary models from 0.85 to 120 solar masses-Observational tests and the mass limits. Astronomy and Astrophysics, 210, pp.155-173.

[90] Mazzitelli, I., D'Antona, F. and Caloi, V., 1995. Globular cluster ages with updated input physics. Astronomy and Astrophysics, 302, p.382.

[91] McCurdy, E. ed., 1956. The notebooks of Leonardo da Vinci (Vol. 1). Prabhat Prakashan.

[92] Mellor, G.L. and Yamada, T., 1982. Development of a turbulence closure model for geophysical fluid problems. Reviews of Geophysics, 20(4), pp.851-875.

[93] Métais, O. and Ferziger, J.H. eds., 2013. New Tools in Turbulence Modelling: Les Houches School, May 21-31, 1996 (Vol. 5). Springer Science & Business Media.

[94] Mihalas, D., 1978. Stellar atmospheres. San Francisco, WH Freeman and Co., 1978. 650 p.

[95] Mikaelian, K.O. Turbulent mixing generated by Rayleigh-Taylor and Richtmyer-Meshkov instabilities. Physica D, 12:45, 1984.

[96] Moffatt, H.K., 1981. Some developments in the theory of turbulence. Journal of Fluid Mechanics, 106, pp.27-47.

[97] Moin, P. and Mahesh, K., 1998. Direct numerical simulation: a tool in turbulence research. Annual review of fluid mechanics, 30(1), pp.539-578.

[98] Monin, A.S. and Yaglom, A.M., 2013. Statistical fluid mechanics, volume II: Mechanics of turbulence (Vol. 2). Courier Corporation.

[99] Monteiro, M.J., 2008. Evolution and seismic tools for stellar astrophysics. Springer.

[100] Morfill, G.E., 1988. Protoplanetary accretion disks with coagulation and evaporation. Icarus, 75(2), pp.371-379.

[101] Olive, K.A. and Steigman, G., 1995. On the abundance of primordial helium. The Astrophysical Journal Supplement Series, 97, pp.49-58.

[102] Orszag, S.A., 1977. Fluid Dyanmics. ed. R. Bailian and J. L. Peube (New York: Gordon and Breach).

[103] Ossendrijver, M., 2003. The solar dynamo. The Astronomy and Astrophysics Review, 11(4), pp.287-367.

[104] Pasetto, S., Chiosi, C., Chiosi, E., Cropper, M. and Weiss, A., 2016. Theory of stellar convection-II. First stellar models. Monthly Notices of the Royal Astronomical Society, 459(3), pp.3182-3202.

[105] Paxton, B., Cantiello, M., Arras, P., Bildsten, L., Brown, E.F., Dotter, A., Mankovich, C., Montgomery, M.H., Stello, D., Timmes, F.X. and Townsend, R., 2013. Modules for experiments in stellar astrophysics (MESA): planets, oscillations, rotation, and massive stars. The Astrophysical Journal Supplement Series, 208(1), p.4.

[106] Paxton B., Bildsten L., Dotter A., Herwig F., Lesaffre P., and Timmes F., 2011. Modules for experiments in stellar astrophysics (MESA). The Astrophysical Journal Supplement Series, 192(1), p.3.

[107] Paxton, B., Cantiello, M., Arras, P., Bildsten, L., Brown, E.F., Dotter, A., Mankovich, C., Montgomery, M.H., Stello, D., Timmes, F.X. and Townsend, R., 2013. Modules for experiments in stellar astrophysics (MESA): planets, oscillations, rotation, and massive stars. The Astrophysical Journal Supplement Series, 208(1), p.4.

[108] Paxton, B., Marchant, P., Schwab, J., Bauer, E.B., Bildsten, L., Cantiello, M., Dessart, L., Farmer, R., Hu, H., Langer, N. and Townsend, R.H.D., 2015. Modules for experiments in stellar astrophysics (MESA): binaries, pulsations, and explosions. The Astrophysical Journal Supplement Series, 220(1), p.15.

[109] Prandtl, L., 1925. Bericht uber Untersuchungen zur ausgebildeten Turbulenz. Z. Angew. Math. Mech, 5(2), pp.136-139.

[110] Prat, V., Guilet, J., Viallet, M. and Müller, E., 2016. Shear mixing in stellar radiative zones-II. Robustness of numerical simulations. Astronomy & Astrophysics, 592, p.A59.

[111] Pringle, J.E., 1981. Accretion discs in astrophysics. Annual review of astronomy and astrophysics, 19(1), pp.137-160.

[112] Rayleigh, L., 1916. LIX. On convection currents in a horizontal layer of fluid, when the higher temperature is on the under side. The London, Edinburgh, and Dublin Philosophical Magazine and Journal of Science, 32(192), pp.529-546.

[113] Rogers, F.J. and Nayfonov, A., 2002. Updated and expanded OPAL equation-of-state tables: implications for helioseismology. The Astrophysical Journal, 576(2), p.1064.

[114] Sagaut, P. and Cambon, C., 2008. Homogeneous turbulence dynamics (Vol. 10). Cambridge: Cambridge University Press.

[115] Schmitt, F.G., 2007. About Boussinesq's turbulent viscosity hypothesis: historical remarks and a direct evaluation of its validity. Comptes Rendus Mécanique, 335(9-10), pp.617-627.

[116] Schwarzschild, M., 2015. Structure and evolution of stars. Princeton University Press.

[117] Serenelli, A.M. and Basu, S., 2010. Determining the initial helium abundance of the Sun. The Astrophysical Journal, 719(1), p.865.

[118] Shakura, N.I., Sunyaev, R.A. and Zilitinkevich, S.S., 1978. On the turbulent energy transport in accretion discs. Astronomy and Astrophysics, 62, pp.179-187.

[119] Spiegel, E.A. and Veronis, G., 1960. On the Boussinesq approximation for a compressible fluid. The Astrophysical Journal, 131, p.442.

[120] Spiegel, E.A., 1962. Thermal turbulence at very small Prandtl number. Journal of Geophysical Research, 67(8), pp.3063-3070.

[121] Spiegel, E.A., 1963. A Generalization of the Mixing-Length Theory of Turbulent Convection. The Astrophysical Journal, 138, p.216.

[122] Speziale, C.G., 1991. Analytical methods for the development of Reynolds-stress closures in turbulence. Annual Review of Fluid Mechanics, 23(1), pp.107-157.

[123] Stothers, R.B. and Chin, C.W., 1993. Iron and molecular opacities and the evolution of Population I stars. The Astrophysical Journal, 412, pp.294-300.

[124] Stothers, R.B. and Chin, C.W., 1995. Tests of two convection theories for red giant and red supergiant envelopes. The Astrophysical Journal, 440, pp.297-302.

[125] Taylor, G.I., 1938, February. The spectrum of turbulence. In Proceedings of the Royal Society of London A: Mathematical, Physical and Engineering Sciences (Vol. 164, No. 919, pp. 476-490). The Royal Society.

[126] Trampedach, R., 2010. Convection in stellar models. Astrophysics and Space Science, 328(1), pp.213-219.

[127] Umlauf, L. and Burchard, H., 2005. Second-order turbulence closure models for geophysical boundary layers. A review of recent work. Continental Shelf Research, 25(7), pp.795-827.

[128] Viallet, M., Meakin, C., Arnett, D. and Mocak, M., 2013. Turbulent convection in stellar interiors. III. Mean-field analysis and stratification effects. The Astrophysical Journal, 769(1), p.1.

[129] Ventura, P., Carini, R. and Di Criscienzo, M., 2012. Convection Modelling and the Morphology of RGBs in Stellar Clusters. In Red Giants as Probes of the Structure and Evolution of the Milky Way (pp. 69-76). Springer Berlin Heidelberg.

[130] Ventura, P., D'Antona, F. and Mazzitelli, I., 2008. The ATON 3.1 stellar evolutionary code. Astrophysics and Space Science, 316(1-4), pp.93-98.

[131] Weiss, A., 2002, January. Key problems in stellar evolution. In Stellar Structure and Habitable Planet Finding (Vol. 485, pp. 57-64).

[132] Weiss, A., Hillebrandt, W., Thomas, H.C. and Ritter, H., 2004. Cox and Giuli's Principles of Stellar Structure. Cox and Giuli's Principles of Stellar Structure, by A. Weiss, W. Hillebrandt, HC. Thomas, H. Ritter. Cambridge, UK: Princeton Publishing Associates Ltd, 2004.

[133] Woelke, M., 2007. Eddy Viscosity Turbulence Models employed by Computational Fluid Dynamics. Prace Instytutu Lotnictwa, pp.92-113.

[134] Yadav, R.K., Christensen, U.R., Morin, J., Gastine, T., Reiners, A., Poppenhaeger, K. and Wolk, S.J., 2015. Explaining the coexistence of large-scale and small-scale magnetic fields in fully convective stars. The Astrophysical Journal Letters, 813(2), p.L31.

[135] Yamaguchi, S., 1963. On Turbulent Thermal Convection. Derivation of Spectrum Equations and the Spectrum in Inviscid and No-conductive Case. Publications of the Astronomical Society of Japan, 15, p.412.

[136] Zhu, P., Zhang, J.A. and Masters, F.J., 2010. Wavelet analyses of turbulence in the hurricane surface layer during landfalls. Journal of the Atmospheric Sciences, 67(12), pp.3793-3805.

[137] Zakharov, V.E., L'vov, V.S. and Falkovich, G., 2012. Kolmogorov spectra of turbulence I: Wave turbulence. Springer Science & Business Media.

[138] MESA homepage, 2017, http://mesa.sourceforge.net/prereqs.html

[139] MESA2013 Citations List: https://scholar.google.co.za/scholar?cites= $506934602602910157\&as_sdt = 2005$ & sciodt=0,5 & hl=en

[140] MESA2015 Citations List: https://scholar.google.co.za/scholar?cites= $12661982803097889724\&as_sdt = 2005$ & sciodt=0,5 & hl=en